Duality and neutral pion electroproduction

Thomas D. B. Wilkie

Duality and Neutral Pion Electroproduction

by

Thomas D. B. Wilkie

Thesis presented to the University of Durham

for the degree of Doctor of Philosophy

September 1979

And I gave my heart to seek and search out by wisdom concerning all things that are done under heaven; and, behold, all is vanity and vexation of spirit. For in much wisdom is much grief: and he that increaseth knowledge increaseth sorrow.

Ecclesiastes

C O N T E N T S

Abstract

The implications of Duality, in the form of Finite Energy Sum Rules, are examined for the photoproduction and electroproduction of neutral pions off protons. The Collins and Fitton model of high energy pion photoproduction is extended to accommodate the features of the photoproduction FESR. The analysis is extended to electroproduction and it is shown that a simple modification of the model will fit the electroproduction cross-section. The implications of this modification are discussed.

Chapter 1 : Hadronic Physics and Photon-Induced Processes

Section 1 Introduction

It is a commonplace to observe that photoproduction processes are strikingly similar to ordinary hadronic interactions. The distinctive patterns of bumps and dips in hadronic differential cross-sections are found also in photon-induced processes and many attempts have been made to explain photoproduction using the models and ideas appropriate to hadronic physics.

This identification of hadronic and electromagnetic processes was given quantitative expression by Sakurai (1960) in his proposal of the Vector Meson Dominance model (VDM). Essentially this proposed that the coupling of photons to hadrons took place through a transition of the photon into a (virtual) vector meson carrying the same quantum numbers. Indeed, the usage has become so familiar that the isospin singlet part of the electromagnetic current (which is a U-spin scalar and therefore of mixed isospin) is habitually referred to as the ω -part of the photon, and similarly for the I=1 ρ -part.

The hypothesis of vector meson coupling may be illustrated by observing that the annihilation of e^+e^- at centre of mass energies below $\sim$1 GeV is dominated by the production of the vector mesons ρ°, ω and ϕ . It is thus the

case that virtual, or off-mass-shell, photons can couple to vector mesons and the assumption is made that the same thing happens for real and spacelike photons (see figure 1.1). Assuming this vector meson-electromagnetic current coupling (the current field identity), the basic result of VDM is to relate photoproduction or electroproduction processes to the corresponding vector induced reaction

$$A(\gamma a \to bc)_{k^2<0} = \sum_{\rho,\omega,\varphi} \sqrt{\frac{\alpha\pi}{g_V^2}} \left(\frac{1}{1-\frac{k^2}{m_V^2}}\right) A(Va \to bc)_{k^2=m_V^2} \qquad 1.1$$

for transverse polarizations of the photon (which by gauge invariance are the only ones allowed in photoproduction) and a similar expression with an extra factor of $\sqrt{\frac{-k^2}{m_V^2}}$ for the longitudinal polarization. (For the metric, sign conventions, and normalizations used throughout this work, the appendices should be consulted). A vector meson propagator and a coupling constant are thus the only items required in this model to relate the electromagnetic interaction to an entirely hadronic one. One can form some estimate of the relative preponderance of the ρ-like to the ω-like parts of the photon by an argument based on SU(3). The coupling constants g_ρ, g_ω and g_φ may be related within SU(3) by

$$\frac{1}{g_\rho} = \frac{-\sqrt{3}}{\cos\Theta}\frac{1}{g_\varphi} = \frac{\sqrt{3}}{\sin\Theta}\frac{1}{g_\omega} \qquad 1.2$$

where Θ is the ω-ϕ mixing angle:

$$\phi = \cos\Theta\,\phi^0 + \sin\Theta\,\omega^1$$
$$\omega = -\sin\Theta\,\phi^0 + \cos\Theta\,\omega^1$$

For ideal mixing $\tan\Theta = \frac{1}{\sqrt{2}}$ one obtains the ratios

$$\frac{1}{g_\rho} : \frac{1}{g_\omega} : \frac{1}{g_\phi} = 3 : 1 : -\sqrt{2} \qquad 1.3$$

This result can be obtained also by considering the quark content of the particles. This approach is perhaps more satisfying in terms of physical intuition, once one accepts the existence of quarks. It also is more readily generalised to the new vector mesons ψ and Υ.

But the interest of photon-induced reactions is not that they can be reduced to hadronic processes - although there is an extensive literature on VDM trying to do just that - they have two important features which are peculiar to the photon as a probe of hadronic structure. One feature is that it is technically not too difficult to prepare beams of polarized photons - and this is a powerful tool for discriminating among various phenomenological models. Asymptotically, a clean separation may be made of natural and unnatural parity exchanges in the t-channel, since unnatural parity exchanges dominate the cross-section for photons polarized parallel to

the reaction plane (Stichel 1964, Ader et al 1968), and vice-versa.

The other feature of photon beams, in addition to polarization, is that they enable the external mass of one of the scattering particles to be changed almost at will. Referring to figure 1.2 it can be seen that in the case of neutral pion electroproduction the mass of the virtual photon can be varied kinematically (we treat the electrons as massless).

$$k^2 = -4EE' \sin^2 \Theta/2 \qquad 1.4$$

It is with this property of the photon, and with the reaction

$$\gamma p \longrightarrow \pi^0 p$$

that we shall primarily be concerned in this work.

Section 2 General Features of Neutral Pion Photoproduction

We shall briefly discuss the prominent features of neutral pion photoproduction, using the language of t-channel Regge pole (and cut) exchange, and then on to indicate why the reaction was considered to be of particular interest.

In table 1.1, the allowed t-channel exchanges and some of the physical particles which have these quantum numbers are summarised. In figure 1.3, some data on the differential cross-section are plotted. The gross features are clear. There is no forward spike, and the data in fact will turn over in the forward direction. This reflects the fact that pion exchange is forbidden in this process by C-parity conservation. The other prominent feature is the dip in the region $t = -0.5$ which is followed by a secondary maximum.

From a theoretical point of view it is to be expected that the natural parity exchanges will dominate this process as they are higher-lying in the j-plane. As the ρ exchange must couple to the ω -like part of the photon, and the ω exchange to the ρ-part, the argument in the previous section generates the expectation that ω exchange will dominate by a factor of 3 over the ρ-exchange amplitude. Since the ω -couples predominantly to the (s-channel) helicity non-flip at the N-N vertex, it is also expected that the s-channel single flip

amplitudes will be dominant, this is borne out also by the turn-over at t=0 (only the non-flip amplitude is non-zero at t=0). The ratio of the cross-sections for photoproduction off protons and neutrons (figure 1.4) indicates that there is only small interference between the I=0 and I=1 exchanges (the latter changes sign between the two reactions). Similarly, evidence for the dominance of natural parity exchange comes from the large value of the polarized photon assymetry (figure 1.5).

$$\Sigma = \left(\frac{d\sigma_\perp}{dt} - \frac{d\sigma_\parallel}{dt}\right) / \left(\frac{d\sigma_\perp}{dt} + \frac{d\sigma_\parallel}{dt}\right)$$

All this is reasonably well understood and accords with expectation, the real interest of neutral pion photoproduction lies in the mechanism employed to explain the dip at t = -0.5. There are two basic and conflicting philosophies.

One approach observes that the trajectory function of the ω itself has a zero at t = -0.5 and that for a number of reasons (see e.g. the discussion in Chapter 6 of Collins 1977) the inclusion of a factor $\alpha_\omega(t)$ in the residue function of the ω Regge pole might be desirable. This so-called nonsense wrong signature zero (NWZ) in the amplitudes then has to be filled in by a strong cut (which is comparatively featureless in t) to produce the observed dip.

The alternative approach is to use a comparatively featureless t-dependence for the residue of the ω -pole and to produce the dip by strong destructive interference from a cut. Regge cuts may be regarded as arising from multiple exchanges of Regge poles and in this strong cut Reggeized absorption model (SCRAM) the cut expresses the diffractive effect of absorption in the s-channel and the dip in the cross-section is a diffractive minimum. In an explicitly geometrical approach the peripheral single flip amplitude would behave like $J_1 (R \sqrt{-t})$ where J_1 is a Bessel function and R is the interaction radius (~ 1fm). The Bessel function has its first zero at around t = -0.5 with this value for R (Harari 1971).

A large number of fits have been published for neutral pion photoproduction and both approaches reproduce the features of the high energy data (Ross et al (1970), Gault et al (1971), Worden (1972), Barker et al (1974).

Section 3 Variable External Mass

The extension from photoproduction ($k^2=0$) to electroproduction ($k^2 < 0$) was early suggested as a process wherein the two different approaches might be distinguished (Harari 1971).

Although many more amplitudes will be present for electro as against photoproduction it is still possible to measure the production of π^0 by transversely polarized photons and ω exchange will still dominate in the t-channel. If the explanation of the photoproduction dip in terms of a NWZ is subscribed to, its position is unaffected by any variation in the photon mass and so the dip in π^0 electroproduction should remain at $t = -0.5$ with this explanation. However, if the photon's interaction radius were to change with its mass, then the diffractive or geometrical approaches would expect the zeros in t of $J_1(R\sqrt{-t})$ to move.

What evidence is there that the interaction radius of the space-like photon decreases as $-k^2$ increases? A number of models have been proposed (Cheng and Wu 1969, Bjorken et al 1971) suggesting that the photon interaction radius

$$R \sim \sqrt{\frac{1}{-k^2}} \qquad -k^2 \to \infty \qquad 1.5$$

Certainly, Harari (1971) expected significant changes for $0 < -k^2 < 1$ GeV^2. It is the case that in quantum electrodynamics the effective radius for producing lepton pairs in an external potential decreases as $-k^2$ increases, and a similar effect may be expected in the context of a parton model explanation of the hadronic "potential". From the proton's point of view, the incident photon might be regarded as acquiring a finite transverse size. This is created by the transverse recoil acquired by the photon as it produces parton anti-parton pairs in its interaction with the proton. When the photon is far off shell, it lives only a short time (because of the uncertainty principle) and can produce fewer transverse parton pairs, and so have a smaller transverse recoil. Thus a highly virtual photon acquires a smaller radius from the proton's point of view.

Other arguments in favour of photon "shrinkage" can be obtained in the context of the Generalised Vector Dominance model (Fraas et al 1975). In this model a Veneziano-like spectrum is assumed for the vector mesons and interference terms are allowed between different mesons coupling to the external photon.

In the differential cross-section for the photoproduction of vector mesons ρ, ω, ϕ - "elastic" photoproduction - this prediction can most easily be tested. The forward elastic amplitudes are predominantly imaginary and

the effective interaction radius for the diffractive component of the scattering can be determined from this. Assuming that the cross-section has a simple exponential behaviour in t

$$\frac{d\sigma}{dt} = Ge^{ct} \qquad 1.6$$

then in the impact parameter representation, the imaginary part of the diffractive amplitude is

$$\text{Im } A(b) \sim e^{(-b^2/R^2)} \qquad 1.7$$

where the diffractive slope c and the radius of interaction are related

$$c = R^2/4 \qquad 1.8$$

This is reasonably model independent and indicates that a measurement of the slope of "elastic" photon and electroproduction can verify the prediction of photon shrinkage. It should be remembered that this is physical shrinkage in impact parameter space as a function of k^2. This would take place at constant s and should be distinguished from Regge shrinkage of the differential cross-section.

One test proposed by Harari (1971) was ρ^o production. The experimental data are confused in this reaction, some results claim photon shrinkage others deny it (Ahrens et al, 1974; Talman, 1973). Nonetheless Fraas et al claimed

support for their model which gave prominence to higher recurrences of vector mesons having flatter slopes than the elastic reaction. In fact, it is experimentally difficult to obtain a pure ρ^0 signal from a non-resonant π-π background and the shape of the ρ distribution may well be t-dependent. However, some recent experiments (Joos et al 1976, Francis 1977) seem consistently to indicate that any downward trend in the exponent is not significant. One process which gets around these difficulties is ϕ meson electroproduction which is also diffractive in nature. Such an experiment has been carried out (Dixon et al 1977) and as can be seen from table 1.2 the exponential parameter, although shallower than in photoproduction, yields no evidence for a significant variation with $|k^2|$.

(Strictly, a distinction should be made between the radius associated with the diffractive component of the hadronic amplitude which can be determined from the slope of elastic scattering as above, and the non-diffractive part which is related to the first by unitarity in some complex way. Since one expects almost no non-diffractive components in $\gamma p \longrightarrow \phi p$ it might be argued that the above evidence is not completely convincing, but it seems unlikely that the non-diffractive radius will behave radically differently, see Harari and Schwimmer 1972).

Section 4 Neutral pion electroproduction

At the time the experimental evidence for photon shrinkage was ambiguous but the effect was expected theoretically, and so the first data on pion electroproduction above the resonance region were awaited with some excitement.

When published (Brasse et al, 1975) the form of the differential cross-section (figure 1.6) came as a considerable shock.

The dip at t = -0.5 completely disappears or more correctly the secondary maximum after the dip is washed out and the data continue to fall, almost by an order of magnitude. This effect is most clearly seen in figure 11 of Berger et al (1978) which we reproduce as figure 1.7.

The relationship between the electroproduction cross-section and the corresponding photoproduction formalism is discussed at length in appendix B. We here simply quote equns B7 and B8. (We work throughout in the one photon approximation). The electroproduction cross-section is related to the virtual photon scattering cross-section $\left(\frac{d\sigma_v}{dt}\right)$ by a flux factor $\frac{d\sigma}{dk^2 d\phi ds dt} = \Gamma \frac{d\sigma_v}{dt}$

$$\frac{d\sigma_v}{dt} = \frac{d\sigma_u}{dt} + \frac{d\sigma_s}{dt}\varepsilon + \frac{d\sigma_{tt}}{dt}\cos 2\phi + \frac{d\sigma_{lt}}{dt}\sqrt{2\varepsilon(\varepsilon+1)}\cos\phi \qquad 1.9$$

In the experiment by Brasse et al the value of ϕ was chosen to be 90° thus eliminating the scalar-transverse interference terms. Since the unpolarized term and the transverse polarization term can be regarded as respectively the sum and difference of terms polarized parallel and perpendicular to the reaction plane

$$\frac{d\sigma_U}{dt} = \frac{1}{2}\left(\frac{d\sigma_\perp}{dt} + \frac{d\sigma_\parallel}{dt}\right)$$

$$\frac{d\sigma_T}{dt} = \frac{1}{2}\left(\frac{d\sigma_\parallel}{dt} - \frac{d\sigma_\perp}{dt}\right)$$

then the above, at $\phi = 90^{\circ}$, can be written as a sum of positive terms

$$\frac{d\sigma_V}{dt} = \left(\frac{1+\varepsilon}{2}\right)\frac{d\sigma_\perp}{dt} + \left(\frac{1-\varepsilon}{2}\right)\frac{d\sigma_\parallel}{dt} + \varepsilon\frac{d\sigma_S}{dt} \qquad 1.10$$

Assuming that the previous argument in the photoproduction case holds good and that natural parity exchanges dominate $\frac{d\sigma_\perp}{dt}$ and unnatural parity $\frac{d\sigma_\parallel}{dt}$ (and $\frac{d\sigma_S}{dt}$), then the measurements of Brasse et al represent an upper bound for the natural parity exchanges. Berger et al, however, performed their experiment at $\phi = 0$ and so were able to separate $\frac{d\sigma_T}{dt}$ and $\frac{d\sigma_U}{dt}$ and, neglecting the contribution from

$\frac{d\sigma_s}{dt}$ could then make a direct comparison of the real and virtual photon scattering processes, figure 1.7.

Berger et al continued the measurements to small t and found that the forward dip was present as in photoproduction. By using the data of Brasse, they evaluated the photon beam assymetry parameter and its value, together with that of $\frac{d\sigma_T}{dt}$ clearly show that the electroproduction process is indeed dominated by natural parity exchange. They also found an overall k^2 dependence consistent with a ρ-propagator dominance in VDM.

These features of the data are in accord with what would be expected from a continuation of the $k^2 = 0$ mechanisms into the spacelike region (c.f. the discussion in section 2). It is therefore all the more surprising that the data for $|t| \sim 0.5$ diverges wildly from expectation. What is also surprising is that the washing out of the secondary maximum occurs so quickly, at $k^2 = -0.22$. It is ironic that, as we have seen, the non-shrinkage of the photon should have removed the chance of making pion electroproduction a definitive test of dip mechanisms, and the process itself confounds all expectations by having no dip at all.

Section 5 Theoretical model

The basic problem of neutral pion electroproduction having been outlined, an explanation must be sought. We shall do so following the tradition of regarding photon-induced interactions as being hadronic in nature and shall seek an explanation in terms of t-channel Regge pole and cut exchange. However, not enough data exist in the high energy region to determine the features of a model. To supplement the data, a tool that is both phenomenologically useful and theoretically powerful will be employed - Duality.

In the next chapter, a brief sketch will be given of the theoretical importance of the idea of duality; its principal phenomenological tool, FESR, will then be explained and its application in photoproduction reviewed; a brief final section will point to some difficulties in squaring FESR and Regge absorption models. The first hint that perhaps the photon is not as hadronic as has been assumed will be found here.

In the third chapter the behaviour of the individual resonances in photoproduction will be studied in the context of one phenomenological observation arising from Duality - lines of amplitude zeros at constant values of the energy variables. It will be seen that, quite apart from any difficulties of extending Regge models to the low energy

region, the resonances themselves in photoproduction behave in a manner different to π N scattering. An extension will be presented to the photoproduction model of Collins and Fitton (1974) to account for this behaviour as manifested in the finite energy sum rules.

The evaluation of FESR for electroproduction is presented in Chapter 4 together with a discussion of the behaviour of the resonance form factors as a function of $|K^2|$. The extended model of the previous chapter is then made to accommodate this electroproduction behaviour.

Some conclusions, predictions, and suggestions for future development are presented in the final chapter.

As the formalism of electroproduction is exceedingly complicated and the literature confusing, a copious series of appendices are included which, it is hoped, provides a comprehensive and consistent account of the amplitudes, observables, and formalism used in this field. No claim for originality is made for any of the material presented therein.

Table 1.1: Allowed t-channel exchanges in pion photoproduction

	$I^G = 1^+$	$I^G = 1^-$	$I^G = 0^-$
$\gamma p \to \pi^+ n$	1	$\sqrt{\frac{1}{2}}$	0
$\gamma n \to \pi^- p$	-1	$\sqrt{\frac{1}{2}}$	0
$\gamma p \to \pi^0 p$	$-\sqrt{\frac{1}{2}}$	0	$-\sqrt{\frac{1}{6}}$
$\gamma n \to \pi^0 n$	$\sqrt{\frac{1}{2}}$	0	$-\sqrt{\frac{1}{6}}$
	ρ, B	π, A_2, A_1	ω, ϕ, H, H'

Table 1.2: Value of the slope parameter (c) as a function of k^2 for ϕ electroproduction

k^2 (GeV^2)	c (GeV^{-2})
0	4.01 ± 0.23
-0.23	3.40 ± 0.34
-0.43	3.84 ± 0.46
-0.97	3.14 ± 0.38

(From Dixon et al (1977))

Figure Captions

Fig 1.1 e^+e^- annihilation and the formation of a vector meson from an off-mass-shell photon

Fig 1.2 The one photon approximation for neutral pion electroproduction

Fig 1.3 Photoproduction differential cross-section at P_{lab} = 6, 9, 12, 15 GeV/c. (Anderson et al 1971).

Fig 1.4 The ratio of the cross-sections for photoproduction off protons and neutrons at P_L = 4.7 GeV/c.

Fig 1.5 The polarized photon assymetry at 6 GeV/c.

Fig 1.6 Electroproduction cross-sections $\left(\frac{2}{1+\varepsilon}\right)\frac{2\pi\, d^2\sigma_v}{dt\, d\phi}$ $(\phi=90^\circ)$ as a function of t, for $k^2 = -0.22, -0.55, -0.85$. The interaction was measured for s = 6.5 GeV^2.

Fig 1.7 Comparison of electroproduction $\frac{d\sigma}{dt}$ at $k^2=-0.22$ with photoproduction data. The complete disappearance of the secondary maximum can be clearly seen. (From Berger et al, 1978).

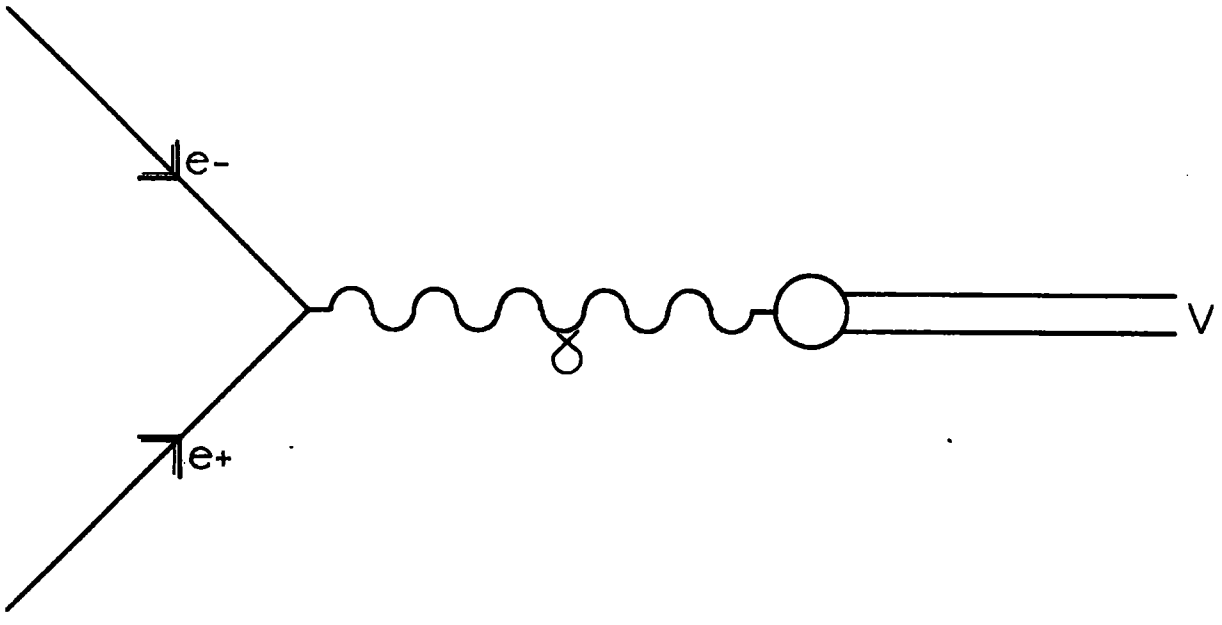

Fig. 1.1

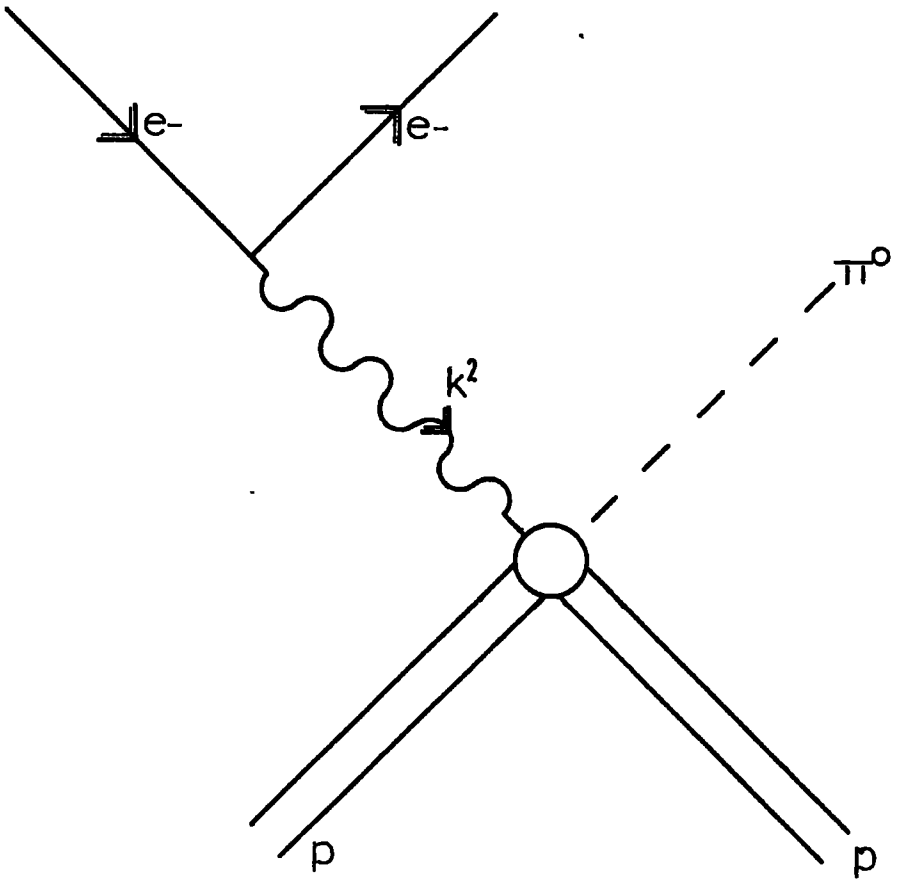

Fig.1.2

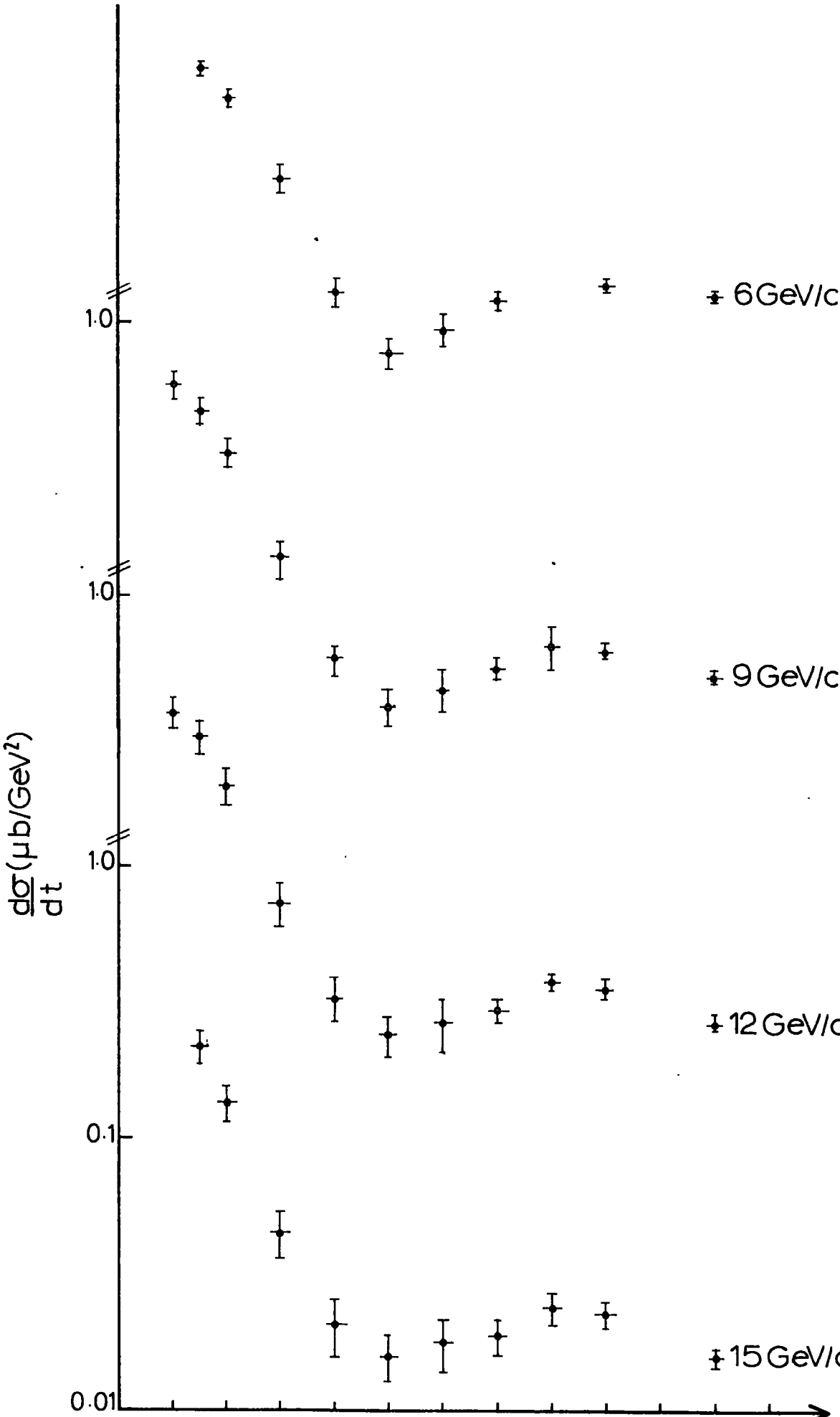
6 GeV/c
9 GeV/c
12 GeV/c
15 GeV/c
1·0
1·0
1·0
0·1
0·01
dσ/dt (μb/GeV²)
0
·2
·4
·6
·8
1·0
1·2
GeV²

Fig.1.3

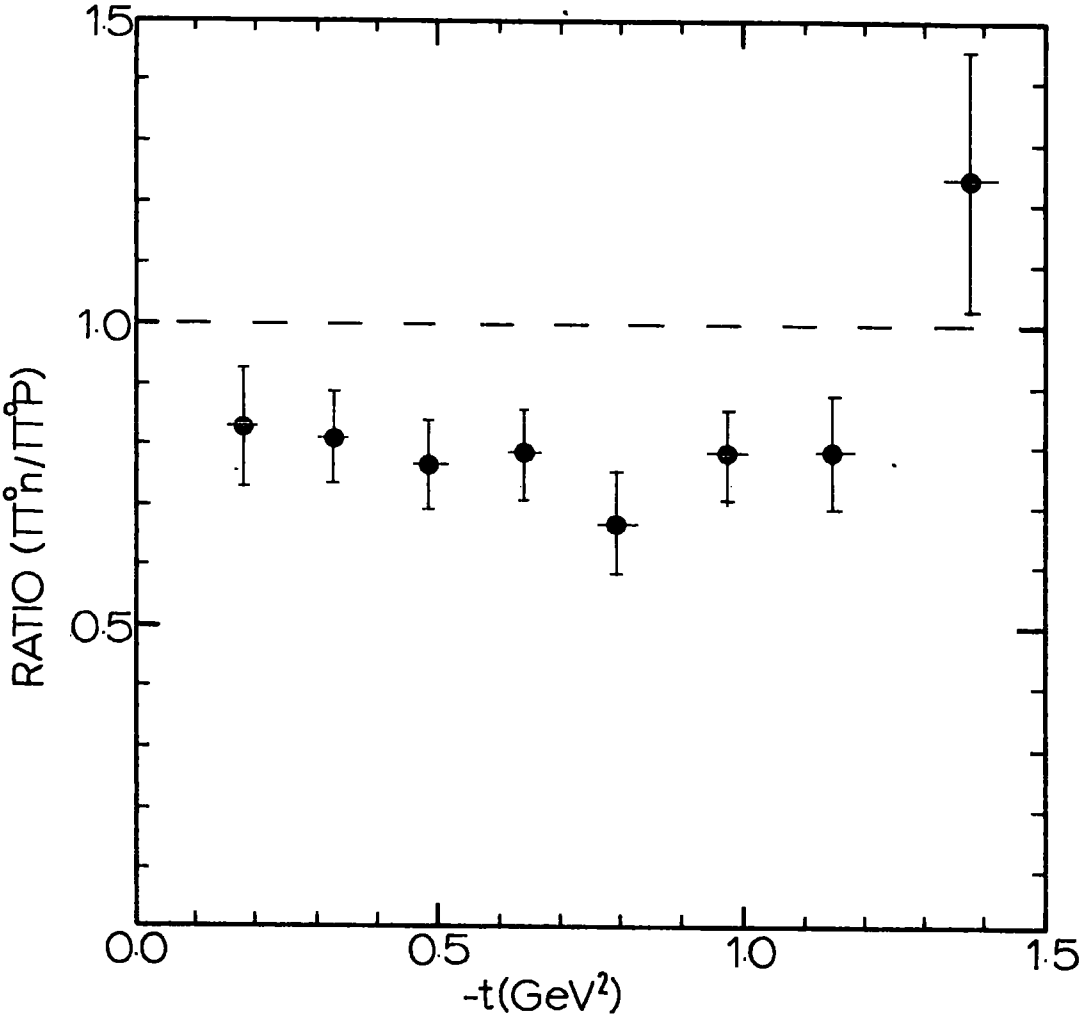

Fig.1.4

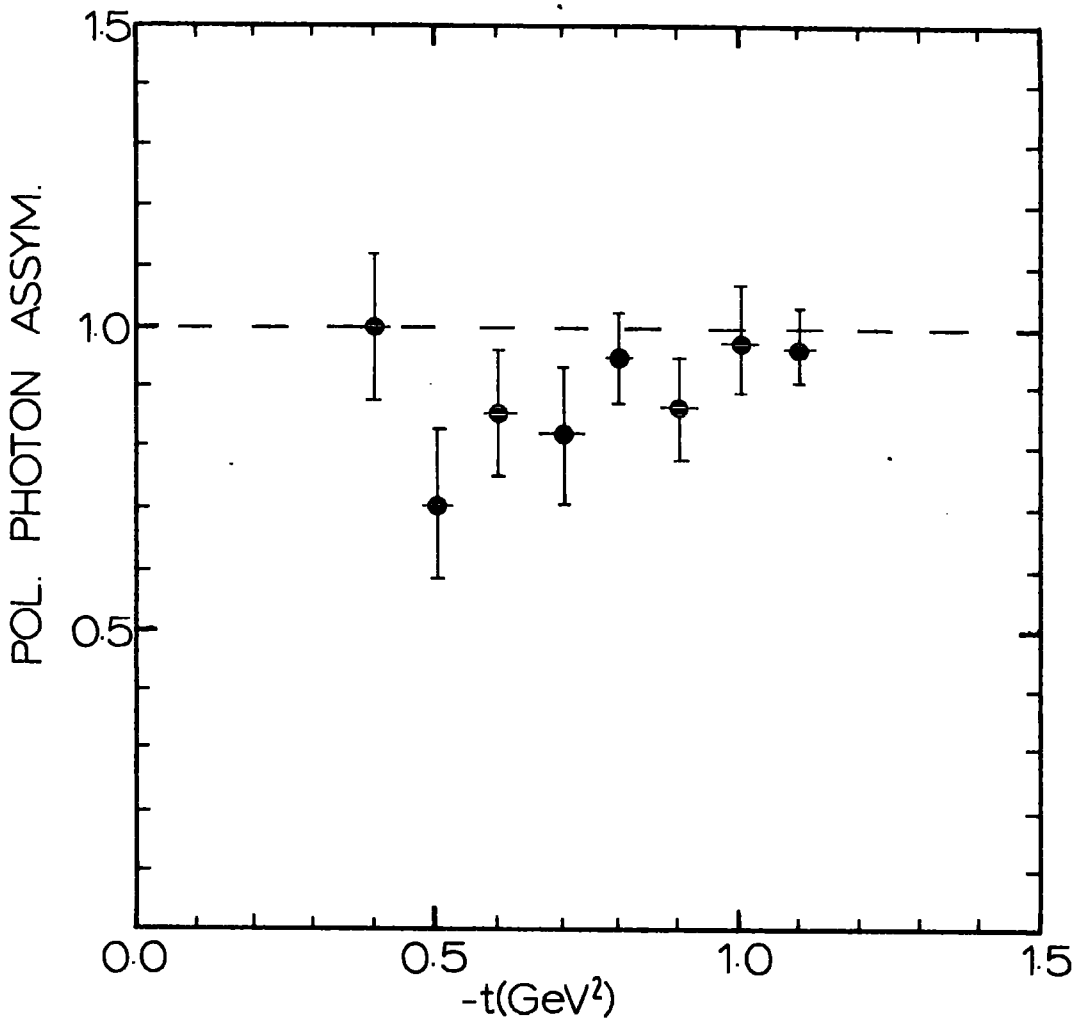

Fig. 1.5

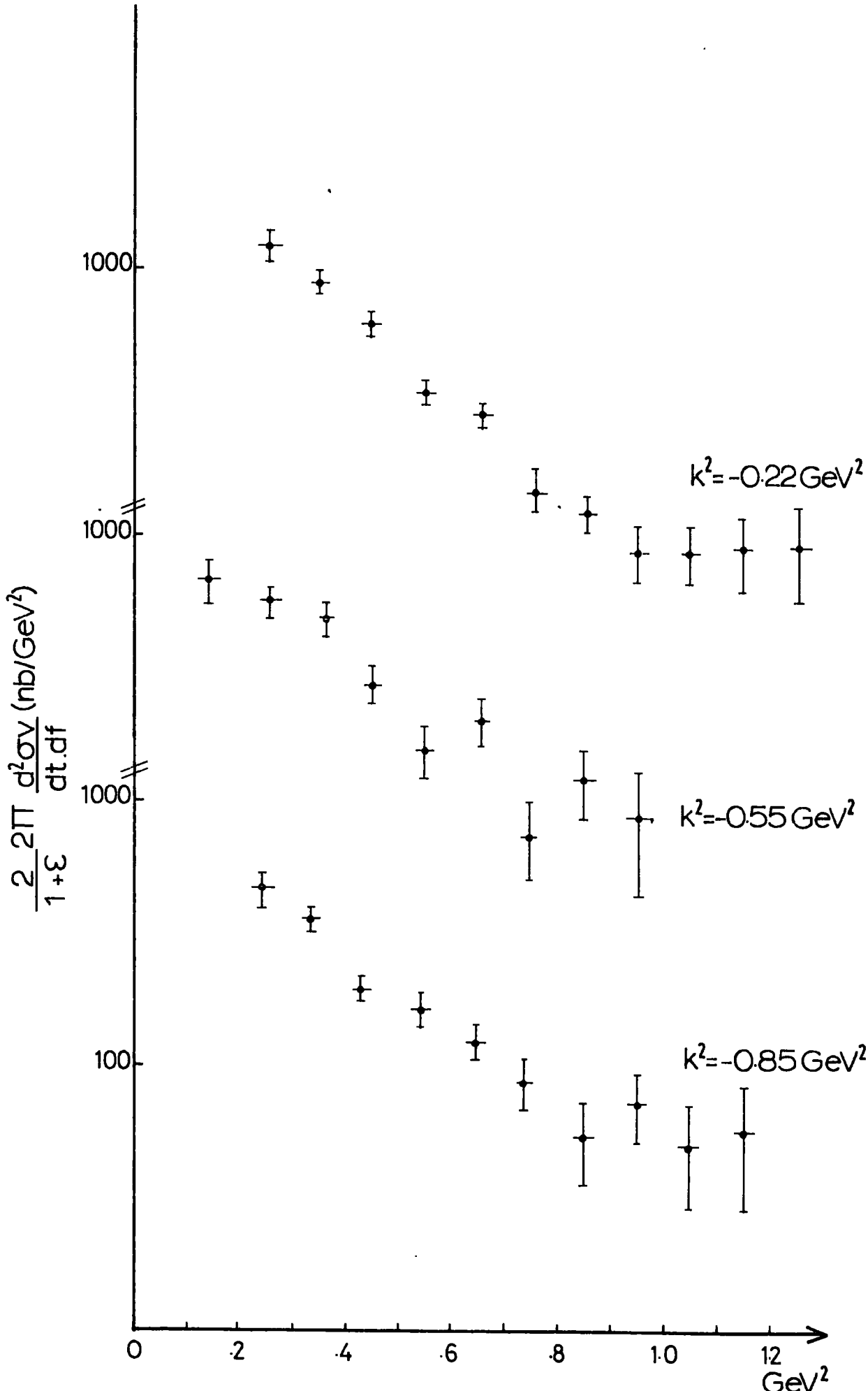
1000
1000
1000
100
k^2=-0.22 GeV^2
k^2=-0.55 GeV^2
k^2=-0.85 GeV^2
$\frac{2}{1+\varepsilon}\frac{2\pi\, d^2\sigma_V}{dt.df}$ (nb/GeV^2)
0
.2
.4
.6
.8
1.0
1.2
GeV^2

Fig.1.6

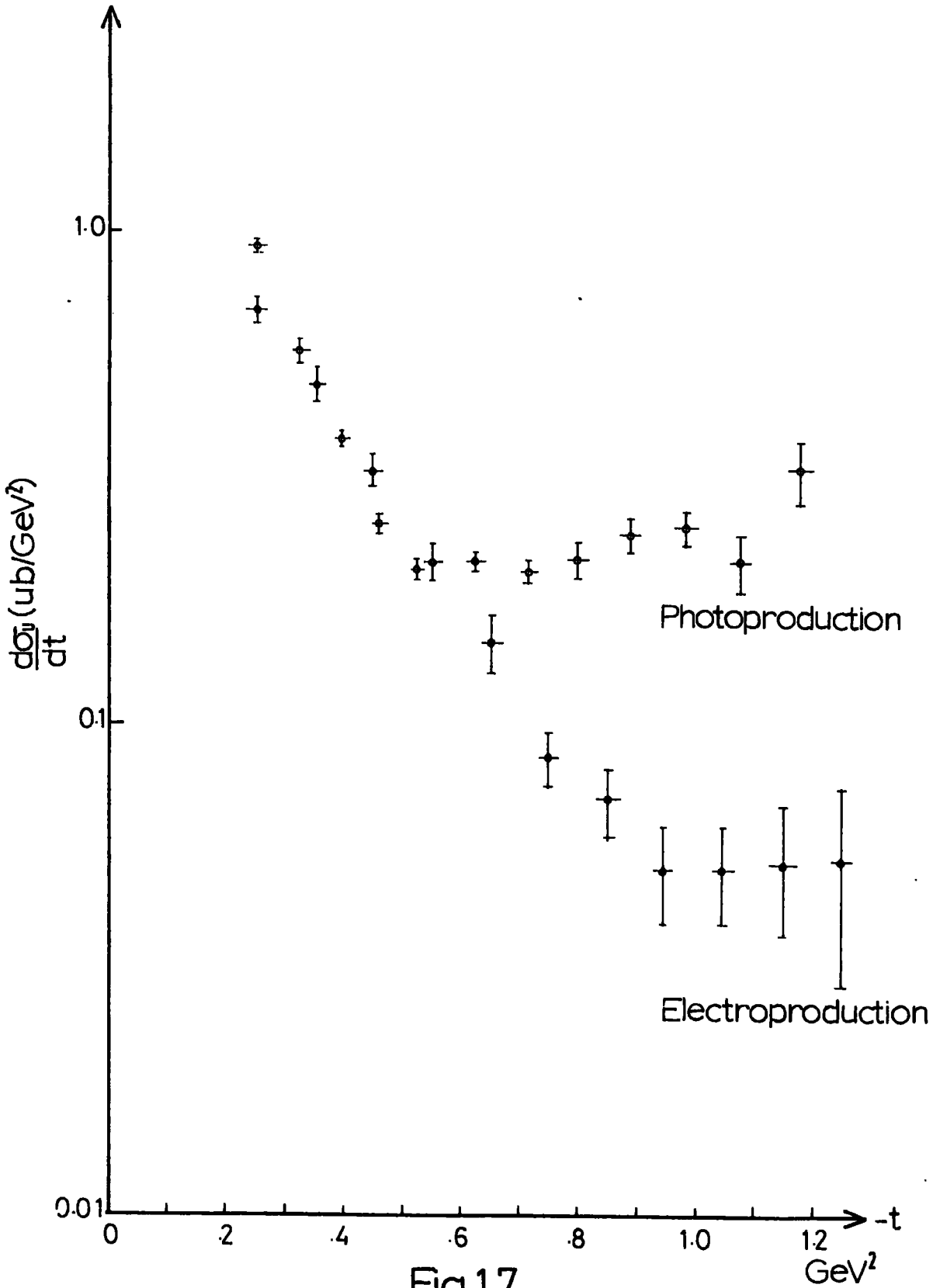
1·0
0·1
0·01
$\frac{d\sigma_{\gamma p}}{dt}$ (ub/GeV^2)
Photoproduction
Electroproduction
0
·2
·4
·6
·8
1·0
1·2
-t
GeV^2

Fig.1.7

Chapter 2 : Duality

Section 1 Theoretical Aspects

The Duality hypothesis was a bold attempt to provide a dynamical postulate completing the theory of the s-matrix. It assumes that all particles are composite and lie on Regge trajectories. These trajectories, however, are presumed to be straight and to rise indefinitely.

The hypothesis was stimulated by the discovery in the 1960s of large numbers of hadrons. Previous attempts at a complete s-matrix theory, such as the Bootstrap model, had predicted a small, finite set of particles and Regge trajectories which eventually turned over and decreased. It was finally shown (Collins et al, 1968) that the measured widths of the Regge recurrences of the ρ were incompatible with the N/D Bootstrap.

A consequence of the indefinitely rising trajectories of the Duality hypothesis is that there are an infinite number of strongly interacting particles. Thus the extraordinary richness of the hadronic spectrum, one of the features which principally distinguishes it from the leptonic spectrum, is used almost as input to the theory.

Of course, some simplifying assumption has to be made before anything can be done with this very general hypothesis;

it happens that the approximation is a physically intuitive one. It is assumed that hadronic scattering proceeds in the resonance approximation. Thus, the s-channel scattering amplitude is built up solely from sums of s-channel resonances. This is well known at low energies where dispersion relation analyses of partial-wave amplitudes have discovered many animals from the hadronic zoo; at higher energies, it is assumed that resonances are so close together that the observed smooth behaviour with increasing energy obtains, and may be represented by crossed-channel (t-channel) Regge poles as an average.

In practice this is not enough: to get any results it is necessary to work in the narrow resonance approximation strictly, the zero-width approximation. This is, of course, a gross violation of unitarity, and therefore of one of the fundamental axioms of s-matrix theory. However, it may be argued that there is sufficient ambiguity, both mathematically and physically, in the location of a resonance in the cut complex plane, for this assumption to be a reasonable starting point. It should be remembered that the conventional, unitary Breit-Wigner formula for a resonance

$$A_{if} = \frac{\Gamma_f \Gamma_i}{s - s_R + i M_R \Gamma_R} \qquad 2.1$$

is a pole on the first sheet, which latter is the

only one since the amplitude has no branch point cut. But it is precisely when one wishes to introduce analyticity i.e. branch points, that the separation of "background" and "resonance" contributions to the amplitude loses clarity. If we demand that scattering proceed only via resonances, then we must be able to distinguish unambiguously the resonance and the background components in the amplitude; the only case for which this is mathematically possible is in the limit of an infinitely narrow resonance. In such a case analyticity is satisfied by poles on the real axis without branch points, and hence with no background.

As a general remark one may assert that appreciation of resonances and their relation to stable particles, holds the key to hadronic physics.

The study of Dual Models, incorporating the above defects and promises, was launched by the publication of the Veneziano Model (Veneziano 1968). This provided a surprisingly simple functional form for a planar dual model.

$$A(s,t) = \frac{\Gamma(1-\alpha_s)\,\Gamma(1-\alpha_t)}{\Gamma(1-\alpha_s-\alpha_t)} \qquad 2.2$$

$$= (1-\alpha_s-\alpha_t)\int_0^1 dx\; x^{-\alpha_s-1}(1-x)^{\alpha_t-1}$$

$$= (1-\alpha_s-\alpha_t)\,B(-\alpha_s,\alpha_t)$$

For a process having resonances in all three channels, the amplitude becomes the sum of appropriate Beta-functions. The third term of such a sum giving rise to Gribov-Pomeranchon poles in the s-channel at nonsense wrong-signature zero points, a role analogous to that of the double spectral function. It was quickly realised that the formulation in terms of beta-functions was susceptible of generalisation from four particle scattering to a generalised Veneziano model of N-point functions. Multiparticle processes are outside our remit however, nor shall we deal, except briefly, with non-planarity of dual models.

The publication of Veneziano's paper revitalised the s-matrix approach to hadronic physics, and a wealth of papers appeared exploring its implications. The theory soon moved from its intuitive physical base to heady mathematical heights (Olive et al, 1974). In recent years there has been some excitement at the similarities between relativistic dual-string models and non-abelian gauge theories. In retrospect this might not be so surprising since both dual-strings and QCD (quantum chromodynamics) are non-perturbative attempts to provide a theory of extended objects. We will not require to go beyond the implications of the 4-point Veneziano function.

It is worth noting that the particle spectrum of the Veneziano model is particularly rich. Not only does the number of levels occupied by particles increase indefinitely

but their degeneracy increases also. The consequence is an exponential growth with mass of the density of levels (Fubini & Veneziano, 1969). This behaviour is characteristic of a system with an infinite number of degrees of freedom and, in fact, the Veneziano multiplicity is similar to that of the statistical model (Chiu et al, 1971). The interest derives from the fact that the number of resonances which couple to k particles of lower mass, grows only polynomially with mass. This fascinating, but seldom explored, area (Gliozzi 1970) has been suggested as a dynamical explanation of the suppression of the two-pion decay mode of the $\rho'(1600)$, by Odorico (1977). The exponential increase in multiplicity of higher mass states also indicates that thresholds infinitely distant in energy still provide a non-zero contribution to the amplitude, evaluated at finite energies. This is a considerable contrast to the bootstrap model.

Section 2 Phenomenology

The preceeding sketch of the theoretical aspects of Duality ignores its historical development. That crossed-channel Regge poles represented an average description of the effects of direct-channel resonances was a concept developed in a paper by Dolen, Horn & Schmid (1967). Prior to this, it had been assumed that at low energies the principal dynamical mechanism was resonance formation to which Regge poles, continued to low energies, provided background; at high energies, the resonance contribution died away and Regge exchange was the only dynamical mechanism. In their critique of this Interference Model (Barger & Cline 1967), Dolen et al showed that it led to inconsistency: sum rules were derived (Gatto, 1967) which would require the sum of positive resonance residues to be zero. A brief rearguard action was fought (Donnachie 1969), showing that a generalized interference model was credible if one allowed each resonance an arbitrary phase, such as occur naturally in nuclear physics; but Duality proved phenomenologically and theoretically too attractive.

It should be noted that our inability rigorously to separate resonance from background still disables a final choice between the two from the experimental evidence alone.

Dolen et al also provided a phenomenological tool of major importance to quantify the "average description" of resonance behaviour in terms of Regge poles: Finite Energy

Sum Rules (FESRs). These were derived from Dispersion Relations, together with the assumption of Regge dominance of the high energy part of the amplitude.

Using the crossing symmetric variable $\nu = \frac{s-u}{2}$ we obtain

$$A(\nu,t) = \frac{1}{\pi}\int_{\nu_T}^{\infty} d\nu' \frac{D_s(\nu',t)}{\nu'-\nu} + \frac{1}{\pi}\int_{\nu_T}^{\infty} d\nu_c \frac{D_u(\nu_c,t)}{\nu_c+\nu} \qquad 2.3$$

$\nu' = \frac{s-u}{2}$ and Ds is the absorbtive part of the s-channel physical amplitude

$\nu_c = \frac{u-s}{2}$ and Du is the absorbtive part of the s-channel physical amplitude

Assuming the amplitude has a Regge asymptotic form

$$A^R(\nu,t) = -\left(-\frac{t}{2\nu_0}\right)^{\frac{m}{2}} \frac{e^{-i\pi\alpha} + \delta}{2\sin\pi\alpha}\, \gamma(t)\left(\frac{\nu}{\nu_0}\right)^{\alpha(t)-1} \qquad 2.4$$

$$\nu \to \infty \Rightarrow \mathrm{Im}\, A^R \to \left(-\frac{t}{\nu_0}\right)^{\frac{m}{2}} \frac{\gamma}{2}\left(\frac{\nu}{\nu_0}\right)^{\alpha-1}$$

$$\nu \to -\infty \quad (\nu_c \to \infty) \Rightarrow \mathrm{Im}\, A^R \to \left(-\frac{t}{\nu_0}\right)^{\frac{m}{2}} \delta\frac{\gamma}{2}\left(\frac{\nu}{\nu_0}\right)^{\alpha-1}$$

$$\Rightarrow A(\nu,t) - A^R(\nu,t) = BT + \frac{1}{\pi}\int_{\nu_T}^{\infty} d\nu' \frac{D_s(\nu',t) - \mathrm{Im}\, A^R(\nu')}{\nu'-\nu}$$

$$+ \frac{1}{\pi}\int_{-\infty}^{-\nu_T} d\nu' \frac{-\mathrm{Im}\, A(\nu'-i\varepsilon) - \mathrm{Im}\, A^R(\nu')}{\nu'-\nu}$$

$$= \frac{R^s}{\nu_B-\nu} + \frac{R^u}{\nu_B+\nu} + \frac{1}{\pi}\int_{\nu_T}^{\infty} d\nu' \frac{D_s(\nu',t) - \frac{\gamma}{2}\left(\frac{\nu'}{\nu_0}\right)^{\alpha-1}}{\nu'-\nu} + \frac{1}{\pi}\int_{\nu_T}^{\infty} d\nu_c \frac{D_u(\nu_c,t) + \delta\frac{\gamma}{2}\left(\frac{\nu_c}{\nu_0}\right)^{\alpha-1}}{\nu_c+\nu}$$

If we have included all Regge poles such that $A(\nu,t) - A^R(\nu,t) \sim \frac{1}{\nu^k} \quad k > 1$, then the LHS of the equation vanishes faster than the right hand side. Performing a binomial expansion of the RHS in terms of $\frac{1}{\nu^n}$ then the coefficient of $\frac{1}{\nu}$ must vanish.

$$A(\nu,t) - A^R(\nu,t) = -\frac{1}{\nu}\left\{R^s\left(1-\frac{\nu_B}{\nu}\right)^{-1} - R^u\left(1+\frac{\nu_B}{\nu}\right)^{-1}\right.$$

$$+\frac{1}{\pi}\int_{\nu_T}^{\infty} d\nu'\left(D_s(\nu';t) - \frac{\gamma}{2}\left(\frac{\nu'}{\nu_0}\right)^{\alpha-1}\right)\left(1-\frac{\nu'}{\nu}\right)^{-1}$$

$$\left.-\frac{1}{\pi}\int_{\nu_T}^{\infty} d\nu_c\left(D_u(\nu_c,t) + \frac{\gamma}{2}\delta\left(\frac{\nu_c}{\nu_0}\right)^{\alpha-1}\right)\left(1+\frac{\nu_c}{\nu}\right)^{-1}\right\}$$

Hence

$$R^s - R^u + \frac{1}{\pi}\int_{\nu_T}^{N} d\nu'\left(D_s(\nu';t) - \frac{\gamma}{2}\left(\frac{\nu'}{\nu_0}\right)^{\alpha-1}\right)$$

$$-\frac{1}{\pi}\int_{\nu_T}^{N} d\nu_c\left(D_u(\nu_c,t) + \frac{\gamma}{2}\delta\left(\frac{\nu_c}{\nu_0}\right)^{\alpha-1}\right) = 0$$

Where, by assumption of Regge saturation of the high energy part, we need not integrate to infinity, but only to a cutoff energy N.

$$\pi\left(R^s - R^u\right) + \int_{\nu_T}^{N} d\nu'\left(D_s(\nu';t) - D_u(\nu';t)\right)$$

$$= \frac{1+\delta}{\alpha}\,\frac{\gamma}{2}\left\{\left(\frac{N}{\nu_0}\right)^{\alpha} - \left(\frac{\nu_T}{\nu_0}\right)^{\alpha}\right\}$$

Only those poles for which $\delta = +1$ contribute to the RHS. If the amplitudes have definite crossing properties: $R^u = \eta R^s$ $D_u = \eta D_s$ then $\eta = 1$, crossing even amplitudes are evaluated using higher moment sum rules.

The lowest moment ($\eta = -1$) sum rule becomes

$$\pi R^s + \int_{\nu_T}^{N} D_s(\nu';t)\, d\nu' = \frac{\gamma}{2\alpha}\left\{\left(\frac{N}{\nu_0}\right)^{\alpha} - \left(\frac{\nu_T}{\nu_0}\right)^{\alpha}\right\} \qquad 2.5$$

Higher moment sum rules are

$$\pi \nu_B^n \left(R^s + (-1)^{n+1} R^u\right) + \int_{\nu_T}^{N} \nu'^n \left\{D_s(\nu';t) + (-1)^{n+1} D_u(\nu';t)\right\} d\nu'$$

$$= \sum_{\substack{\text{Rosse}\\ \text{ptles}}} \left(1 + (-1)^n \beta\right) \frac{\gamma}{2} \frac{1}{\alpha+n} \left\{\left(\frac{N}{\nu_0}\right)^{\alpha+n} - \left(\frac{\nu_T}{\nu_0}\right)^{\alpha+n}\right\} \qquad 2.6$$

Functions which are crossing odd/even contribute only to even/odd values of n.

The zeroth (n=0) moment sum rule was obtained by requiring the first term in the expansion of powers of $\frac{1}{\nu}$ to vanish, the nth moment sum rule comes from setting the (n+1) th term in the expansion equal to zero.

Section 3 Applications

A complete review of the use of sum rules in hadronic physics will be found in Ferro Fontan et al (1972). Their review includes an extensive treatment of FESRs, their extension Continuous Moment Sum Rules, and the related superconvergence relations.

Dolen Horn and Schmid used FESRs to examine the properties of Reggeized t-channel ρ-exchange in πN charge exchange scattering. They obtained from the low energy data an effective one-pole trajectory function $\alpha_{eff}(t)$ close to that of the ρ as determined from fits to high energy, cross-sections. They also evaluated a secondary trajectory (using high energy values for the itself) but obtained a rather high $\alpha : 0.3 + 0.8t$. This value probably reflects the inaccuracies consequent upon evaluating higher moment sum rules. Resonance parameters, as obtained from partial wave analyses, have a not inconsiderable uncertainty associated with them; evaluating higher moment sum rules weights the integral towards the upper limit of integration and it is precisely the higher mass resonances contributing there whose parameters are most uncertain.

As noted in Chapter 1, the differential cross-section for a given process is characterized by a given pattern of peaks and dips. Dolen et al succeeded in identifying such

features of the high energy cross-section as consequences of the low energy resonance behaviour. Thus the near-forward peak in π N charge exchange was identified with the fact that the spin-flip amplitude is an order of magnitude larger than the non-flip near t = 0 in the resonance region. Similarly the dip at t = -0.5 GeV^2 was identified with a zero in the spinflip amplitude at low energies. It should be noted that these are model independent features, they occur because the resonances, at t = 0, enter the spin flip amplitude with the same sign but with alternating sign to the non flip; that all prominent resonances have their first zero in the flip amplitude simultaneously within the range $-0.6 < t < -0.4$. GeV^2, excepting the nucleon and P_{33} which cancel each other.

The great success of this technique and its apparent predictive power, soon led to applications to other processes. The kinematically similar KN process has been investigated (Elvekjaer & Martin 1974), as has $\pi^- p \rightarrow \eta^0 n$ (Harnard 1972). In photoproduction, one of the first applications of the technique and its extension, Continuous Moment Sum Rules, was a rather unhappy one: an attempt to identify the mechanism of the forward spike in charged pion photoproduction. The conservation of angular momentum imposes certain constraints on the complete scattering amplitude at t = 0, but Regge exchange amplitudes have a definite parity - that of the exchanged Reggeized particle. Exchange of the unnatural parity pion cannot by itself satisfy the constraints on the amplitude at t = 0; a popular solution

(Leader 1968, Capella et al 1969) was to suggest the existence of a Reggeon of opposite parity which would conspire to meet the constraint. A model of the forward spike in charged pion photoproduction, using such a conspiracy mechanism, was put forward by Ball et al (1968). As a result of a CMSR analysis, Bietti et al and Di Vecchia et al (1968 a, b) claimed positive evidence for the existence of the pion conspirator, and they enumerated its properties. No such scalar particle has been seen and it has been shown by Le Bellac (1969) that such conspiracy is incompatible with other π-exchange processes.

In a masterly couple of papers, Jackson & Quigg (1969, 1970) showed that a model containing "evasive" Regge poles could fit both the high energy data and the CMSRs: the forward spike was attributed to an associated pion cut. The cut is of mixed parity and so can conspire with itself to satisfy the angular momentum constraint. Jackson and Quigg gave a more sophisticated analysis of the properties of the relevant FESRs and they showed, by developing a "pseudomodel", that it is possible to relate directly the FESRs and the high energy, data without a definite commitment to a specific dynamical model. Thus, echoing the result of Dolen et al, that the high energy properties of a process can be deduced in a model-independent manner from the FESRs, Jackson and Quigg concluded that there was no evidence in favour of a pion conspirator in charged pion photoproduction.

FESRs assume that the high energy part of a scattering amplitude is superconvergent once the leading Regge contributions have been removed. Given this assumption, model independent information may be obtained from the low energy region about the high energy behaviour. However, consistency with FESRs may be used as a test of particular high energy models. Thus the remark of Dolen et al becomes important, "if a secondary pole or a cut is unimportant in a high energy fit above the integral cut-off, then this singularity is unimportant to exactly the same extent in the low energy sum rules".

Worden (1972) produced an exhaustive comparison of all the then available models for pion and eta photo-production. He pointed out that pion photoproduction provides a highly constrained test of Regge models. The residues of the dominant exchanges can be estimated approximately using factorization, exchange degeneracy, vector meson dominance, SU(3) and the naive quark model. The high energy data are accurately measured, cross-sections are available for all four charge states, and polarized photon and polarized target asymmetries have been measured. Finally, the low energy data are sufficiently precise to allow partial wave analysis and FESR evaluation. Worden concluded in favour of a Regge absorption model with nonsense wrong signature zeroes (NWZ) as being in best agreement with the triangular consistency conditions

outlined. It is of interest to note that he dismissed the SCRAM model (Strong Cut Reggeized Absorption Model - Kane et al, 1970) mainly because "the sum rules are strong evidence against it ".

Since then, a number of different fits to high energy pion photoproduction have appeared which have made use of FESR constraints on the parametrization. One of the most interesting (Barker et al 1974) used the constraints not only of FESR, but also simultaneously of fixed-t dispersion relations (FTDR) from which FESRs (with the assumption of Regge dominance) are derived.

Guided by general Regge-style ideas rather than a specific model Barker et al obtain a parametrization of the data involving a large number of parameters which are then interpreted in the language of Regge poles and cuts. This interpretation was more fully carried out in a later paper (Barker and Storrow 1977). The main conclusions of the first paper concerned the zero structure of the imaginary part of the non-flip amplitude: Barker et al found no zero at $t \sim -0.2$. In the context of the Dual Absorptive Model (which does not require explicit pole/cut separations) and most Reggeized Absorption Models (Collins & Fitton 1974), such a zero in the non-flip amplitude is to be expected. Barker et al also find evidence for NWZs in the contributions to the single flip amplitudes identified as being pole-like.

There is, however, a slight puzzle as to why the position of the zero of the same pole in two contributions to the single flip amplitudes should vary slightly in t : one occurs at $-0.4 < t < -0.5$ and the other at $-0.5 < t < -0.6$. Since our interest here is only in the application of FESRs as a constraint to Regge models, we will discuss specific features of this model later.

Section 4 Regge Models and Duality

At the time duality and FESRs were proposed, there was considerable doubt as to the importance of the Regge cut contribution in describing high energy scattering data. But the presence of diffractive phenomena, such as the cross-over effect in $\pi^{\pm}p$, $K^{\pm}p$, $p^{*}p$ scattering, required the introduction of a t-channel mechanism which could accommodate this. The mechanism of absorptive cuts to provide peripheral t-dependent amplitudes was adopted.

In the resonance region, prominent resonances also occur in the peripheral partial waves and so the introduction of cuts provides a qualitative correspondence between the crossed and direct channels, reflected in the continuation of the fixed-t structure from high to low energies. However, a rather startling result has been obtained by Worden (1973) who showed, in the context of π N scattering, that <u>all</u> current Regge absorption models do not obey duality in the form of FESR constraints and that no simple satisfactory modification can be made.

The basic problem is that the models, at high energy, are required to have strong absorption of the imaginary parts of the amplitudes in order to reproduce the peripheral behaviour of the resonances contributing to the low energy region; the real parts of the high energy

amplitudes however do not possess a peripheral structure and therefore are only weakly absorbed. To achieve this, most absorption models have one component which contributes with opposite sign to the real and imaginary parts of the amplitudes and which is low-lying in the j-plane $0 > j > -1$. As these Regge amplitudes are continued to low energies, the low-lying cut component increases relative to the pole contribution until it completely swamps the pole and there is too much absorption. This over-absorption, linked with the shrinkage of the Regge pole contribution to the peripheral partial waves, removes any simple peripheral impact parameter structure.

One way out of the impasse is provided by the Dual Absorptive Model, which explicitly prescribes a peripheral structure to the imaginary part of the high energy amplitude but makes no statement regarding the real part. This model is claimed by Harari (1971) to provide at least qualitative understanding of the dip structure of many processes. However, the elucidation of the j-plane structure of the DAM is not clear and could be extremely complicated as no attempt is made to distinguish cut from pole.

It has, however, been suggested (Bronzan & Jones 1967) that a finite branch-point discontinuity, which arises when cuts are calculated in the eikonal approximation and which gives rise to the differing energy dependence of pole

and cut noted above, in fact may be theoretically unsatisfactory, since it violates t-channel unitarity. One alternative which has been explored (Cardy & White 1974) suggests that the cut discontinuity vanishes at the branch point and that the coupling of Regge cuts to external particles proceeds through the pole. This pole enhancement of the cut would yield a similar energy dependence for both components of the π^- N amplitudes and so would continue the peripheral structure of the high energy amplitudes down to low energies without over-absorption, or the components getting out of step. This would essentially provide the "shrinking cut" model required by Worden (1973) and which seems to be indicated by an analysis of the large $|t|$ effective trajectories in π^-N , KN scattering (Collins and Fitton 1975).

It should be noted that although this "pole enhanced" or "shrinking cut" model was successfully applied by Collins and Fitton to π^- N charge exchange scattering, they could not get a fit to neutral pion photoproduction using it. It is significant, phenomenologically, that this process does not exhibit large -t shrinkage, and interesting that, theoretically, the process is not constrained by t-channel unitarity since, as mentioned in chapter 1, we work only to first order in the electromagnetic coupling. This transition from soft to hard cuts is illuminated by the results of Irving (1975). He compared the magnitudes of the poles and cuts contributing

to $\pi N \to \rho N$, $\gamma p \to \pi^+ n$, and $\gamma_v p \to \pi^+ n$ and found that the magnitude of the cut contribution increased as the variable external mass became more space-like. He suggested that this was connected with the transition from structured hadrons, whose coherent scattering is represented by Regge-pole like behaviour, to point-like hadrons in the scaling region of electroproduction.

If the option of a "shrinking cut" model of absorption is not tenable, as the above Collins and Fitton argument indicates is the case for photoproduction, then we are left with Worden's alternative of altering the very low-lying j-plane structure in order to accommodate the discrepancies between the high and low energy regions. In this regard it is interesting to note that Barker and Storrow, who are not constrained by any of these Regge model problems, find an important role, nonetheless, for low-lying contributions.

Chapter 3 : Photoproduction

Section 1 Photoproduction FESR

In the previous chapter we surveyed the theoretical motivation for, and some phenomenological applications of, duality. We saw that the constraints of FESR were early applied to relate high energy features of scattering data to low energy behaviour. We have seen, also, that in a departure from this original programme FESR have been used to discriminate between specific models of high energy processes. That such a departure might not be justified follows from one analysis which found that all Regge models of $\pi^- N$ scattering require modification to accommodate the features of FESR.

In this chapter the FESR for neutral pion photoproduction will be presented, and the integral over the resonance region will be compared to that of a specific model of the high energy region. It will be shown that, for this process, the discrepancy between left- and right-hand sides of the FESR equation do not stem solely from deficiencies in the high energy model. Rather, we will see that the dip at $t = -0.5$ which characterises high energy $\frac{d\sigma}{dt}$ data cannot easily be related to the behaviour of the data in the low energy region. To establish this conclusion, we shall examine the behaviour of individual resonances and see that their behaviour contradicts the expectation even of a naive

Veneziano-type model. We shall see that in other, related processes such naive behaviour is found.

We will find that, in photoproduction, duality is satisfied (even semi-locally) but for the contribution of the Born term and the P_{33} resonance. To cope with this unexpected behaviour of these low energy contributions within the framework of the chosen high energy model, we must extend the model by adding a term, low-lying in the j-plane, specifically to be dual to these terms. This daughter-like addition to the high energy model is in the manner of the modifications suggested by Worden (1973) for reconciling Regge models with FESR.

Section 1a The resonance integral

As may be seen from eq 2.3, FESR are derived from dispersion relations. The amplitudes appearing in dispersion relations, and hence in the FESR integrals, are considered to have only dynamical singularities in the ν-plane. However, we shall be discussing a Regge model which is parametrized to yield Regge-type behaviour in s-channel helicity amplitudes and it is these amplitudes which will appear on the right hand side of the FESR equation. Such amplitudes have a simple singularity at t=0 arising from the half angle, or angular momentum conservation factors. These are the factors $\left(-\frac{t}{s_0}\right)^{\frac{m}{2}}$ appearing in A^R (eq 2.4). It should be noted that they are simply dropped to obtain a kinematic singularity free (KSF) amplitude, before the FESR is derived in eq 2.5. s-channel helicity amplitudes are used as we shall be going on to discuss a Regge absorption model, and this is most easily described as an s-channel phenomenon.

At low energies the s-channel helicity amplitudes are linear combinations of multipole moments, each multipole being an eigenamplitude of parity and angular momentum. The multipoles contain kinematic singularities such as square root branch points in s at threshold and pseudo-threshold, as well as the half-angle singularities in t. The singularities in s cannot be removed as simply as the half-angle factors. However, there is an invariant amplitude decomposition of neutral pion photoproduction

where all the kinematic singularities in s and t are siphoned off into spinor terms leaving the amplitudes with dynamic singularities only. (In fact, for photoproduction there are several such decompositions). Further, one can form linear combinations of the invariant amplitudes which are still KSF and which, at high energies away from the energy region of the singularities, approximate the s-channel helicity amplitudes.

In our case, the choice of invariant amplitude is determined by one further condition. We are going to examine electroproduction and so the amplitudes should be capable of extension into $k^2 \neq 0$ regions without kinematic singularity in k^2. This last dictates the use of Ball's (1961) invariant amplitudes Bi (s, t, k^2) i = 1, ... 8. Appendix C and D contain a full account of the definitions of the Ball amplitudes. The inter-relationship of these three sets of amplitudes - the multipoles and helicity amplitudes in which physical quantities are easily described, and the Ball amplitudes - is set out in appendix C, and only a few points will be noted here.

Kinematically, one requires 16 independent amplitudes to describe a reaction with the spin structure $1 + \frac{1}{2} \longrightarrow 0 + \frac{1}{2}$. Because parity is conserved in electromagnetic interactions this number is reduced to eight. The fact that the photon current is conserved further reduces the independent amplitudes to six. For photoproduction the masslessness of the photon introduces the further con-

straint of gauge invariance which results in only four independent amplitudes. Note that gauge invariance arises only when the photon is massless and it is therefore inappropriate to use a set of amplitudes constrained by this, when an extension to electroproduction is contemplated.

For helicity amplitudes we use the notation $f_{\mu_2\mu_1\lambda}$ where $\mu_2(\mu_1)$ denote the final (initial) nucleon helicity, and λ is the photon's helicity ($\lambda = 1$ for photoproduction). The four independent amplitudes are therefore

f++1, f--1	s-channel single helicity flip
f-+1	s-channel zero helicity flip
f+-1	s-channel double helicity flip

The relationship between these amplitudes and the KSF Ball amplitudes at high energies is (Appx D).

$$
\begin{aligned}
f_{++1} + f_{--1} &\cong -\frac{1}{\sqrt{2}}\sqrt{-t}\,\nu B_6 \\
f_{-+1} &\cong -\sqrt{2}\,\nu(B_1 - m B_6) - t\sqrt{2}\,B_3 \\
f_{+-1} &\cong -t\sqrt{2}\,B_3
\end{aligned}
\qquad 3.1
$$

where $\nu = \frac{s-u}{2}$

The terms discarded in making approximation 3.1 are lower order terms in ν , and even at a $p_L \sim 5$ GeV/c they represent factors smaller than 10%. The approximations hold good also for $k^2 \neq 0$. The combination of single flip amplitudes isolates the natural parity contribution. The unnatural parity combination is expected to be superconvergent since there are no Regge poles with the quantum numbers of the t-channel in this combination. (This conventional wisdom has been disputed by Barker et al (1974).

It may be seen from appendix E that, for $\gamma p \to \pi^0 p$, the amplitudes B_1 and B_6 are crossing even, and the amplitude B_3 is odd under $s \leftrightarrow u$ crossing. We must use odd-moment sum rules for B_1 & B_6 and even moment rules for B_3, if we are to evaluate right-moment FESR. For these right moment FESR we can thus add the s and u-channel discontinuities of eq. 2.6 to yield:

$$-\frac{\pi \nu_B R_6}{\sqrt{2}\, N} - \frac{1}{\sqrt{2}\, N}\int_{\nu_T}^{N} \nu\, B_6(\nu,t)\, d\nu = \frac{1}{N}\int_{\nu_T}^{N} \frac{d\nu}{\sqrt{-t}} \left(f_{++1}(\nu) + f_{--1}(\nu)\right)$$

$$-\sqrt{2}\,\frac{\pi \nu_B}{N}\left(R_1 - m R_6\right) - \frac{\pi\sqrt{2}\, t\, R_3}{N} - \frac{\sqrt{2}}{N}\int_{\nu_T}^{N} \nu\left(B_1(\nu,t) - m\, B_6(\nu,t)\right) d\nu$$

$$- \frac{t\sqrt{2}}{N}\int_{\nu_T}^{N} B_3(\nu,t)\, d\nu = \frac{1}{N}\int_{\nu_T}^{N} d\nu\, f_{-+1}(\nu,t) \qquad 3.2$$

$$\frac{\pi\sqrt{2}\, R_3}{N} + \frac{\sqrt{2}}{N}\int_{\nu_T}^{N} B_3(\nu,t)\, d\nu = \frac{1}{-t\,N}\int_{\nu_T}^{N} d\nu\, f_{+-1}(\nu,t)$$

The Born term residues are listed in Table 3.1. The angular decomposition of the invariant amplitudes may be obtained in terms of multipole moments, the eigenamplitudes of parity and angular momentum, by substituting equations C10 in eq. C12. The multipole moments were defined by Chew et al (1957) and are now used mainly for historical reasons: as can be seen from eq C12 the relation between multipoles and invariant amplitudes is a complicated one.

The main dynamical input (as opposed to formal requirements) is to characterise the energy behaviour of the resonances. As we shall later make extensive use of the Devenish and Lyth (1975) analysis of electroproduction, we follow their Breit Wigner parametrization. For each multipole amplitude $M_{l\pm}$

$$M_L(s) = \frac{W_R \Gamma \left(\frac{q_R}{q}\right)^{l+1}}{s_R - s - i W_R \Gamma} M_R$$

$$\Gamma = \Gamma_R \left(q/q_R\right)^{2L+1} \left(\frac{q_R^2 + X^2}{q^2 + X^2}\right)^L \qquad 3.3$$

$$X = 0.35$$

Γ_R is resonance width, W_R resonance mass, q is π N com mentum, and M_R is the multipole coupling. However, Devenish and Lyth adopt a rather more complicated parametrization for the P_{33} (1232) magnetic multipole:-

$$M_{1+}(s) = \frac{kq}{k_R q_R} \frac{c q_R^3}{(q_R^2 - q^2)(1 + q^2 a^2) - i c q^3} M_{P_{33}} \qquad 3.4$$

where $a^2 = 21.4$, $c = 4.27$, $q_R = 0.2254$. The relation between the magnetic and electric multipoles is given by

$$E_{1+}(s) = (1.19 x - 0.25)\, e^{-3x}\, M_{1+}(s)$$

$$x = \frac{s - m^2}{2m} - 0.15 \qquad 3.5$$

The structure of $\gamma p \to \pi^0 p$ scattering in the resonance region has been frequently studied, and there are several multipole analyses available (Moorhourse et al 1974, Metcalf and Walker 1974, Devenish et al 1974). Only the last of these has been extended to electroproduction and so we use the multipole moments, determined by that analysis: they are listed in table 3.2. However the resonance parameters in neutral pion photoproduction cannot be uniquely determined, each of the above three analyses reflects the preferences of its authors. Regardless of the powerful tools employed, such as dispersion relations, some model-dependence inevitably creeps in. It is advisable, then, to check that conclusions derived from FESRs using these parameters are not affected by changing the parameter set. Therefore, in addition to the FESR evaluation discussed here, the calculation was performed using the other data sets. The results were not inconsistent with the evaluation using Devenish et al's parameters. Any numerical differences were within a 10% band.

This procedure of taking multipole parameters from different analyses of the experimental data probably provides the most realistic estimate of the overall errors in the calculation. As explained above, the absolute errors in the FESR calculation reflect not only experimental uncertainties in the parameters but also a systematic bias from the underlying analysis. For that reason, rather than attach errors to any one set of multiple parameters and check how they are propagated through the calculation, we have chosen to regard the FESR error band as being determined by the spread of the three analyses. We used a maximum value of W = 2.07 GeV/c as the integral cut-off.

A computer program was written to evaluate the integrals of equations 3.2: the numerical method adopted was the trapezoidal rule. The results, evaluated at -t values of 0, 0.3, 0.5, 0.7, 0.9, are displayed on graph 3.1. Higher moment sum rules were evaluated with a view to calculating an effect $\alpha(t)$ for photoproduction purely from the resonance data. However, since the next right moment sum rule for the single and non-flip amplitudes involves ν^3 terms in the integral, the process is weighted unacceptably to the higher mass resonances. But the fourth resonance region is quite badly understood, so the results of the evaluation are essentially meaningless.

Section 1b : Evaluating the Regge integral

Graph 3.1 contains also the results of the integration over the Regge amplitudes continued down into the resonance region. We use the SCRAM model of Collins and Fitton (1974), hereafter referred to as the CF model. This represents an extension to photoproduction of a model developed to describe πN charge exchange scattering (Collins and Swetman 1972).

A complete analysis (R.L. Kelly 1972) of the πN scattering amplitudes had provided a determination of the amplitude phases which contradicted the phases of then extant Regge cut models. (Incidentally the analysis confirmed an earlier prediction of πN amplitude phases, resulting from FESR calculations). To solve this problem Collins and Swetman modified the phase of the $I_t = 0$ amplitude by including $\rho\otimes(P+P')$ strong cuts, calculated using the eikonal/absorptive model.

To fit photoproduction, Collins and Fitton used the t-channel isoscalar part of Berger and Phillips' (1969) five-pole fit to πN as the absorbing amplitude. That this amplitude is applicable to photoproduction follows from the work of Chadwick et al (1973) who showed that the couplings of P and P' to ρp and γp (scaled by vector dominance) were almost identical to those for πN. The only Regge poles needed in this analysis were the ρ and ω. With this comparatively

economical parametrization, which nonetheless has a satisfactory physical interpretation, the differential cross-section, the neutron/proton ratio, polarized target assymetry, and the polarized photon assymetry were all fitted for pion photoproduction. However, SU (3) provides a very strong constraint on such $\gamma p \to \pi^0 p$ amplitudes: a linear combination of the Regge exchange amplitudes for neutral pion photoproduction must also fit $\gamma p \to \eta p$. One of the most convincing tests of the Collins and Fitton model is that it fits $\gamma p \to \pi^0 p$ and $\gamma p \to \eta p$ simultaneously.

Following CF we define the photoproduction differential cross-section to be (Equ. B6).

$$\frac{d\sigma}{dt} = \frac{1}{32\pi(s-m^2)^2}\; 0{\cdot}3893 \sum_{\mu_2\mu_1} |f_{\mu_2\mu_1}|^2 \qquad (mb/GeV^2) \qquad 3.6$$

where the factor of 0.3983 is explicitly extracted to afford dimensionless amplitudes. In particular

$$\frac{d\sigma}{dt}(\gamma p \to \pi^0 p) \sim \Sigma |f^\omega + f^\rho|^2$$

$$\frac{d\sigma}{dt}(\gamma n \to \pi^0 n) \sim \Sigma |f^\omega - f^\rho|^2$$

Where

$$f^R_{\mu_2\mu_1} = i(-t)^{\frac{n+x}{2}} \left(\frac{s}{s_0} e^{-\frac{i\pi}{2}}\right)^{\alpha^R(0)} G_{\mu_2\mu_1} e^{c^R_{\mu_2\mu_1} t}$$

$$c^R_{\mu_2\mu_1} = a^R_{\mu_2\mu_1} + \alpha'^R\left(\log\frac{s}{s_0} - \frac{i\pi}{2}\right) \qquad 3.7$$

$$x = |\lambda| + |\mu_1 - \mu_2| - n \qquad n = |\lambda - (\mu_1 - \mu_2)|$$

$G^{R}_{\mu_2\mu_1}$ is the trajectory coupling strength at t=0 (see table 3.3) $a^{R}_{\mu_2\mu_1}$ is the t-slope parameter of the Regge residue.

The absorbing P + P' amplitude has a similar form

$$A = i\sigma_T s e^{c_P t} + E_0 e^{c_{P'} t} s_0 \alpha^{P'}(t) \left(e^{-\frac{i\pi}{2}} \frac{s}{s_0}\right)^{\alpha^{P'}(0)}$$

$$c_P = h_1 + \alpha'_P \left(\log \frac{s}{s_0} - \frac{i\pi}{2}\right) \qquad 3.8$$

$$c_{P'} = h_2 + \alpha'_{P'} \left(\log \frac{s}{s_0} - \frac{i\pi}{2}\right)$$

The parameters for the absorbing amplitude are displayed in table 3.4.

The cut amplitude can now be calculated from the absorptive/eikonal prescription. For x = o

$$f^{cut}_{\mu_2\mu_1} = i\left(\frac{s}{s_0} e^{-\frac{i\pi}{2}}\right)^{\alpha^R(0)} G^{R}_{\mu_2\mu_1} (-t)^{\frac{n}{2}} \left\{ -\frac{\lambda^R_n \sigma_T}{8\pi c_P} \right.$$

$$\left(\frac{c_P}{c_P + c_R}\right)^{n+1} \exp\left(\frac{c_R c_P t}{c_R + c_P}\right) + \alpha^{P'}(0) \left(1 + \frac{\alpha'_{P'}}{\alpha_{P'}(0)} \frac{\partial}{\partial c_{P'}}\right) \qquad 3.9$$

$$\left.\left(\frac{i E_0 \lambda^R_n}{8\pi c_{P'} s}\right) \left(\frac{c_{P'}}{c_{P'} + c_R}\right)^{n+1} \exp\left(\frac{c_R c_{P'} t}{c_R + c_{P'}}\right) \left(\frac{s}{s_0} e^{-\frac{i\pi}{2}}\right)^{\alpha_{P'}(0)} \right\}$$

For n=o, x=2 the terms of $\left(\frac{c_P}{c_P + c_R}\right)^{n+1}$ are replaced by

$$\left[\frac{1}{c_P} \left(\frac{c_P}{c_P + c_R}\right)^2 - t \left(\frac{c_P}{c_P + c_R}\right)^3 \right]$$

The λ_n are the SCRAM cut enhancement factors. It should be noted that the above parametrization differs in sign for n=o, x=2 from CF's published paper, and will produce f-+1 amplitudes of opposite sign to those graphed on fig 6 of that paper. The above sign convention is correct and was, in fact, used in CF's actual numerical work.

As noted before, this model gives an excellent representation of the high energy differential cross-section data for energies down to $P_L = 6$ Gev.

However, FESRs are conventionally evaluated in terms of ν and the Collins and Fitton model has Regge behaviour in s. We have therefore taken the opportunity of repeating the CF fit to photoproduction, this time expressing the amplitudes in terms of ν. It was found that the quality of the original fit could be retained with a slight variation in the Regge trajectorys' slope parameters (which determines the energy dependence of the amplitudes). It is these parameter values which are listed in Table 3.4.

Modified in this manner, the CF model was used as input to the FESR integral. Although they have a physically simple interpretation, the model's amplitudes are extremely complicated formulae. It is not possible

to evaluate their integrals analytically and so a computer program was written to evaluate the FESR numerically. The results are graphed on figure 3.1 for comparison with the resonance integrals.

Section 2 Behaviour of the Amplitudes

It can easily be seen from figure 3.1 that the two sides of the FESR differ in magnitude, t-dependence, and sign, in the single flip and the non-flip amplitudes. Before attempting to repair the disagreement, we shall look at certain interesting features of each component of the FESR equation.

As remarked in the introduction to this chapter, an FESR is not merely a convenient way of constraining particular models of the high energy region: the integral over the resonances is supposed to give model independent information on the behaviour of the interaction at higher energies. But it is difficult to see from fig. 3.1 how one could be expected to predict that the high energy cross-section should have a dip at $t = -0.5$. We need not be constrained to a particular model to expect that dip to manifest itself as a zero in the single flip amplitude. As we shall go on to discuss, there are strong theoretical reasons for believing that such a zero at $t = -0.5$ should propagate down to low energies, and therefore that the resonance FESR integral should have a zero at this point. We might also expect the non-flip FESR to exhibit a zero at $t = -0.2$, as explained in chapter 2 (section 3).

The quickest way to understanding the resonance FESR is to look at the integrand itself. The individual amplitudes are graphed, at selected t-values, as a function of W (com energy) in figure 3.2. It can clearly be seen that in the single flip amplitude, on which our discussion will focus, most of the resonance contributions do fall to zero for $0.3 < -t < 0.5$. However, the contribution of the P_{33} (1232) is dominant in the single flip amplitude and, although it does fall with -t, it does not have a zero near t = -0.5. It is largely the exceptional behaviour of this resonance, clearly illustrated in the graphs of the amplitudes, which is responsible for the -t behaviour of the FESR, (there is also a contribution from the D_{13} (1514)). The final item which determines that the FESR should not have a zero in the place expected from continuing high energy behaviour down to the resonance region, is that the Born Terms in photoproduction are comparatively small and are unable to cancel the P_{33} or the D_{13}, Odorico (1975).

The graphs of Fig. 3.1 show the "global" duality breaks down. However, Armenian et al (1974) showed that the much stronger constraint of "semi-local" duality is obeyed by neutral pion photoproduction - except for the P_{33}. This is a conclusion which might be expected from fig 3.2 and the remarks above: apart mainly from the P_{33} the resonances do appear to be locally dual. For Armenian et al, semi-local duality also requires that

the imaginary part of the low energy amplitude should oscillate about the values extrapolated from high energy data. However, the real part of the low energy amplitude should, they argue, be more slowly varying and given approximately by the Regge phase applied to the averaged imaginary part. This follows because the sign of the real part changes as energy increases through the resonance; thus, if the next resonance is roughly of the same width, spaced one width higher in energy, and its imaginary part has the same sign, then the real parts will interfere destructively.

Armenian et al used these simple observations to relate the imaginary part of an effective Reggeized simple flip amplitude to the square root of the differential cross-section at low energies, i.e. on average

$$-\frac{\nu}{2} \mathrm{Im}\ B_6^{Regge} = \nu \cos\left(\frac{\pi\alpha}{2}\right) \sqrt{\frac{1}{K}\frac{d\sigma}{dt}} \qquad 3.10$$

(where K is a kinematic factor).

They found that the expression on the right hand side did indeed oscillate about the Regge extrapolation and thus that semi-local duality formed a powerful constraint on both real and imaginary parts of the amplitudes in the resonance region.

However, their argument depends on having densely packed resonances, so that the smoothing of the real part actually holds. The P_{33} is separated from the higher resonances by a large gap in energy and so its real part is not altered. They ignored the detailed j-plane structure of the process by using an effective trajectory and it is precisely in the low energy region that the Regge extrapolation is most sensitive to low lying singularities in the j-plane.

The twin conclusions of Armenian et al: that duality implies relationships among resonances and that the P_{33} does not cooperate in such relations, were highlighted by Odorico (1975). He pointed out that the Veneziano model was explicitly designed to satisfy FESR (Veneziano 1968), and that it entailed constraints among resonances. Although the higher resonance contributions in $\gamma p \to \pi^0 p$ have zeroes in t at approximately the desired position, this is not necessary for duality to hold. Thus the Legendre functions for these resonances do behave like $J_n\left(R\sqrt{-t}\right)$: their zeroes are approximately coincident with the lowest t zeroes of the Bessel functions for the amplitude of spin flip = n. The positions of the zeroes are uniquely fixed by the resonance mass and spin. Where the resonance contribution does not $\sim J_n$, then two resonances can conspire to produce a zero amplitude at the appropriate t-value.

If the Veneziano formula (2.2) is used in an FESR expression we obtain

$$\frac{1}{\pi}\int_1^{j_0} d\alpha(s)\ \mathrm{Im}\, V(s,t) = \sum_{j=1}^{j_0} \frac{\Gamma(j+\alpha(t)-1)}{\Gamma(\alpha(t))\,\Gamma(j)}$$

$$= \frac{1}{\alpha'}\,\frac{\Gamma(\alpha(t)+j_0)}{\Gamma(\alpha(t))\,\Gamma(j_0)} \qquad 3.11$$

The right hand side of the expression is zero for $\alpha(t)$ = -1, -2, ... $-j_0+1$. If we regard the middle expression of 3.11 as a sum of s-channel resonances of spins up to j = jo which form the resonance contribution to the FESR, then the zero at $\alpha(t) = -1$ can only arise from a cancellation between the j=1 and j=2 resonances. The shape of the j=1 pole is already fixed (since it has a zero at $\alpha(t)=0$) and so, to get the $\alpha(t) = -1$ zero, the strength of the j=2 resonance pole must be fixed with respect to that of the j=1 residue. The zero condition completely determines the residue of the j=2 pole. In fact the Veneziano model is very highly constrained, the j=3 s-channel resonance residue is similarly fixed by the $\alpha(t) = -2$ zero, and so on. In order to get more zeroes one has to introduce more parameters (resonances) on a one-to-one basis. Veneziano (1968) showed that his formula satisfied FESR for $|\alpha(t)| < \alpha(s_0)\ (= j_0)$. This limit may now be understood in terms of a balance between the number of amplitudes and FESR zeroes and the number of free resonance parameters available.

This Veneziano illustration exemplifies how, at bottom, duality demands a lot more than that of the resonance amplitude should mimic the Bessel function zero structure for the amplitude. We should not necessarily expect local duality in the sense of matching high energy and resonance zeroes, but also a set of cancellations among resonances which, in theory, could be strong enough uniquely to fix the resonance couplings.

However, we have seen that, in practice for $\gamma p \to \pi^0 p$ this theoretical expectation is not fulfilled in our analysis of the FESR. We have seen our conclusions echoed in a different analysis by Armenian et al. Two questions arise: do such cancellations actually occur in other processes and, if they do, why is pion photoproduction different?

It will suffice to mention only one example where resonance contributions which do not individually have a Bessel function zero structure cooperate to produce the required zero. In the classic πN charge exchange reaction there are only two invariant amplitudes, conventionally denoted A and B. In the non-flip combination $A + \nu B$ the Born term makes a sizeable contribution and, because of the simple t behaviour of the Born residues, there is no possibility of a dip in the required place of $t = -0.14$. However, once again the

P_{33} contribution is large and the two combine to produce a zero in the required place, in the averaging FESR sense. Similarly, at t = -2.5 the F_{33} , D_{13} and F_{15} (1682) all combine to cancel out in this amplitude, although this may be considered too high a -t value for FESRs to be applicable.

Further evidence for the cooperative behaviour of resonance contributions to scattering amplitudes may be found in the papers by Odorico (1974). He found a consistent pattern of lines of zeroes in the Mandelstam s, t, u plane for a variety of processes. Once again these patterns were held to determine the couplings of leading resonances in the amplitudes. From the observation of linear zeroes, Odorico derived dual constraints on certain resonance decay modes which previously had been explained only in a Quark Model context. But there are some couplings e.g. $K^{**} \rightarrow K\eta$ whose experimental suppression is inexplicable in the quark model and which can easily be accommodated in the linear zero dual constraint picture. More recently Odorico has sought to show that the model can comprehend the experimental suppression of the low pion multiplicity decay modes of the $\rho'(1600)$.

Neutral pion photoproduction differs in three respects from the processes which can be fitted into a consistent pattern on the lines sketched above. At a fundamental

level the interaction is electromagnetic, not purely hadronic, in nature. It still remains an hypothesis that the two can be explained in the same terms. Secondly, the photon is a vector particle which introduces spin complications. Most of the processes in which dual constraints have been observed are pseudoscalar-fermion interactions. Finally, the photon is a U -spin scalar, it is not in a definite eigenstate of isospin.

Odorico suggested the extra amplitudes, introduced due to the vector nature of photon, might hold the key to the movement of the zero in t. But he was unable to suggest a set of amplitudes in which the desired resonance conspiracies would operate. (It is easy to check that they do not operate, for example, in t-channel helicity amplitudes). In any case, there is a fundamental difficulty in proposing a unique set of amplitudes in which to perform FESRs. There is no reason to justify an arbitrary choice of amplitudes apart from their success in obtaining the desired conspiracies - which seems slightly circular.

The best way of investigating Odorico's suggestion is to look at the behaviour of the zeroes in a process with a similar spin structure to pion photoproduction. Since no vector projectile other than the photon exists, it is necessary to look at a process where a vector particle is produced in the final state, and apply time reversal. One such process, which is experimentally accessible, is

$\pi N \to \rho N$. This has been recognised for a long time (Contogouris 1967) as an important process. For if all the scattering charge states are measured, then a clean, model-independent separation of the t-channel Regge exchanges can be made and an unambiguous determination made of a single trajectory's properties.

If I_0 and I_1, represent the t-channel isoscalar and isovector components respectively then

$$\begin{aligned} \pi^+ p \to \rho^+ p \quad &\sim \quad |I_0 + I_1|^2 \\ \pi^- p \to \rho^- p \quad &\sim \quad |I_0 - I_1|^2 \\ \pi^- p \to \rho^0 n \quad &\sim \quad 2|I_1|^2 \end{aligned}$$

The I_0 component can be extracted from these three interactions

$$\left.\frac{d\sigma}{dt}\right|_{I_0} = \frac{1}{2}\left(\frac{d\sigma_+}{dt} + \frac{d\sigma_-}{dt} - \frac{d\sigma_0}{dt}\right) \qquad 3.12$$

and only the ω has the correct quantum numbers for this exchange.

A number of people (Crennell et al, 1971; Michael and Gidal, 1972) have isolated the ω-exchange, the most recent analysis (Haber et al, 1974) coming down in energy to Wcom = 2.86 GeV. All find a pronounced dip and secondary maximum for the ω-exchange component.

However, the photon has mixed isospin and is uncharged, it is therefore impossible to separate the relative ρ and ω exchange contributions to $\gamma p \to \pi^0 p$ without recourse to a specific model. Many high-energy analyses, indeed, do not make such an explicit separation. (Barker et al 1974). One cannot therefore learn much from comparing the pure ω -exchange process of eq 3.12, with one contaminated by ρ-exchange.

In the resonance region of pion photoproduction, however, one can separate components corresponding to t-channel isovector and isoscalar exchanges. This follows because the scattering proceeds (in the s-channel) through resonances of definite isospin, whose coupling to an isospin configuration can be determined. We separated the resonance amplitudes into components corresponding to definite t-channel isospin and found that the behaviour of the Born term and P_{33} contributions to the ω-exchange component did not differ from the behaviour of the full amplitude: neither a Bessel function zero nor a cancellation was observed.

Unfortunately, the ω -exchange behaviour is only accessible in the resonance region for photoproduction, and has only been measured in the high energy region for $\pi N \to \rho N$. It is singularly frustrating that a direct comparison cannot, therefore, be made. As one comes down in energy through the resonance region in photoproduction,

the $t = -0.5$ dip in the cross-section will be washed out as the influence of the P_{33} grows. If this arises from the spin complications introduced by a vector incident particle, then the same behaviour will be seen in the $\pi N \to \rho N \quad I_t = 0$ cross section. If, however, the complication is due to the electromagnetic nature of the photon, then the dip will persist in $\pi N \to \rho N$.

The resolution of this question is of considerable importance. For if Odorico's conjecture is correct and the zero movement follows from the complexities introduced by spin, then the undeniable success of FESR in πN (and to a lesser extent in KN) appears more as a lucky coincidence than a manifestation of a deeper dynamics. If, on the other hand, the behaviour follows from the electromagnetic nature of the photon, then it confirms the indications (section 2.3) that neutral pion photoproduction is not as purely hadronic as had been thought.

Section 3 Extending the Regge Model

To illustrate the behaviour of the Regge contributions to the FESR, we provide in figure 3.3 a comparison of the FESRs and the amplitudes at p_{Lab} = 6 GeV/c (fig. 6 of Collins & Fitton (1974)). It can easily be seen that the zero at t = -0.4 in the single flip amplitude is not present in the FESR. Instead, this zero is shifted out to t = -0.9. However, the zero at t = -0.2 in the non-flip amplitude is retained in the FESR. The higher -t behaviour of the non-flip FESR does not reflect the amplitude's t-structure. (It should be remembered that the FESR in Fig. 3.3 contain $(-t)^{n/2}$ factors for ease of comparison).

The amplitudes (and therefore the FESR integrals) in the CF model are the result of a complicated interplay of poles and cuts, each with their own energy dependence. If the Regge amplitudes were controlled by a "shrinking cut model" as described in the previous chapter, then the single flip amplitude would be expected to maintain the zero at fixed t down to threshold energies and so provide a zero at t = -0.5 in the FESR. We saw in the last chapter that it was not possible to describe photo-production using such a model, and we have seen from the preceeding section of this chapter that such a model could not satisfy photoproduction FESR constraints.

In the Collins and Fitton model two poles are exchanged, and each pole has two associated cuts which are determined by the position of the cut discontinuity in the j-plane and not by the pole position. Everyone of the exchanges therefore has its own energy dependence, and their relative contributions to the amplitude change as the value of ν decreases into the resonance region. Since the effective α's of the cut contributions to the CF amplitudes are higher than the α's of the poles at large -t, the zero in the single flip amplitude, produced by pole/cut interference, is shifted to larger -t as the energy decreases. The interplay of the six contributions to each amplitude (and FESR) is very complicated; in figure 3.3 we show also the FESRs without the P' cuts. It is clear, particularly from small -t single flip FESR, that the CF amplitudes are heavily over-absorbed as the energy decreases. This was the main reason that Worden (1972) rejected SCRAM models in preference to NWZ models for photoproduction. But it is not clear that the alternatives are actually more successful. Barker et al (1974) provide a comprehensive fit to the high energy data, the dispersion relations and the FESRs; in particular they avoid the t = -0.2 zero in the non-flip amplitude and the t = -0.5 zero in the single flip FESR. To achieve the latter, they require a number of Regge-like terms in their amplitude, and the identification with physical exchanges is somewhat heuristic. But more importantly,

as we have seen in the preceeding section, the single flip amplitude (as determined from the resonances) does not exhibit a zero shifted from t = -0.5 until one reaches energies $p_{lab} \sim 0.8$ GeV/c. The FESR zero shift for this amplitude reflects the large weighting of the P_{33} in the FESR integrand and not the amplitudes behaviour for $0.8 < p_{lab} < 1.5$ GeV/c. The "zero shifting mechanism" of Barker et al's amplitudes starts to operate before this and so only "global", not semi-local, duality is retained.

We have thus seen that the strong cut reggeized absorption model fails to meet FESR constraints in photoproduction; that the modified "shrinking cut", absorption model would fail also, even were it available to us; and that although abandoning absorption in favour of NWZ apparently offers one way out, even this is not without difficulties. Since it is the behaviour of the P_{33} which is the principal feature of the resonance amplitudes, the most reasonable way of meeting the FESR constraints while retaining the main features of the CF eikonal model, may be locally to simulate the P_{33} behaviour. In other words we shall introduce a "daughter" pole, lying low in the j-plane, to provide a reasonable approximation to the resonance amplitude. When integrated over in the FESR, this term will rectify the mis-match between the two sides of the FESR.

It is interesting to note that this approach is one of the alternatives proposed by Worden (1973) in his discussion of duality and absorption models. However, there is an extra element to our introduction of a daughter. Worden's difficulty was to persuade the Regge models to continue the high energy t-structure down to the resonance region. Our problem concerns also the behaviour of the resonances themselves, a feature whose interest is independent of specific high energy models.

Our method was, in fact, to obtain a fit to the FESR using CF + daughters and then to check the correspondence with the individual amplitudes. Care was taken to ensure that the quality of the fit to high energy data was maintained.

A number of parametrisations were tried to fit the FESR without undermining the high energy fit, the simplest successful one was an effective daughter term, $\alpha^d \sim \alpha^\omega - 2$ with the following form:

$$f_{++1} = i(-t)^{1/2}\left(\frac{\nu}{\nu_0}e^{-\frac{i\pi}{2}}\right)^{\alpha^d(0)} G^d_{++}\, e^{c^d_{++}t}(1+bt)$$

$$f_{-+1} = i\left(\frac{\nu}{\nu_0}e^{-\frac{i\pi}{2}}\right)^{\alpha^d(0)} G^d_{-+}\, e^{c^d_{-+}t}(\alpha_d+2)$$

$$f_{+-1} = i(-t)\left(\frac{\nu}{\nu_0}e^{-\frac{i\pi}{2}}\right)^{\alpha^d(0)} G^d_{+-}\, e^{c^d_{+-}t} \qquad 3.13$$

$$c = a + \alpha'^d\left(\log\frac{\nu}{\nu_0} - \frac{i\pi}{2}\right)$$

We list the values of the parameters in table 3.5 and display the resultant (CF + daughter) fit to the FESR on figure 3.4.

In the next chapter we will examine this extended model in the light of the electroproduction data.

Table 3.1 The Born Term Residues

Amplitude	Residue
B_1	$-\frac{g}{2}(F_1 + 2m\,F_2)$
B_2	$\frac{g}{2}F_1$
B_3	$\frac{g}{4}F_1$
B_5	0
B_6	$-g\,F_2$
B_8	$-\frac{g}{2}F_2$

F_1 and F_2 are proton electromagnetic form factors

g is πNN coupling constant

Table 3.2 Resonance parameters

Resonance	$I^{\pm}$	Mass	Width	E_1	M_1
S_{11}	1+	1.505	0.1	0.502	0.0
S_{11}	0+	1.688	0.11	0.099	0.0
P_{33}	1+	1.232	0.114	-0.071	3.51
P_{13}	1+	1.850	0.3	0.0	0.0
F_{37}	3+	1.940	0.2	0.014	0.156
P_{11}	1-	1.434	0.2	0.0	0.495
D_{13}	2-	1.514	0.33	0.721	0.269
D_{13}	2-	1.680	0.07	-0.071	0.05
D_{13}	2-	1.971	0.1	0.171	0.036
D_{33}	2-	0.649	0.15	-0.340	0.028
F_{15}	3-	1.682	0.14	0.332	0.113

Mass and width are in GeV/c^2

Couplings are in $\mu b^{1/2}$

Table 3.3 Parameters of the CF model

	ρ	ω
α'	0.72	1.01
G_V	2.19	15.56
G_T	10.07	20.02
a_{++}	4.42	1.07
a_{+-}	0.02	1.61
λ_0	2.88	1.51
λ_1	2.93	2.89
λ_2	2.70	1.65

Table 3.4 Parameters for the P, P' poles

	P		P'
σ_T	19.92	E_0	-43.31
h_1	2.02	h_2	0.23
α'_P	0.49	$\alpha'^{\circ}_{P'}$	0.55
		$\alpha'_{P'}$	1.1

Table 3.5 Parameters of the daughter amplitudes

$\alpha(0)$	-1.71
α'	0.94
G_{++}	-12.4
G_{-+}	17.2
G_{+-}	-0.46
a_{++}	1.64
a_{-+}	1.26
a_{+-}	-0.03
b	1.45

Figure Captions

Fig 3.1 The results of the FESR analyses. The resonance integral is the unbroken line and the Regge integral is the dashed line.

a) is the FESR of the natural parity combination of the single flip amplitudes
b) is the double flip amplitude FESR
c) is the non-flip amplitude FESR

Fig 3.2 The resonance amplitudes as a function of centre of mass energy for selected values of t.

a) Single flip amplitude
b) Double flip amplitude
c) Non-flip amplitude

Fig 3.3 The shape of the imaginary parts of the Regge amplitudes at p_L = 6 GeV/c compared with the FESRs. In both cases the unbroken line is the full amplitude, and the amplitude without $R \otimes P'$ cuts is shown as a dashed line. (Note that the half angle factors are present in the amplitudes, and also in the FESRs).

Fig 3.4 The fit to the resonance integrals of the extended CF + daughters model of equation 3.13.

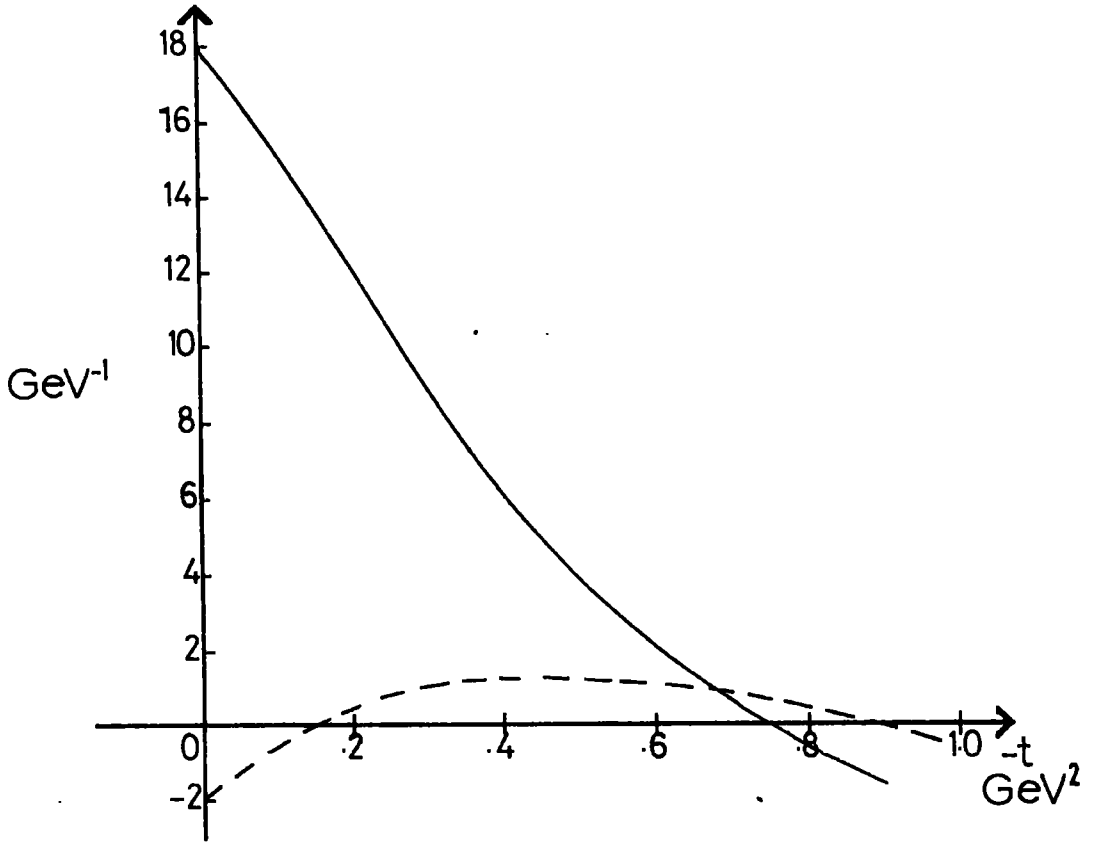

Fig. 3.1(a)

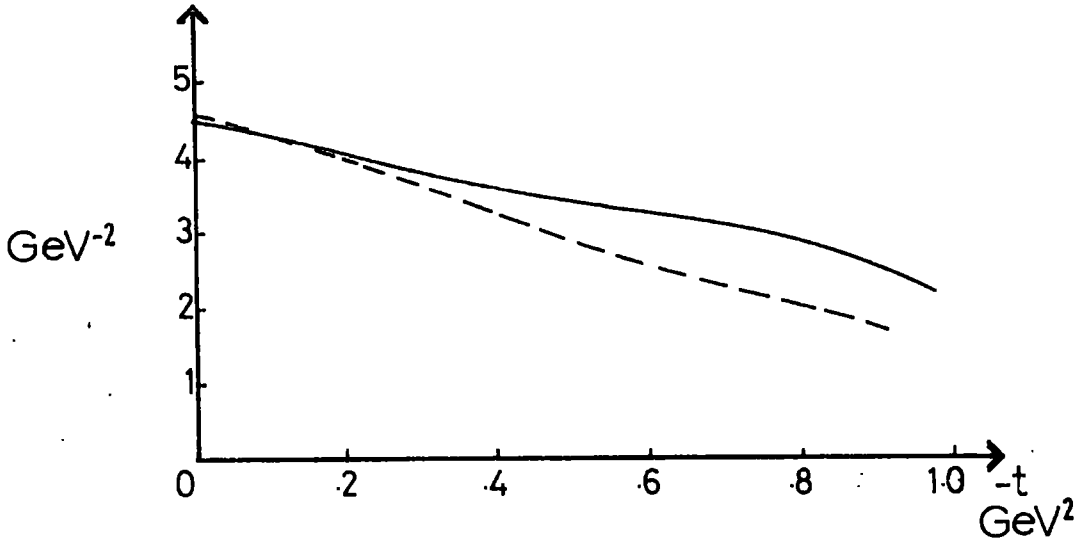

Fig. 3.1(b)

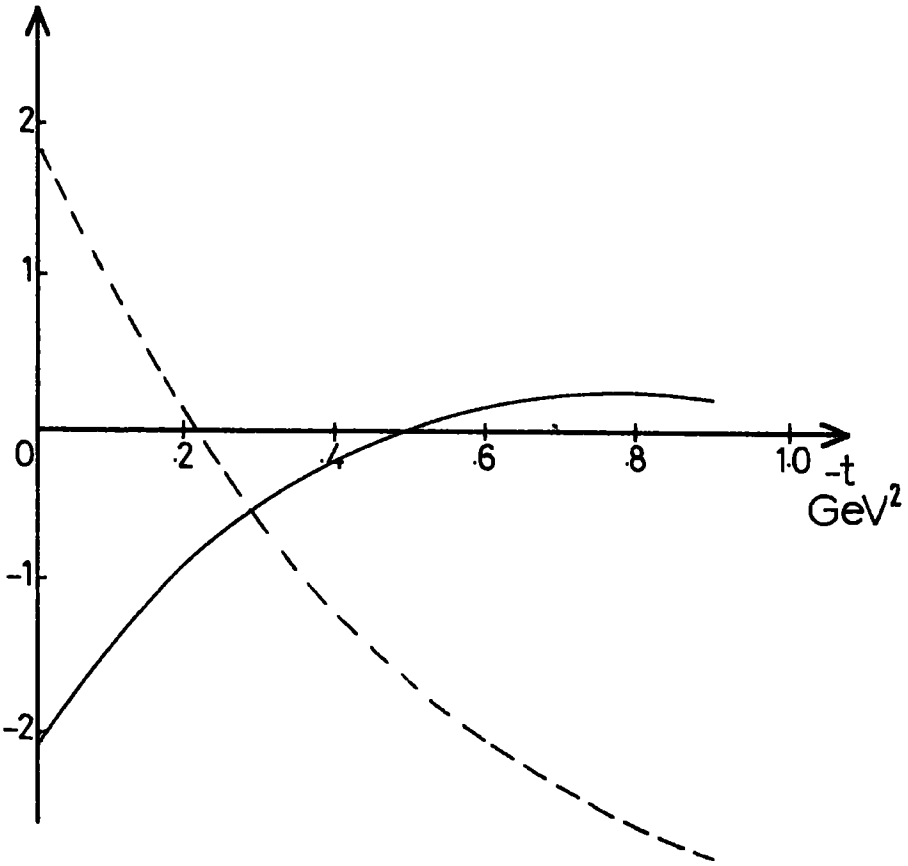

Fig. 3.1(c)

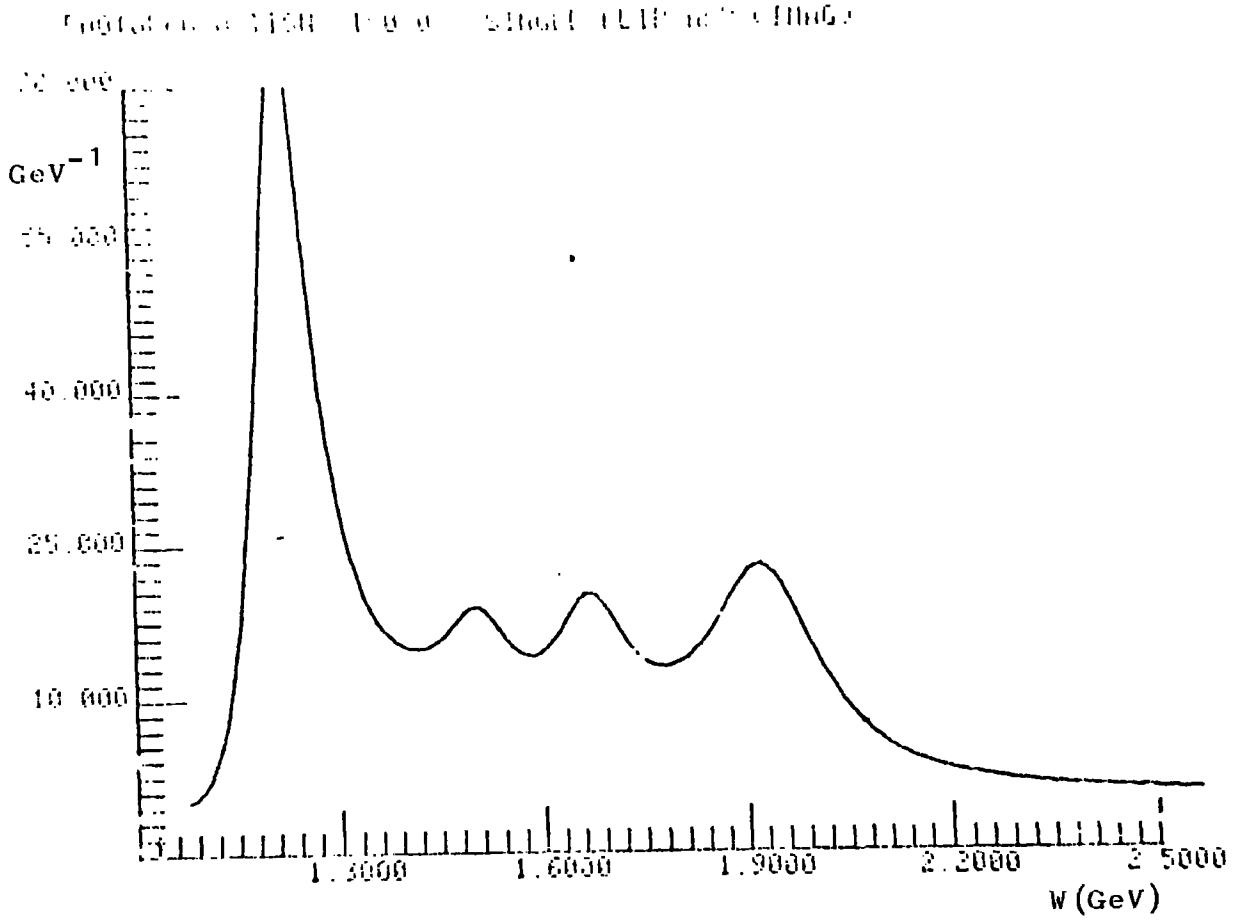
GeV^{-1}
40.000
25.000
10.000
1.3000
1.6000
1.9000
2.2000
2.5000
W(GeV)

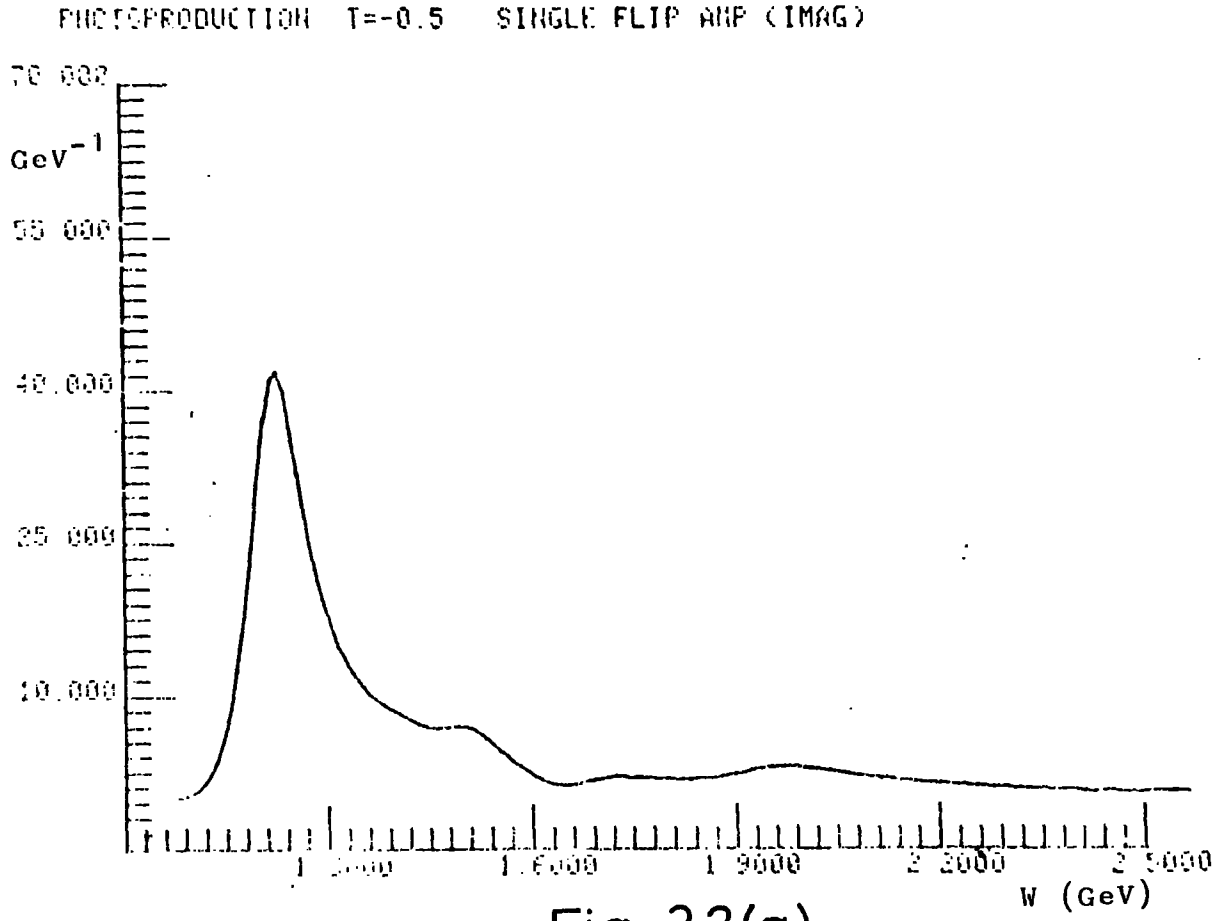
PHOTOPRODUCTION T=-0.5 SINGLE FLIP AMP (IMAG)
GeV^{-1}
55.000
40.000
25.000
10.000
1.9000
2.2000
2.5000
W (GeV)

Fig. 3.2(a)

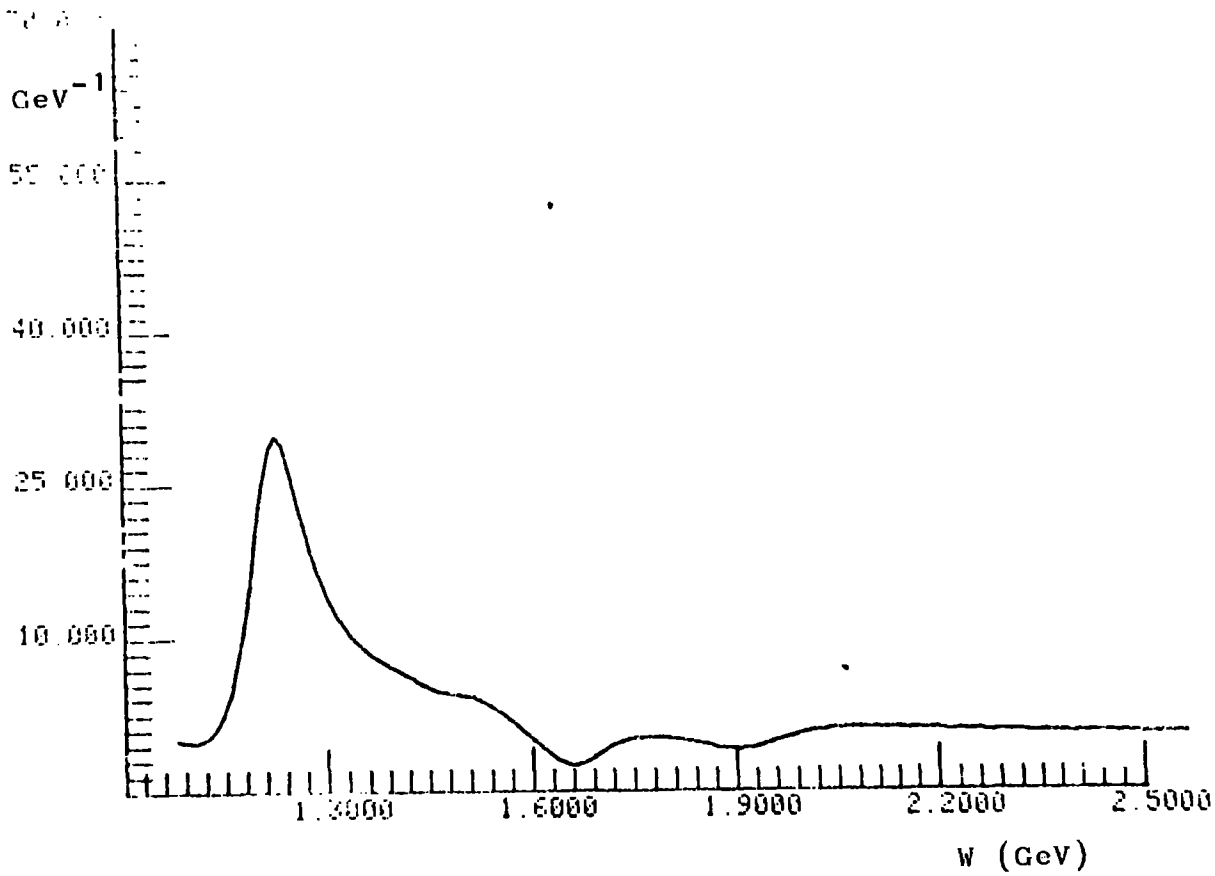

PHOTOPRODUCTION T=-0.9 SINGLE FLIP AMP (IMAG)

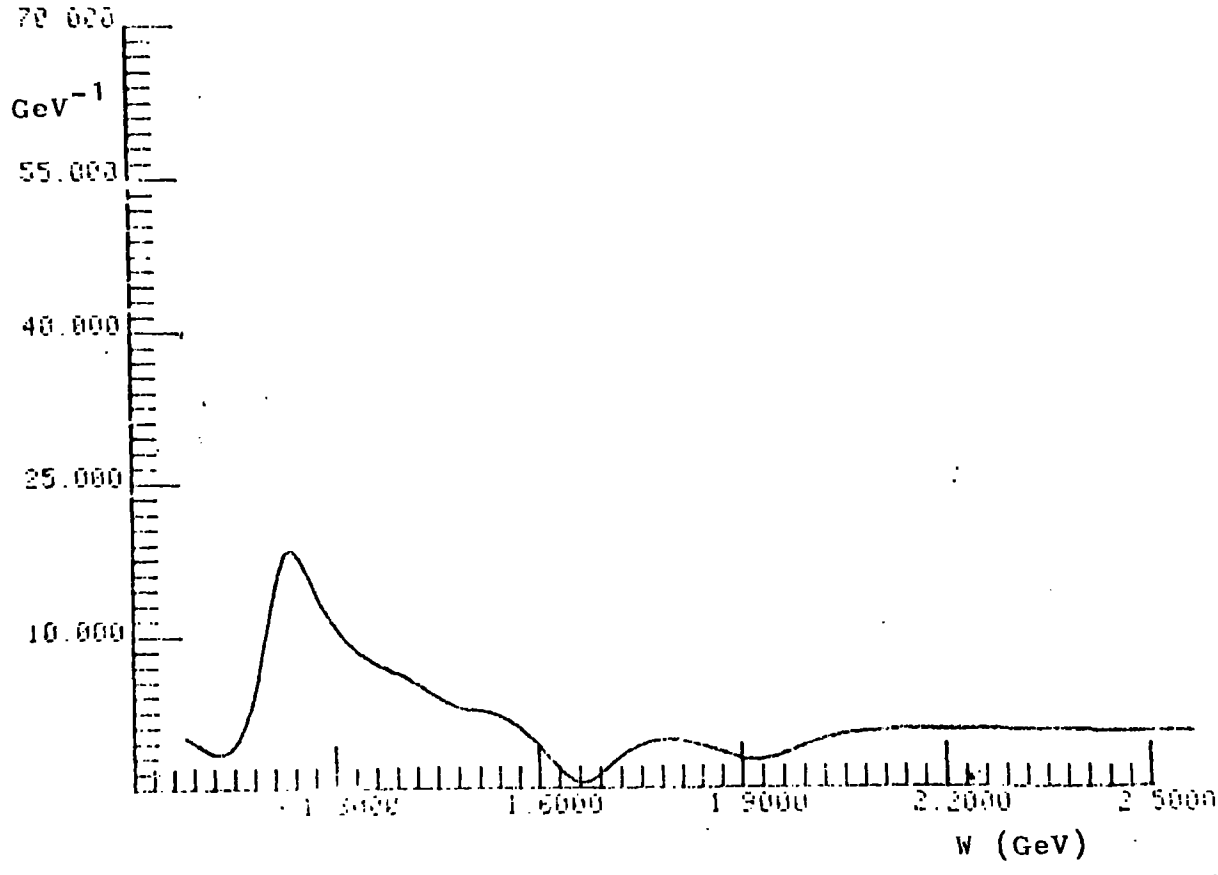

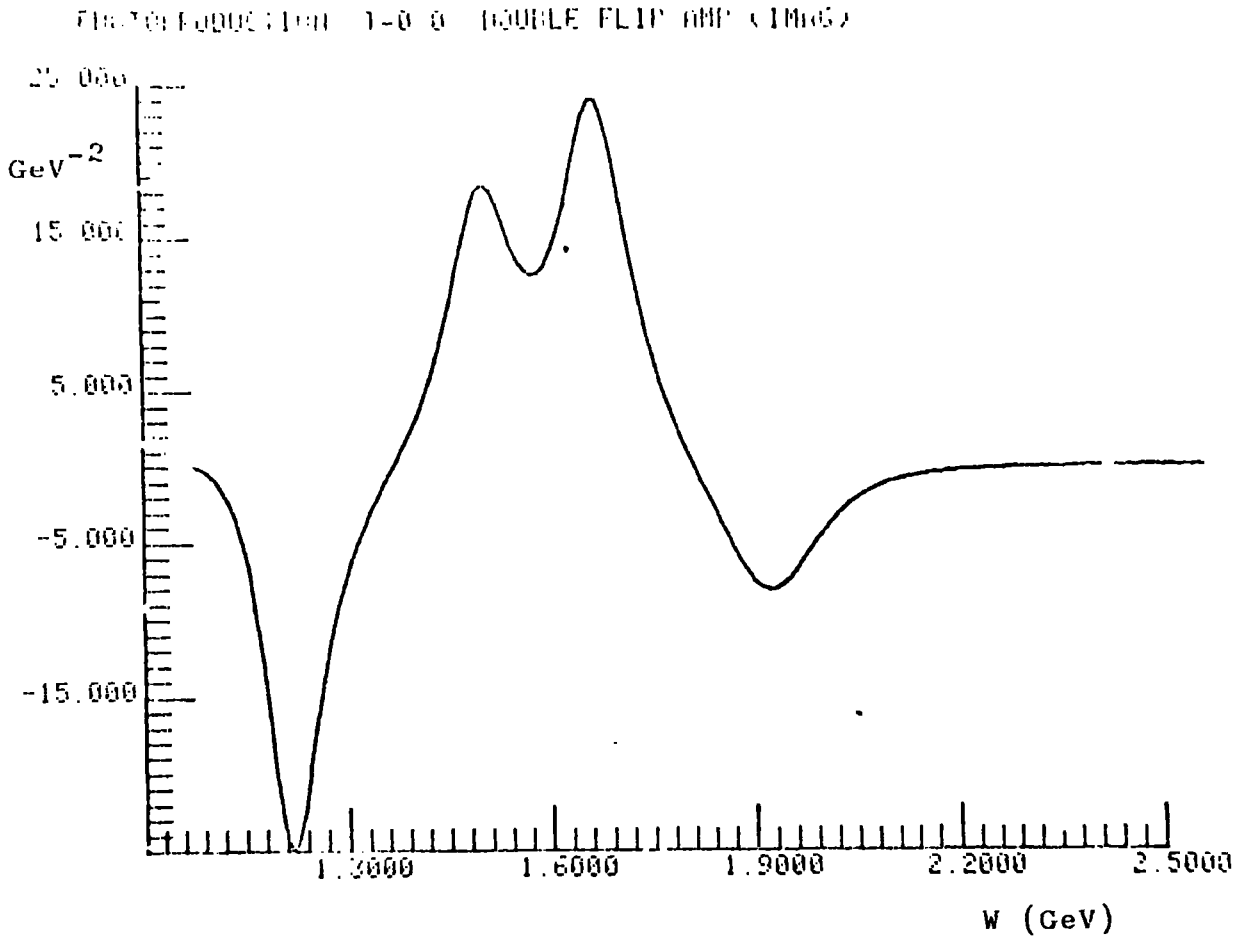
25.000
GeV^{-2}
15.000
5.000
-5.000
-15.000
1.3000
1.6000
1.9000
2.2000
2.5000
W (GeV)

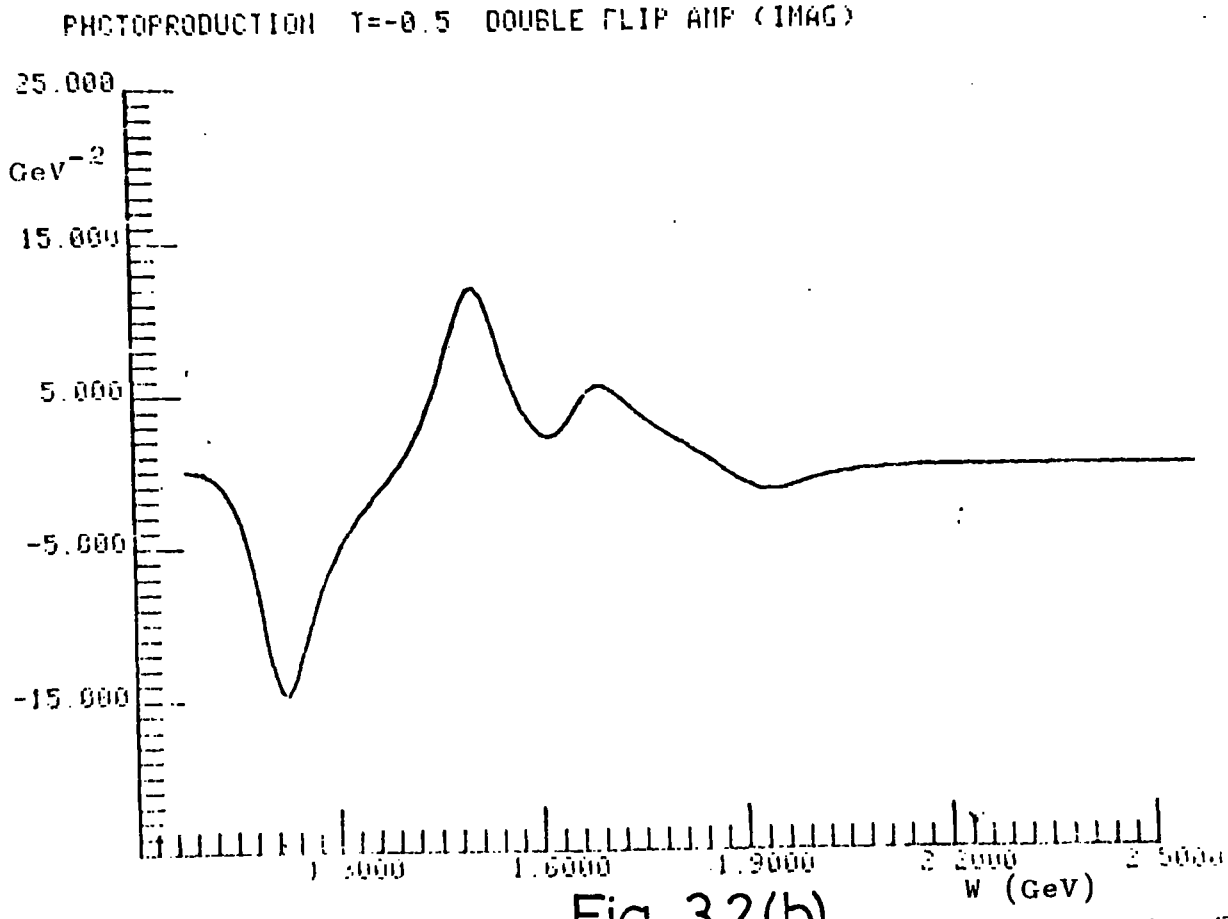
PHOTOPRODUCTION T=-0.5 DOUBLE FLIP AMP (IMAG)
25.000
GeV^{-2}
15.000
5.000
-5.000
-15.000
1.6000
1.9000
W (GeV)

Fig. 3.2(b)

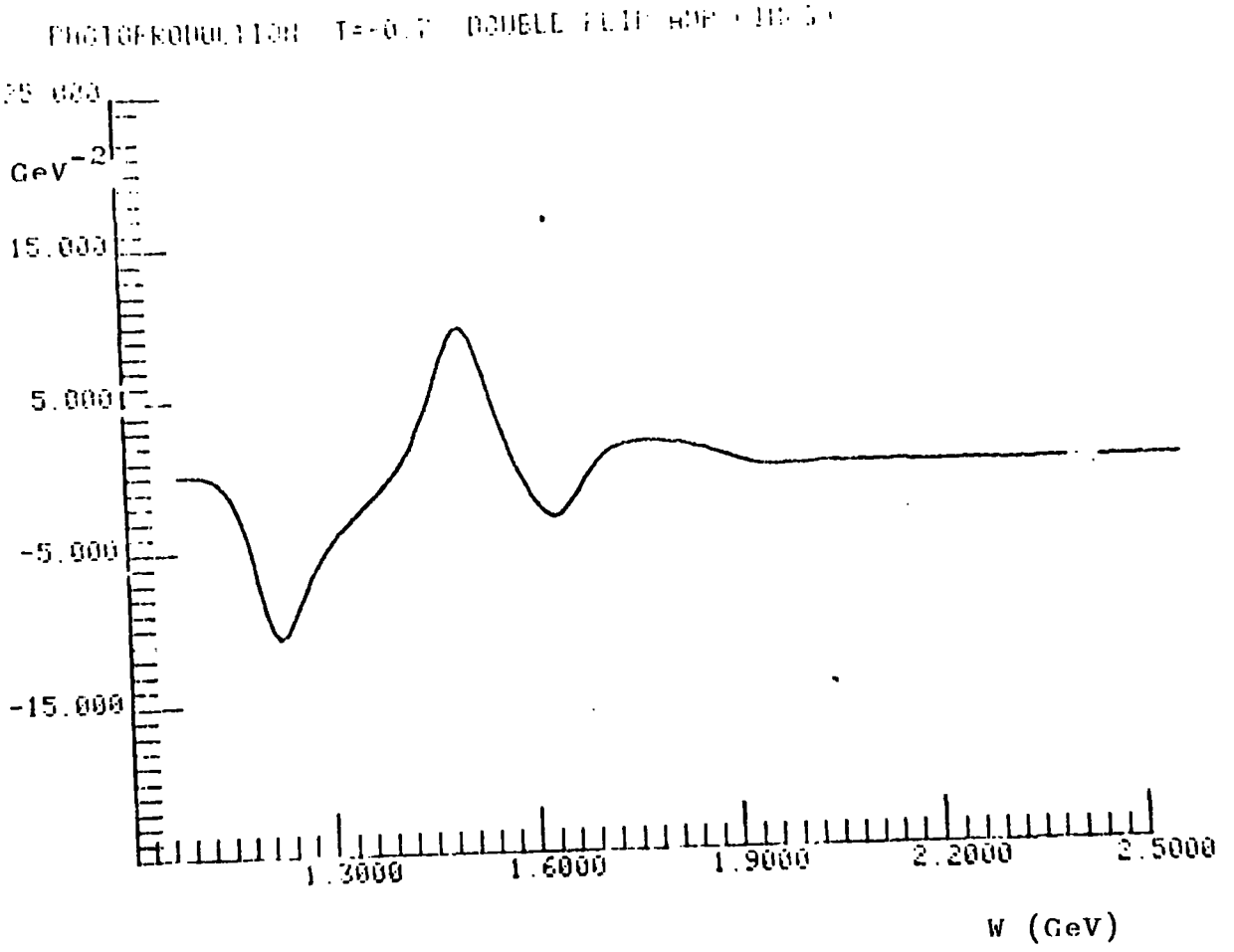
GeV^{-2}
15.000
5.000
-5.000
-15.000
1.3000
1.6000
1.9000
2.2000
2.5000
W (GeV)

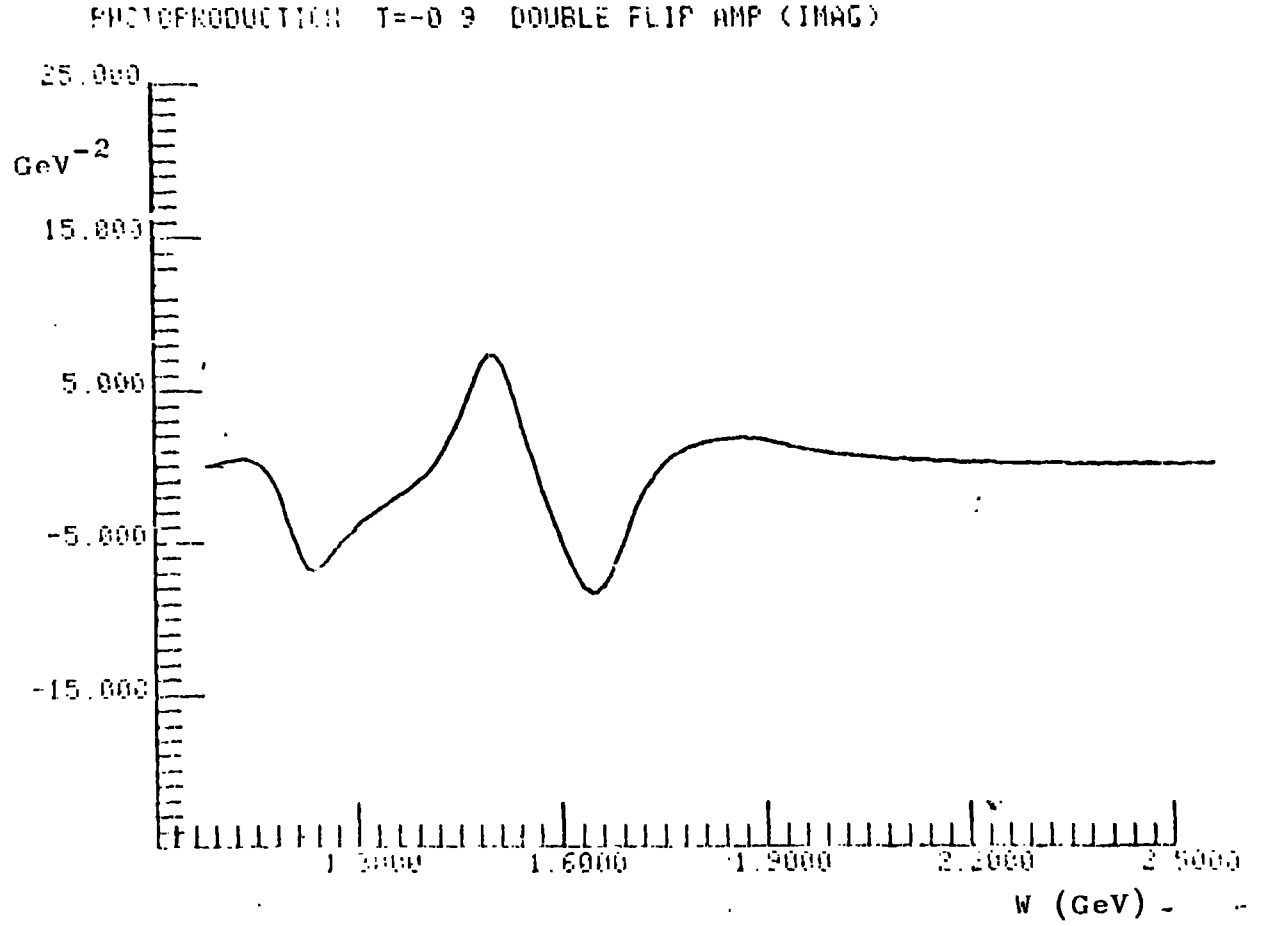
25.000
GeV^{-2}
15.000
5.000
-5.000
-15.000
1.6000
1.9000
2.2000
W (GeV)

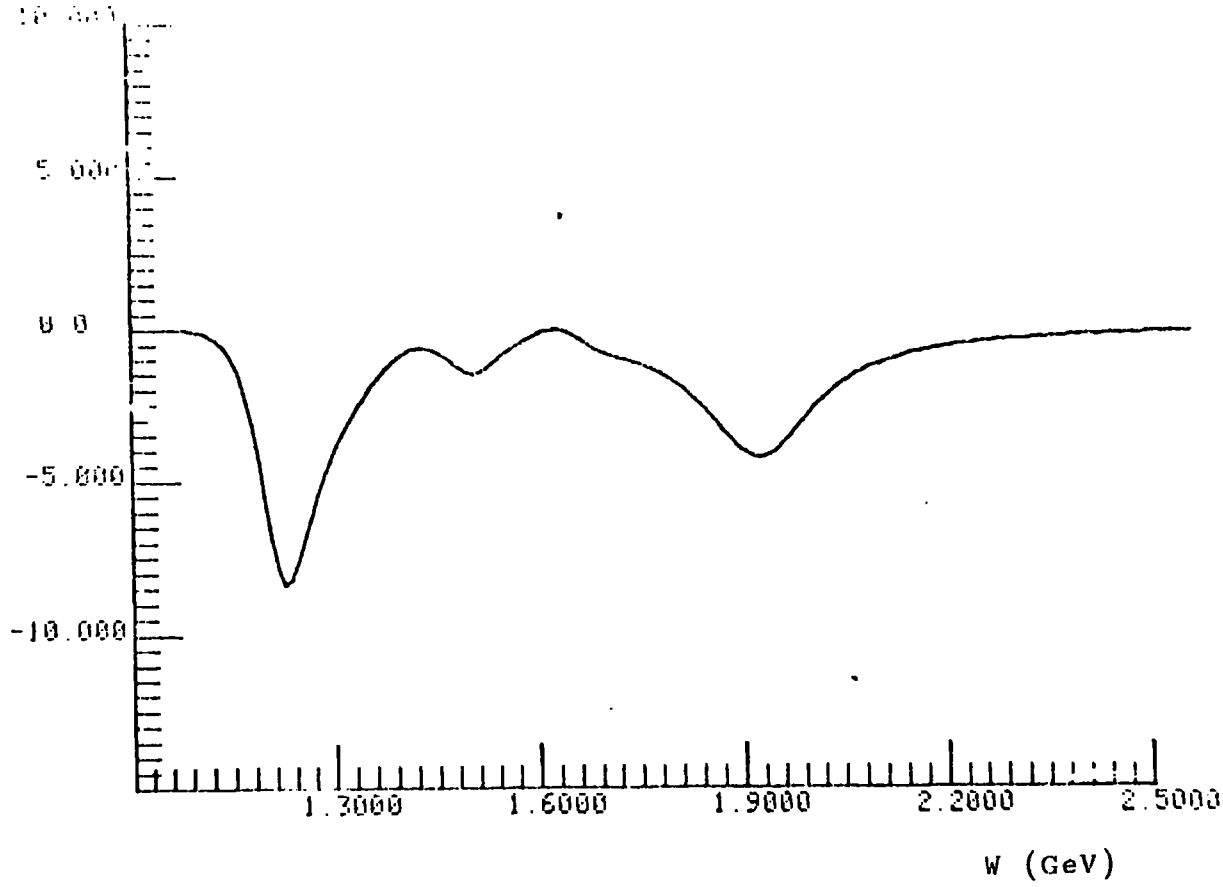
5.000
0.0
-5.000
-10.000
1.3000
1.6000
1.9000
2.2000
2.5000
W (GeV)

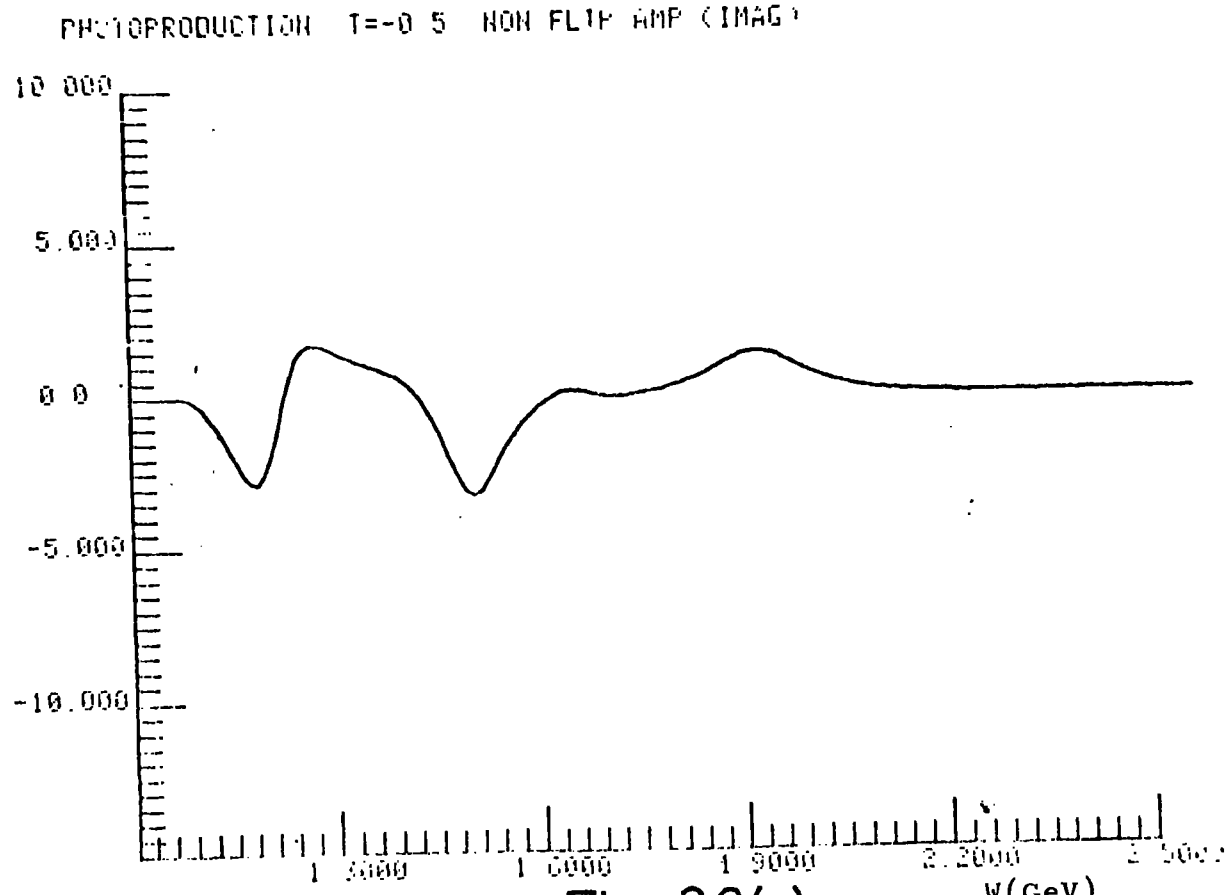
10.000
5.000
0.0
-5.000
-10.000
W(GeV)

Fig. 3.2(c)

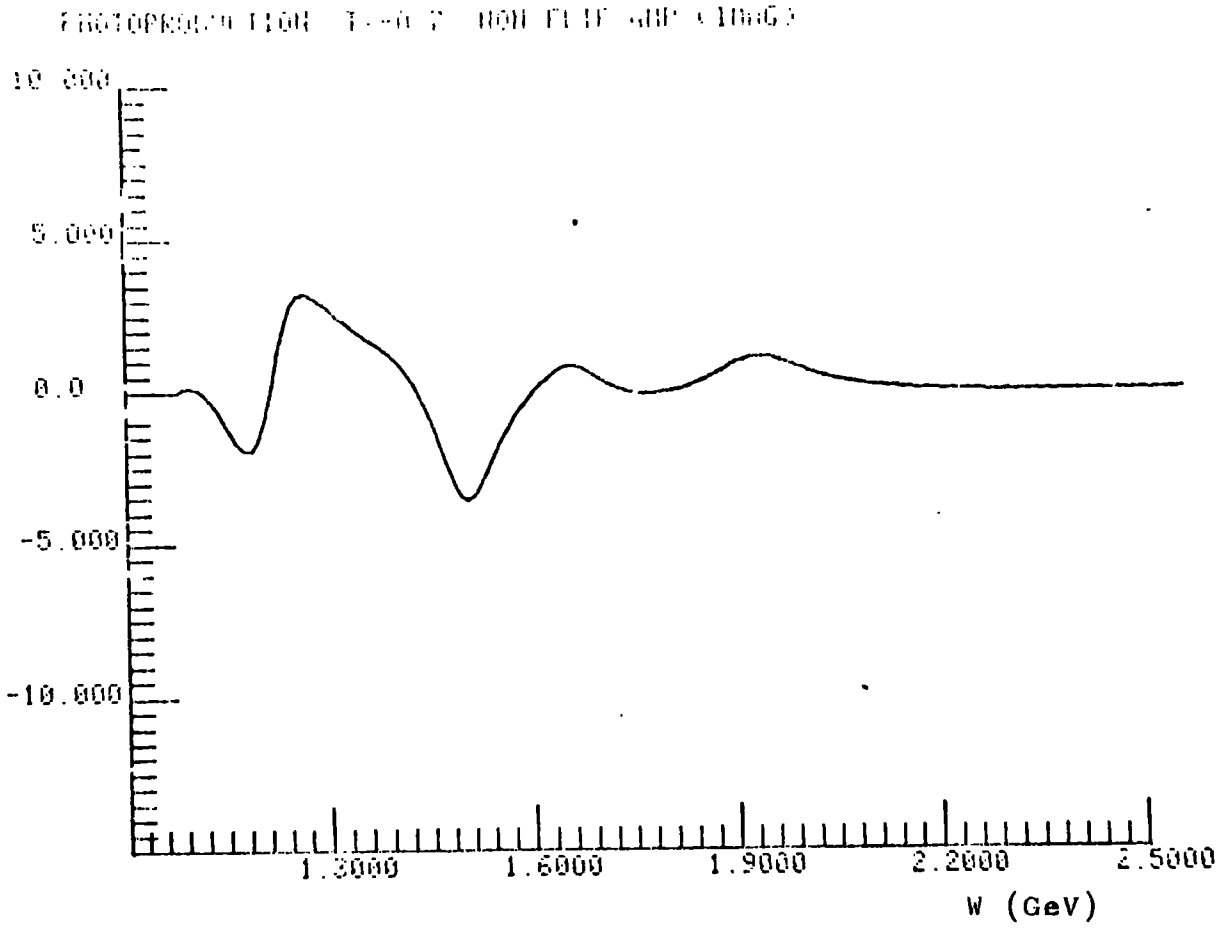

PHOTOPRODUCTION T=-0.9 NON FLIP AMP (IMAG)

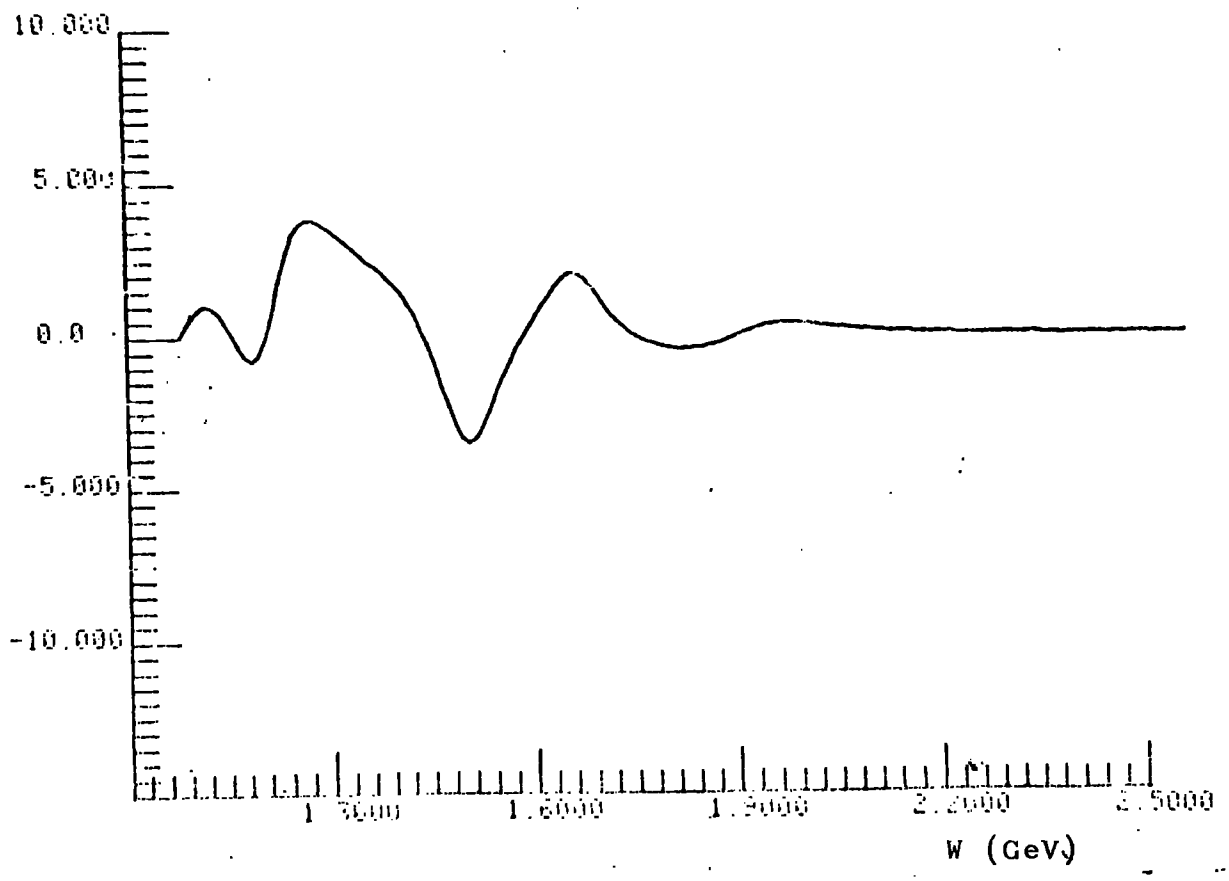

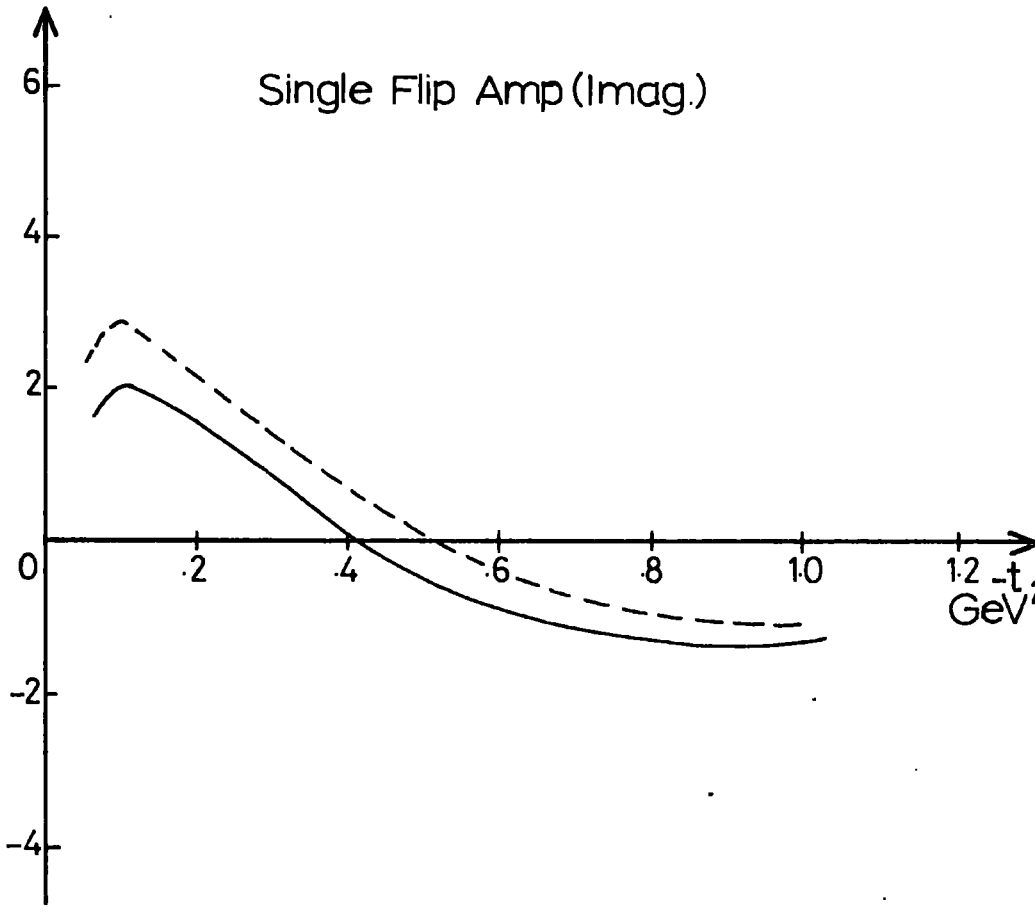
Single Flip Amp (Imag.)
6
4
2
0
-2
-4
.2
.4
.6
.8
1.0
1.2
-t
GeV

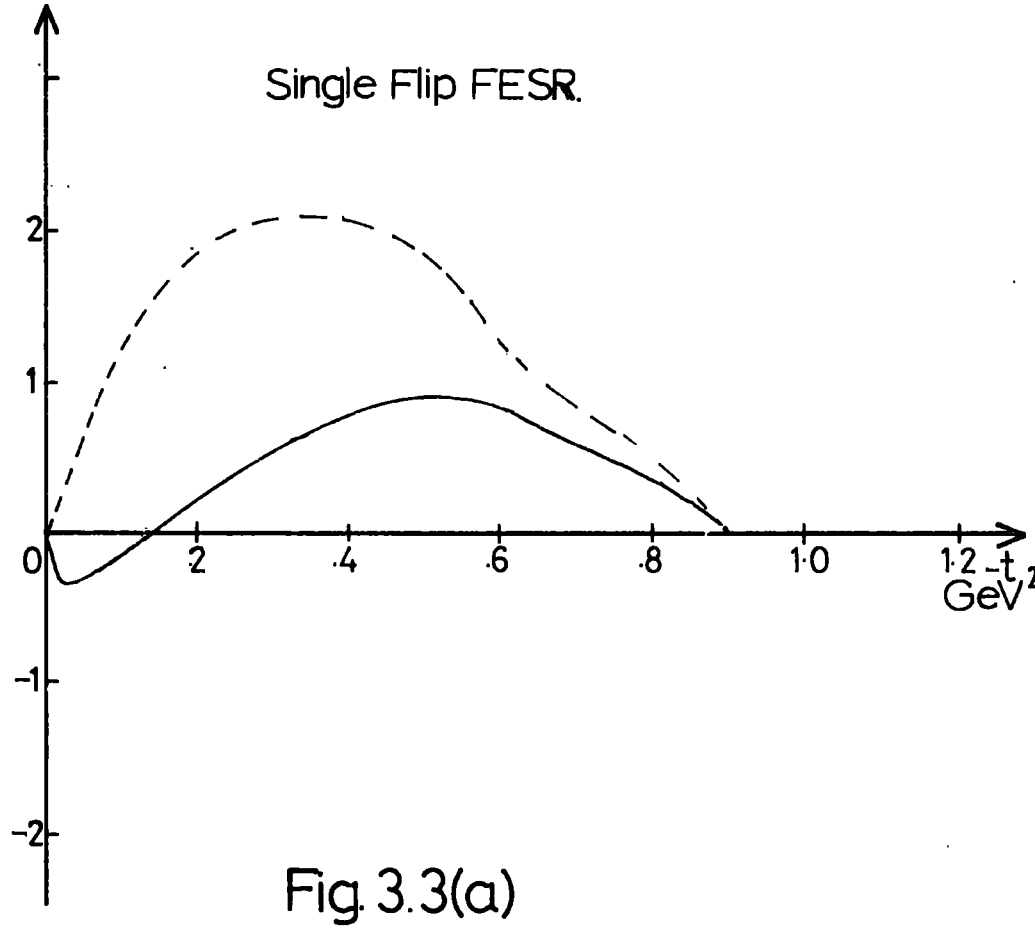
Single Flip FESR.
2
1
0
-1
-2
.2
.4
.6
.8
1.0
1.2
-t
GeV

Fig. 3.3(a)

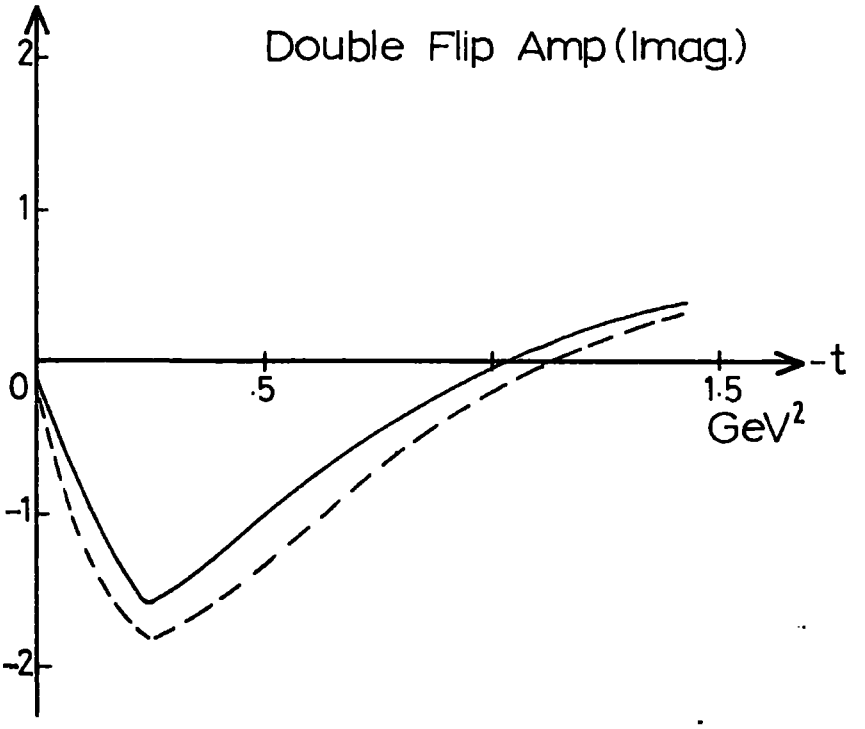
Double Flip Amp (Imag.)
2
1
0
-1
-2
·5
1·5
GeV²
-t

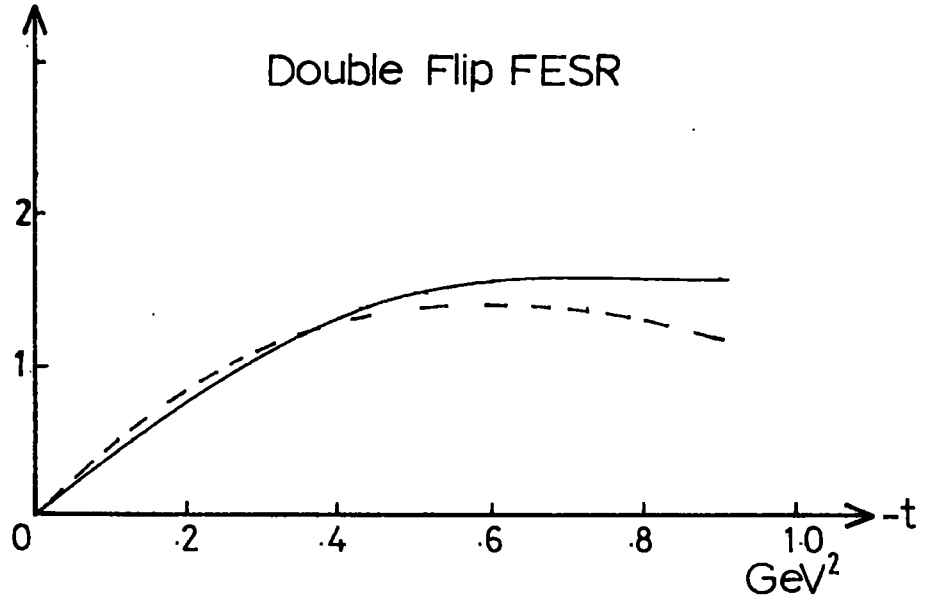
Double Flip FESR
2
1
0
·2
·4
·6
·8
1·0
GeV²
-t

Fig. 3.3 (b)

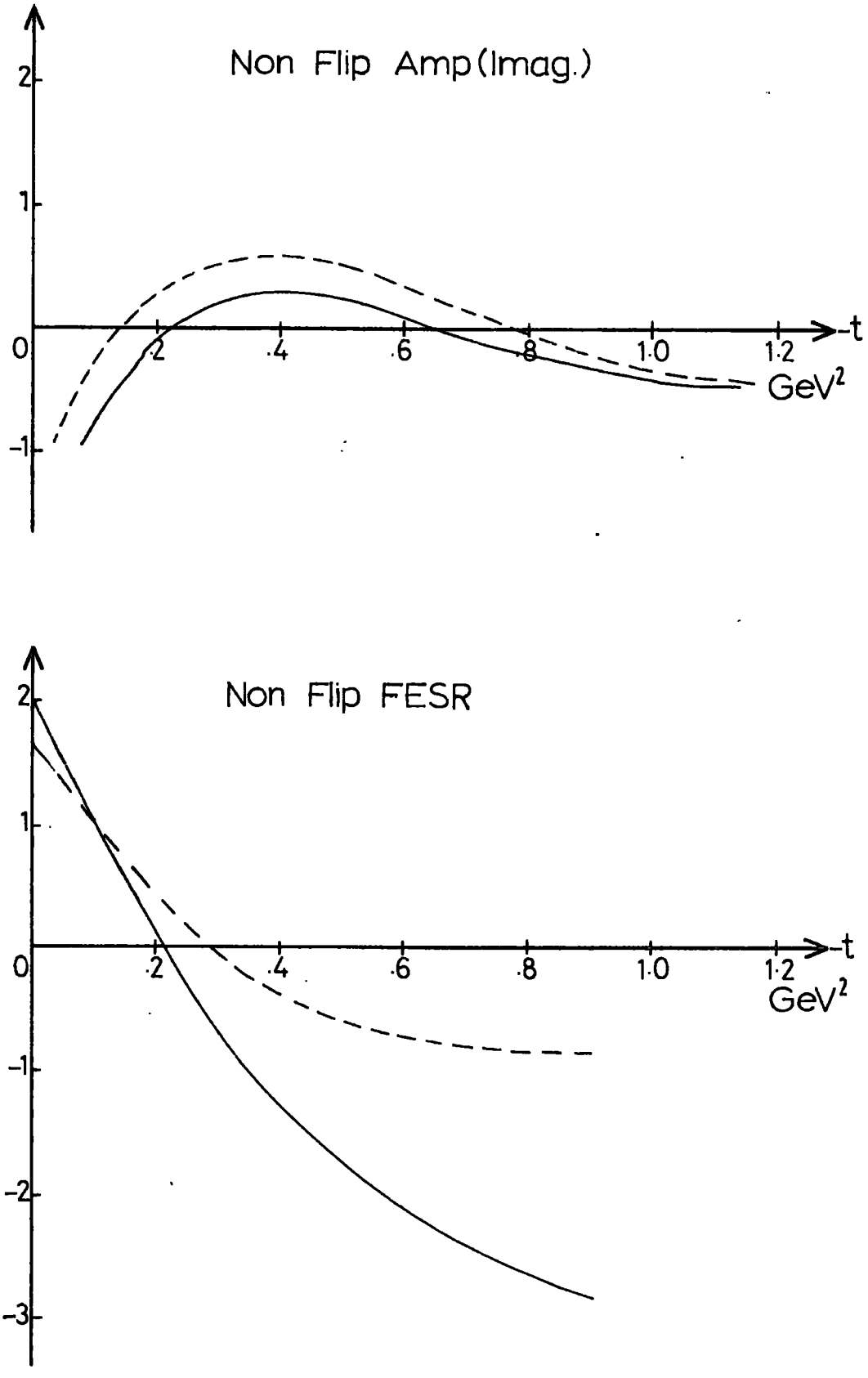
Non Flip Amp(Imag.)
2
1
0
-1
.2
.4
.6
.8
1.0
1.2
-t
GeV²
Non Flip FESR
2
1
0
-1
-2
-3
.2
.4
.6
.8
1.0
1.2
-t
GeV²

Fig. 3.3(c)

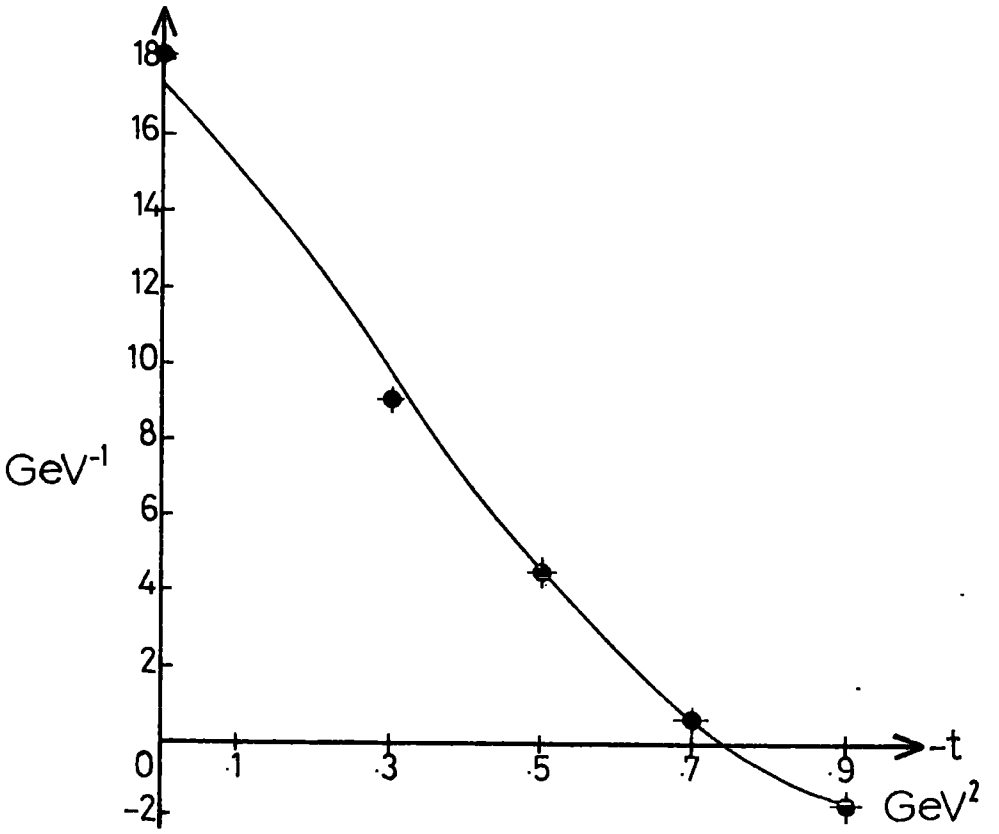

Fig. 3.4(a)

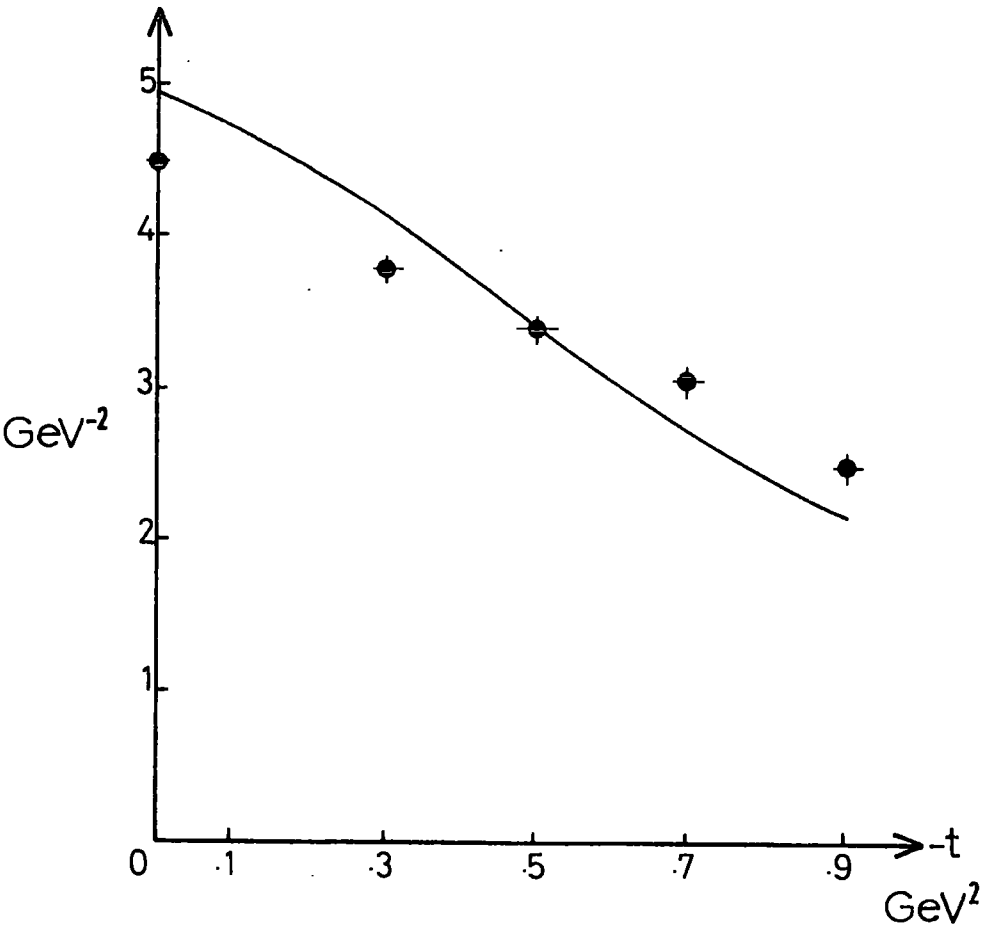

Fig. 3.4(b)

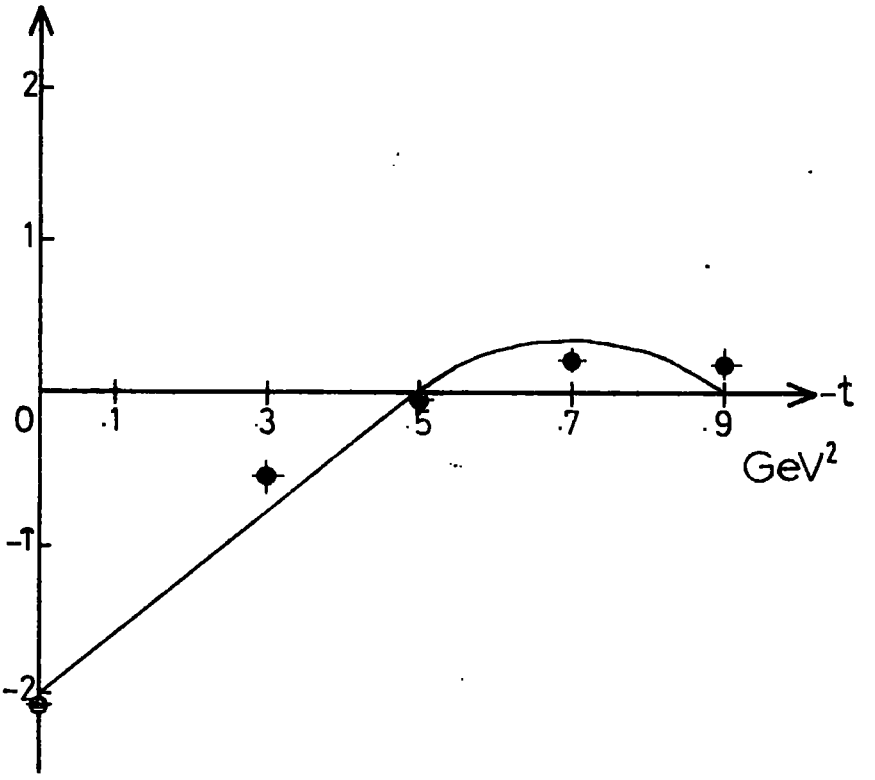

Fig. 3.4(c)

Chapter 4 : Electroproduction

Section 1 : Introduction

How does the analysis presented in the preceeding chapter generalise to electroproduction? We have seen that the resonances in photoproduction have an unexpected t-dependence, due principally to the P_{33}. This makes it difficult to relate the high and low energy regions. We have seen that our chosen high energy model does not fit the resonance FESR integral and has to be modified to take account of the over-absorption inherent in a SCRAM model extrapolated to low energies, and to account for the unexpected t-dependence of the resonances. Two questions immediately present themselves. Does the unexpected behaviour of the P_{33} persist to $k^2 \lesssim 0$? If so, can the daughter terms introduced in section 3 of the last chapter accommodate this?

However, as we saw in Chapter 1, neutral pion electroproduction has a peculiar interest. The dip at $-t \sim 0.5$ and the secondary maximum, such prominent features of photoproduction, are not present in the electroproduction differential cross-section, see fig. 1.6 (Brasse et al 1975). Since we have already identified problems in the region $-t=0.5$ for photoproduction, it is tempting to try to connect the two phenomena. The first part of this chapter

will describe this attempt.

In fact, we will find that the behaviour of the resonances cannot be extrapolated to account for the cross-section. Rather we will find that a simple modification of the absorbing amplitude which is used to generate the cut in the CF model provides an excellent phenomenological description of the electroproduction data for all $-t$ and for all $-k^2$.

Section 2a Resonance Integral

In section 1a of the last chapter we discussed the reasons for choosing Ball invariant amplitudes as the kinematic-singularity-free approximation to the single, double, and non-flip s-channel helicity amplitudes. The only amendment needed now is to parametrize the k^2 dependence of the resonances. The electromagnetic form factors of the resonances in pion electroproduction have been evaluated by Devenish and Lyth (1975) and we follow their determination.

Devenish and Lyth parametrized the k^2 dependence for each resonance multipole as a multiplicative form factor i.e.

$$M(s,k^2) = G(k^2)\, M(s) \qquad G(0) = 1$$

where $G(k^2)$ is itself a product of poles lying on the real k^2 axis: (There is a cut along this axis from a pseudothreshold of $2\mu^2$ to $(m_R+m)^2$

$$G(k^2) = \prod_{i=1}^{n} \left(1 - \frac{k^2}{k_i^2}\right)^{-1}$$

$$k_i^2 = k_1^2 + \frac{i}{n}\left(k_2^2 - k_1^2\right) \qquad 2\mu^2 \leq k_1^2 \leq k_2^2 \leq (m_R+m)^2 \qquad 4.1$$

The k_1^2 and k_2^2 are the variable parameters in Devenish and Lyth's fit to the electroproduction data.

However, the physical multipoles, considered as functions of k^2, have kinematic singularities and are subject to constraints at thresholds and pseudothresholds in k^2; and the form factors parametrized above apply only to multipoles with the singular behaviour divided out. That such problems arise can be seen from equation F3 in Appendix F:

$$M_L \sim \sum_i a_i X_i |\underset{\sim}{k}_i|^{L_i} \operatorname{Im} F_i$$

Since Fi is a singularity-free combination of Ball amplitudes, the singularities arise from the $X_i |\underset{\sim}{k}_i|^{L_i}$ factors and take the form of square-root branch points

as $k^2 \longrightarrow$ threshold or pseudothreshold (equation F2)

Defining $\phi_{\pm} = \left(1 - \frac{k^2}{(m_R \pm m)^2}\right)$ where m_R = mass of resonance, the threshold and pseudothreshold behaviour, $k^2 \longrightarrow m_R \pm m$, is determined by looking for the slowest decrease in F3 as $\phi_{\pm} \to 0$. In fact one may take linear combinations of the physical multipoles to remove the slowest decrease. Devenish and Lyth chose the following combinations:

$$\alpha_{l+} = \left(\frac{1}{l+1}\right)\left(l M_{l+} + E_{l+}\right) = \phi_-^{l}\, \phi_+^{l+1}\, \bar{\alpha}_{l+}$$

$$\beta_{l+} = \left(\frac{1}{l+1}\right)\left(M_{l+} - (l+2) E_{l+}\right) = \phi_-^{l}\, \phi_+^{l-1}\, \bar{\beta}_{l+}$$

$$S_{l+} = \phi_-^{l+1}\, \phi_+^{l}\, \bar{S}_{l+} \qquad 4.3$$

$$E_{l-} = \phi_+^{l-1}\, \phi_-^{l-2}\, \bar{E}_{l-}$$

$$M_{l-} = \phi_+^{l-1}\, \phi_-^{l}\, \bar{M}_{l-}$$

$$S_{l-} = \phi_+^{l}\, \phi_-^{l-1}\, \bar{S}_{l-}$$

It is only the reduced amplitudes $\bar{\alpha}_{L+}$, $\bar{\beta}_{L+}$, $\bar{S}_{L+}$, $\bar{E}_{L-}$, $\bar{M}_{L-}$, $\bar{S}_{L-}$ which are analytic functions of k^2, and which have the form factors described above (4.1).

The factor n in equation 4.1 now becomes, for each reduced multipole,

$$n_\alpha = L + \tfrac{1}{2}(n+1)$$

$$n_\beta = L + \tfrac{1}{2}(n-1) \qquad j = L + \tfrac{1}{2}$$

$$n_E = L + \tfrac{1}{2}(n-3) \qquad \text{4.4}$$

$$n_M = L + \tfrac{1}{2}(n-1) \qquad j = L - \tfrac{1}{2}$$

where the n on the RHS of Eq 4.4 is the asymptotic power of $(k^2)^{-1}$ required for the resonance contribution to the total cross-section. It is set equal to 3, except for the P_{33} which has n = 5.

As noted in appendix F, the scalar multipoles have to satisfy certain constraints at $q_\pm = 0$, these are accommodated by

$$S_{L+} = \frac{c\,|\underset{\sim}{k}(m_R, k^2)|}{(k^2-a)(k^2-b)}\, E_{L+}(k^2)$$

$$S_{L-} = \frac{c\,|\underset{\sim}{k}(m_R, k^2)|}{(k^2-a)(k^2-b)}\, \frac{1}{L}\left(M_{L-} - (L-1)\,E_{L-}\right) \qquad \text{4.5}$$

where

$$b = \left(3 m_R^2 + m^2 - a\right)\left(1 + a\left(m_R^2 - m^2\right)^{-1}\right)$$

$$c = 2 m_R^2 \left((m_R + m)^2 - a\right)\left(a - (m_R - m)^2\right)\left(m_R^2 - m^2 - a\right)^{-1}$$

and a is a free parameter

and $$S_{o+} = \frac{c\,|\underset{\sim}{k}(m, k^2)|}{k^2 - a} E_{o+}$$

It is interesting to note that the results sketched in Appendix F are identical to those obtained by Devenish, Eisenschitz and Komer (1977). These authors derived the multipoles' constraint structure by expressing the reaction's vertices in terms of kinematic covariants. Their purpose, however, was to obtain a universal form factor behaviour, the phenomenological parametrisation outlined above is more than adequate for our purposes.

Devenish and Lyth published several fits to the electroproduction data. They found that the parameters of their fourth fit yielded the best representation of the coincidence data for $ep \to ep\pi^o$, and recommended that these parameters be used. We have therefore used this set of parameters. They are listed in table 4.1. It is doubtful

that the FESR would be seriously affected by using other fits from Devenish and Lyth's paper. Having amended the photoproduction program to take account of the k^2 dependence noted above, the FESR integrals were evaluated for $k^2 = -0.22, -0.55, -0.85$. The results are graphed on figure 4.1.

It may be seen that the integrals all have a reasonably smooth k^2 dependence. In particular, there seems to be no evidence for a fixed pole in any of the amplitudes. Fixed poles are not excluded by unitarity, when we work with a process to first order in the electromagnetic coupling constant. (However, such poles would only be expected in pion electroproduction if the pion is elementary, according to the parton model (Brodsky, 1972)). For the single flip amplitude the magnitude of the integral increases for $-t \gtrsim 0.5$, the zero moving out in t as $-k^2$ increases. In view of the previous chapter's discussion, such behaviour is perhaps not surprising.

Section 2b Amplitudes' Behaviour

In fact some qualitative explanation of this behaviour of neutral pion electroproduction can be found in terms of the quark model (Moorhouse 1975). Using naive constituent quark models one can calculate the transition amplitude for

radiative decay of an N^* to the nucleon ground state. This is simply the time reversed reaction to the transition of interest to us here. In the quark model description, certain helicity amplitudes are preferentially excited, contributing to the removal of the zero from $-t \sim 0.5$ for those amplitudes.

It is usually assumed that the N^* is de-excited by photon emission from a single quark: the orbital angular momentum, l, of the N^* thus resides on that quark and the photon is emitted in an $M_L \pm 1$ or E_L state. To first order, these naive constituent models give the correct answer for radiative transitions in photoproduction. However difficulties arise for $k^2 \neq 0$ even in the neighbourhood of photoproduction. Indeed, even the nucleon form factor is an unsolved problem for quark models in the region $-k^2 < 2\ \mathrm{GeV}^2$. For larger k^2, asymptotic expressions may be used and seem to yield answers more in accord with experiment.

Using a non-relativistic harmonic oscillator model, Close and Gilman derived expressions for the k^2 behaviour of the $N^* \to \gamma p$ helicity amplitudes for the D_{13} and F_{15} resonances.

$$A_{1/2} = a\left(\frac{9}{\alpha^2}|\underline{k}|^2 - 1\right) \exp\left(-|\underline{k}|^2/6\alpha^2\right) \qquad 4.6$$

$$A_{3/2} = -\sqrt{3}\, a \exp\left(-|\underline{k}|^2/6\alpha^2\right)$$

These amplitudes are linear combinations of the multipoles used throughout the rest of this work; the above simple form occurs in the proton Breit frame, elsewhere we have used the centre of mass frame. α is the spring coupling constant for the harmonic oscillator, g is the quark gyromagnetic ratio, and a contains the quark magnetic moment.

It was observed that : consistently with other aspects of the quark model (Copley et al 1969).

leads to the vanishing of $A_{\frac{1}{2}}$ in photoproduction. This occurs for both the D_{13} and F_{15}, and is borne out by experiment. The exponential terms in the above expression are most model dependent and thus least reliable, but since they are common to both helicities we can make reasonable statements about the ratio of the two. Clearly, $A_{\frac{1}{2}}$ increases with respect of $A_{3/2}$ as the photon moves further off-shell, and for $|\underset{\sim}{k}|^2 \sim 1$ the D_{13} should be predominantly helicity $\frac{1}{2}$. However the helicity $\frac{1}{2}$ amplitude does not give a zero at -t = 0.5. This switch from helicity 3/2 to helicity $\frac{1}{2}$ means that the magnetic multipole decreases more slowly than the electric with k^2. The Devenish and Lyth analysis agrees qualitatively with the quark model's predicted helicity structure.

The argument has been taken one stage further by Alcock et al (1977). These authors showed that the form factor behaviour found by Devenish and Lyth was compatible with the algebra of the relativistic quark model (Feynman et al, 1971). Guided by this model, they expressed the helicity amplitudes as linear combinations of form factors (three for the transverse, and two for the longitudinal, amplitudes). They did not derive a functional form for these but regarded them as free parameters for all the resonances in the l=1 multiplet (with a second set of five parameters for the l=2 multiplet). They found that the quark model could fit the Devenish and Lyth analysis very well and that there was no deterioration in quality of fit as $-k^2$ increased.

In figure 4.2 we present the form of the resonance amplitudes for selected values of t and k^2. That the P_{33} still dominates the amplitudes can clearly be seen.

Section 2c : Regge FESR

The Collins and Fitton Regge absorption model used in this work has no explicit k^2 dependence. In our modification there is of course, an dependence implicit in the definition of

$$\nu = s - m^2 + \frac{t - \mu^2 - k^2}{2}$$

Since we have adopted Regge behaviour in ν (not s) the Regge integral does vary with k^2. This is demonstrated in figure 4.1.

Before any comparison can be made with the resonance FESR, there is one further factor. Guided by the ideas of vector meson dominance, we multiply the Regge amplitude by an effective vector meson propagator (see equation 1.1). Our model amplitudes are therefore, the sum of the CF pole-and-cut exchanges and the daughter terms of equation 3.13:

$$A(k^2) \sim \left(1 - \frac{k^2}{m_v^2}\right)^{-1} \left\{ R(\nu) + D(\nu) \right\}$$

If VDM were taken literally then a separate ρ-propagator should multiply the ω-exchange term of the CF model, and an ω-propagator the ρ-term. However, we have already obscured such distinctions by using an effective daughter-term. We therefore treat m_v^2 as a free parameter and assume the propagator represents the effect of several vector mesons.

In fact, m_v^2 is the only parameter which can be varied to ensure the prescribed equality between the resonance integral and the Regge model. Unfortunately, it is easy to show that such agreement cannot be obtained

simply by varying m_v^2 . It turns out that the modified -t dependence of the resonances necessitates a similar alteration to the Regge side of the equation.

In the preceeding section we saw that the variation of t with k^2 followed from the anomalous behaviour of the P_{33}, D_{13} and the F_{15}. In Chapter 3 we introduced the daughter terms to accommodate such a low-energy effect. Once again, therefore, we use the daughter terms to improve the agreement. The simplest parametrization was found to be (referring to equation 3.13)

$$
\begin{aligned}
G^d_{++}(k^2) &= G^d_{++}(0)\,(1 - g_{++}k^2) \\
b(k^2) &= b(0)\,(1 + B k^2) \\
G^d_{+-}(k^2) &= G^d_{+-}(0)\,(1 - g_{+-}k^2) \\
a_{+-}(k^2) &= a_{+-}(0)\,(1 + A_{+-}k^2) \\
G^d_{-+}(k^2) &= G^d_{-+}(0)\,(1 - g_{-+}k^2) \\
a_{-+}(k^2) &= a_{-+}(0)\,(1 + A_{-+}k^2)
\end{aligned}
\qquad 4.7
$$

The agreement between the two sides of the FESR equation can be seen in figure 4.1. The parameters are listed in table 4.2.

Section 3 : Electroproduction cross-section

As discussed in Chapter 1, the high energy differential cross-section for neutral pion electroproduction was considered an interesting and possibly crucial experiment. That the actual measurements confounded all expectations has also been noted. The experiments confirmed the conventions of dominance by natural parity exchange, and justified the neglect of scalar terms in the cross-section. The disappearance of the dip and secondary maximum, which occurs at small $-k^2$ presented something of a mystery, however.

Two related attempts have been made to try to understand the puzzling electroproduction behaviour. In the first, Vanryckeghem (1976) carried out an FESR analysis. He confirmed that in the resonance region, at least, the contribution of scalar amplitudes is small enough to be neglected. He also found no evidence to suggest that a fixed pole might contribute to electroproduction. He modified the photoproduction model of Barker, Donnachie and Storrow (BDS, 1974) to obtain a fit to electroproduction differential cross-section. Following BDS, Vanryckeghem chose a Regge-style paramatrization of the imaginary parts of his amplitudes (calculating real parts from the phase-energy relation rather than FTDR as BDS had done for photoproduction).

$$\mathrm{Im}\, A_i(\nu, t, k^2) = \sum_j C_{ji}(t, k^2)\, \nu^{\alpha_j - 1}$$

$i = 1,3 \qquad j = 1,3,4.$

(Note that these amplitudes are t-channel helicity amps) where

$$\alpha_1 = 0.477 + 0.9t$$
$$\alpha_3 = 0.477 + 0.33t$$
$$\alpha_4 = -0.177 + 0.5t$$

α_1 represents an effective ω/ρ pole, α_3 the corresponding cut, and α_4 is a low-lying singularity. Vanrykeghem chose to explain the k^2 dependence of the cross-section in terms of this fourth component. (It is interesting to note that BDS claimed this could be replaced by a J=0 fixed pole in photoproduction). He allowed the residue and the Regge slope to vary as free parameters for the three values of $k^2 \neq 0$. Vanrykeghem thus obtained a fit to the FESR and to $\frac{d\sigma}{dt}$, but at the cost of a strange $|k|^2$ dependence of his free parameters. He chose to explain the electroproduction data in terms of a cancellation between ω -exchange and a strongly enhanced singularity lying low in the j-plane. He showed that, in this model, the dip's absence from $\frac{d\sigma}{dt}$ persisted up to at least $s = 12\ \mathrm{GeV}^2$. But it is apparent that at higher energies

the low-lying singularity will disappear and the conventional photoproduction-like form will re-assert itself.

Barker and Storrow (1978) later extended the work of BDS. As part of that, they extended their model to electroproduction also. Guided by general ideas about cut enhancement as a function of k^2 (Irving, 1975) they parametrised the k^2 dependence of their cut residues as

$$G(k^2,t) = (1 + A\,(1 - e^{-Bk^2}))\,G(o,t) \qquad 4.8$$

Like Varnykeghem they also had an overall k^2 dependence in the form of the ρ-meson propagator, this being common to all terms.

Barker and Storrow claim a qualitative success for their cut enhancement model, using $A = 0.5$ and $B = 8$. But they are not able to explain the $k^2 = -0.22$ data, no matter how rapidly the cut enhancement switches on. They attribute this to low energy effects.

Since these two analyses stress the low-energy contributions to the electroproduction cross-section, and since we have already seen some interesting features in the t and k^2 dependence of the resonances, one might look

to the electroproduction model of section 3 to provide an explanation of the differential cross-section. However, it can easily be seen that this does not happen. The daughter parametrisation of chapter 3 was chosen for two reasons. It had to mimic the very low energy behaviour of some resonances. Since the Collins and Fitton model provided a good fit to the photoproduction cross-section the daughters had to fall sufficiently fast with energy not to damage the high energy fit. For these two reasons, it turns out that the daughter contributions are too small to effect the drastic alteration in the behaviour of the cross-section in going from photoproduction to electroproduction.

In fact it is possible to obtain a very satisfactory fit to the electroproduction cross-section for all values of $-k^2$, with only a simple modification of the CF model. Our path is somewhat similar to that of Barker and Storrow in that we modify the behaviour of the cut term as a function of k^2. This is in spite of the observation by Barker and Storrow that cut enhancement depends on having predominantly real cuts rather than as we have Michigan-style phases.

Modifying the "high-energy" part of the Regge model means, of course, that the parametrization of equation 4.7

will no longer hold. It thus becomes necessary to modify both parts of our Regge model simultaneously to obtain a fit to the cross-section and to the FESR simultaneously. We shall discuss them separately and since the modification of the CF model introduces some unexpected points we will deal with it first.

We choose to modify the absorbing $P + P'$ amplitude as a function of k^2 as follows. For $k^2=0$, equation 3.8 gives us

$$A = i\,\sigma_T\, s\, e^{c_P t} + \bar{E}_0\, e^{c_{P'} t}\, s_0\, \alpha_{P'}(t) \left(e^{-\frac{i\pi}{2}}\, \frac{s}{s_0} \right)^{\alpha_{P'}(0)}$$

$$c_P = h_1 + \alpha'_P \left(\log \frac{s}{s_0} - \frac{i\pi}{2} \right) \qquad c_{P'} = h_2 + \alpha'_{P'} \left(\log \frac{s}{s_0} - \frac{i\pi}{2} \right)$$

We alter both the residue and the t-dependence of the absorbing amplitude

$$\sigma_T(k^2) = \sigma_T(0)\,(1 - r k^2) \qquad E_0(k^2) = E_0(0)\,(1 - r k^2)$$

4.9

$$h_1(k^2) = h_1(0)\,(1 - H k^2) \qquad h_2(k^2) = h_2(0)\,(1 - H k^2)$$

The only other k^2 dependence comes from the factor $\left(1 - \frac{k^2}{m_v^2}\right)^{-1}$ which is common to both poles and cuts. There are thus only three parameters in this extension of the CF model r, H, m_v^2.

This parametrization of the cuts is common to all the helicity amplitudes. The remarkably good fit to the electroproduction data is demonstrated in figure 4.3. The three parameters for this fit are listed in column (a) of table 4.3.

As mentioned above, this modification to the high-energy part of the model is reflected in a modification to the parametrization of equation 4.3. This part of the fit is displayed in figure 4.4 and the revised parameters are listed in table 4.4. The best fitting parametrization is (see equations 3.13 and 4.7)

$$
\begin{aligned}
G^{d}_{++}(k^2) &= G_{++}(0)\left(1 - g_{++}k^2\right) \\
a_{++}(k^2) &= a_{++}(0)\left(1 + A_{++}k^2\right) \\
b(k^2) &= b(0)\left(1 + Bk^2\right) \\
G^{d}_{+-}(k^2) &= G^{d}_{+-}(0)\left(1 - g_{+-}k^2\right) \\
a_{+-}(k^2) &= a_{+-}(0)\left(1 + A_{+-}k^2\right) \\
G_{-+}(k^2) &= G_{-+}(0)\left(1 - g_{-+}k^2\right) \\
a_{-+}(k^2) &= a_{-+}(0)\left(1 + A_{-+}k^2\right)
\end{aligned}
\qquad 4.10
$$

However, a fit to the differential cross-section of equal quality to that obtained by equation 4.9 is possible through modifying only the single flip amplitude. In fact we took a functional form identical to that of equation 4.9 but assumed it applied only to the single flip amplitude cut. Thus the other helicity amplitudes had no k^2 dependence. The parameters for this fit are listed

in column (b) of table 4.3. As can be seen, these parameters are very close in magnitude and sign to those of fit (a) which were common to all the cut amplitudes. It happens therefore that the single flip parametrization of equation 4.10 is adequate to describe the FESR.

The two fits to the differential cross-section agree so closely that we have not plotted the second one - figure 4.3 will suffice. A chi-squared of 1.05 per point (30 points) was obtained for both fits to the cross-section. The implications of these fits, and of the value of the parameters, will be examined in the next chapter.

Table 4.1

Resonance form factor parameters

Resonance	Mass	Multipole	λ_1^2	λ_2^2	a
S_{11}	1.505	E_{0+}	3.63	4.02	
		S_{0+}			0.09
S'_{11}	1.688	E_{0+}	5.16	5.18	
		S_{0+}			0.04
P_{33}	1.232	α_{1+}	0.545	4.715	
		β_{1+}	0.43	4.715	
		S_{1+}			2.867
P_{13}	1.850	S_{1+}			3.34
F_{37}	1.940	α_{3+}	1.61	4.0	
		β_{3+}	0.11	0.43	
		S_{3+}			0.04
P_{11}	1.434	M_{1-}	0.04	0.041	
		S_{1-}			0.046
D_{13}	1.514	E_{2-}	0.82	1.59	
		M_{2-}	0.9	1.92	
		S_{2-}			2.19
D'_{13}	1.680	E_{2-}	6.85	6.851	
		M_{2-}	0.04	0.045	
		S_{2-}			6.85
D''_{13}	1.971	E_{2-}	0.08	0.25	
		M_{2-}	0.82	2.29	
		S_{2-}			8.46

Table 4.1 Continued

Resonance form factor parameters

Resonance	Mass	Multipole	λ_1^2	λ_2^2	a
D_{33}	1.649	E_{2-}	1.09	1.94	
		M_{2-}	4.1	4.12	
		S_{2-}			6.69
F_{15}	1.682	E_{3-}	0.53	1.51	
		M_{3-}	1.14	2.98	
		S_{3-}			6.59

Table 4.2 Coefficients of k^2 for daughter parametrisation of equation 4.7 and figure 4.1.

g_{++}	2.34
g_{-+}	1.27
g_{+-}	4.92
A_{-+}	0.97
A_{+-}	47.2
B	0.919
m_v^2	0.5

Table 4.3 Parameter of equation 4.9 yielding fit to electroproduction cross-sections displayed on figure 4.3.

	(a)	(b)
m_v^2	0.68	0.54
r	1.4	2.54
H	15.25	19.1

The parameters of column (a) result from modifying the absorptive contribution to all the amplitudes; column (b) results from modifying only the single flip amplitude.

Table 4.4 Revised parameters for daughter pole (equation 4.10) giving fit displayed on figure 4.4.

g_{++}	2.38
g_{-+}	1.26
g_{+-}	0.506
A_{++}	0.886
A_{-+}	0.649
A_{+-}	48.1
B	0.252
m_v^2	0.68

Figure Captions

Fig 4.1 The results of the electroproduction FESR analyses for $k^2 = -0.22, -0.55, -0.85$. The results of the integrals over the resonances are plotted as full points at $t=0, -0.3, -0.5, -0.7, -0.9$. The integrals of the Regge model of equations 3.6 - 3.9 are plotted as a broken line to display the k^2 dependence resulting from the ν behaviour, see page 80. The solid line is the fit resulting from equation 4.7 of the Collins and Fitton model extended to incorporate k^2 dependent daughter terms.

a) is the FESR of the natural parity combination of the single flip amplitudes
b) is the double flip amplitude FESR
c) is the non-flip amplitude FESR

Fig 4.2 The resonance amplitudes as a function of centre of mass energy for selected values of t and k^2.

Fig 4.3 The fit to the electroproduction differential cross-section of the parametrization of equation 4.9, fit (a).

Fig 4.4 The fit to the FESR resulting from the parametrizations of equations 4.9 and 4.10. As in figure 4.1 the resonance integral is plotted as full points and the Regge fit is the solid line. The integral of the modified Collins and Fitton model of equation 4.9 (i.e. without the daughter terms) is shown as the broken line.

a) is the natural parity combination of the single flip amplitudes

b) is the double flip amplitude FESR

c) is the non-flip amplitude FESR

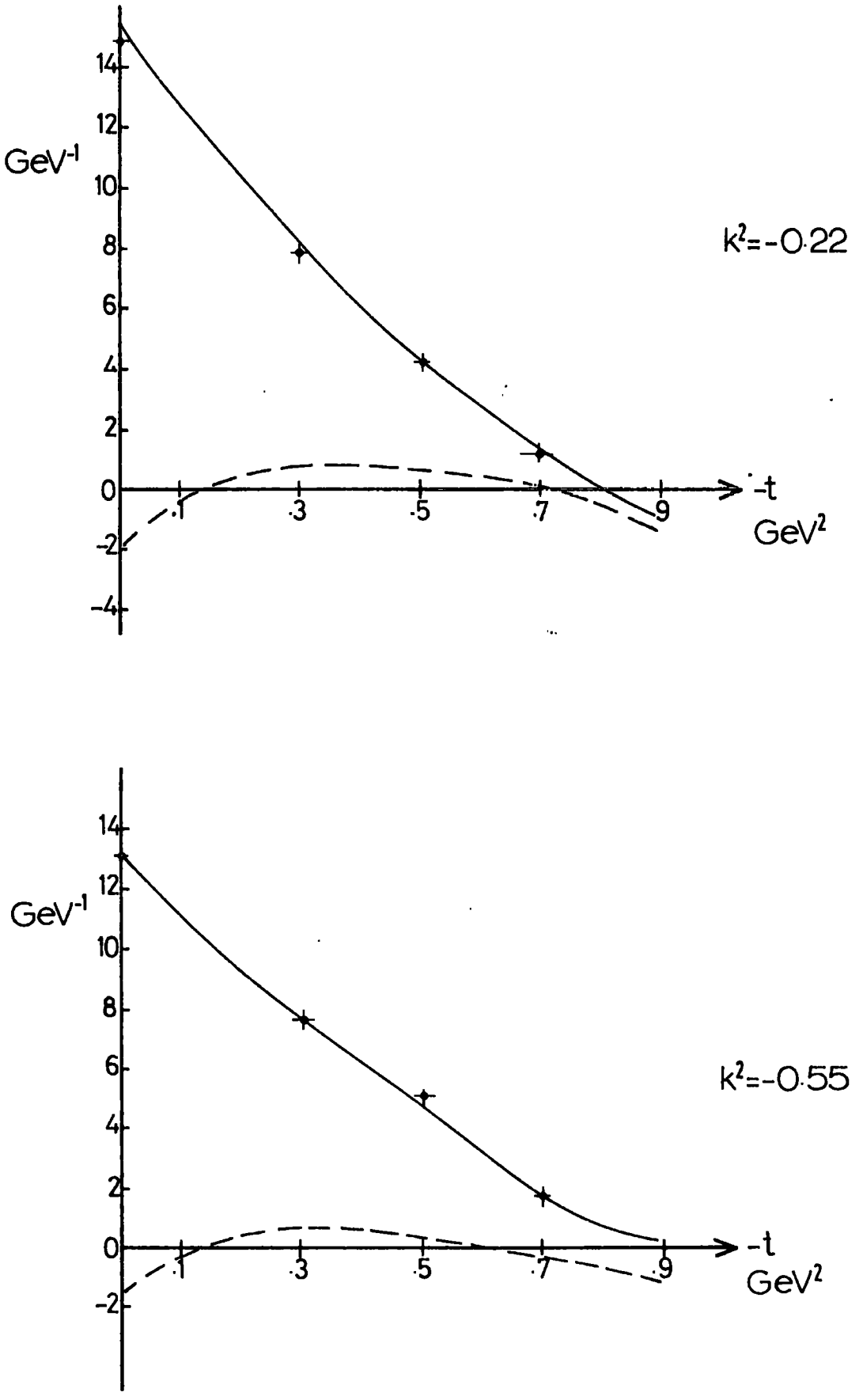
GeV⁻¹
14
12
10
8
6
4
2
0
-2
-4
.1
.3
.5
.7
.9
-t
GeV²
k²=-0.22
GeV⁻¹
14
12
10
8
6
4
2
0
-2
.1
.3
.5
.7
.9
-t
GeV²
k²=-0.55

Fig. 4.1(a)

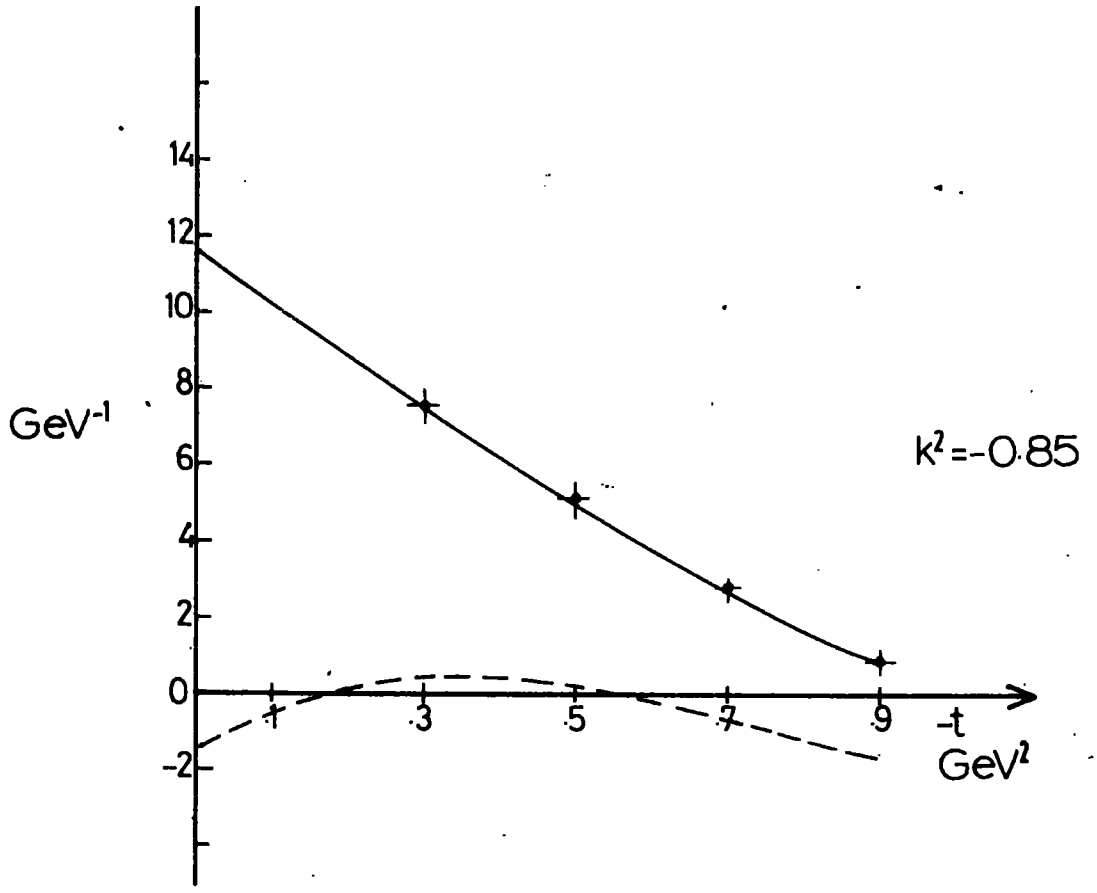

Fig. 4.1(a)

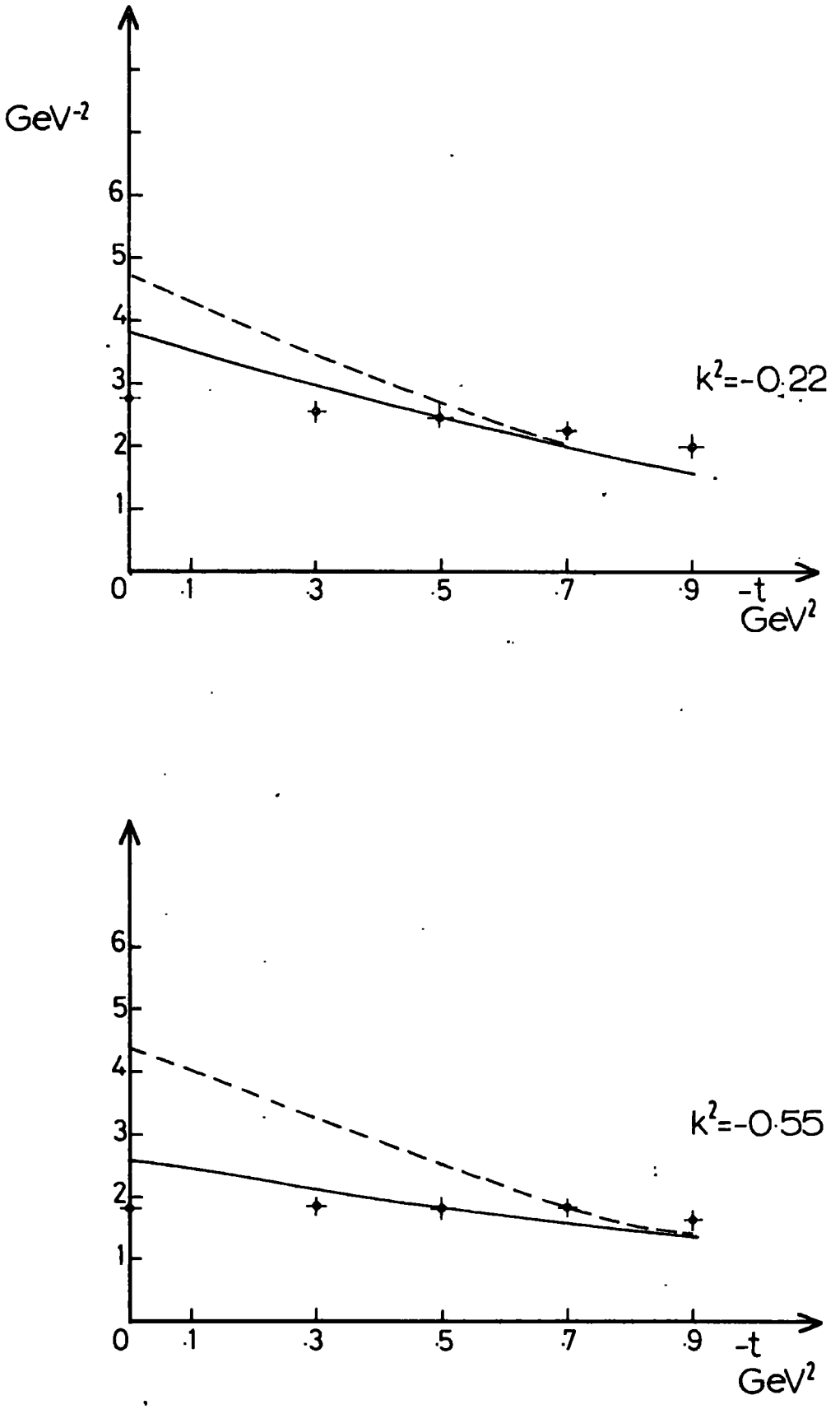

Fig.4.1(b)

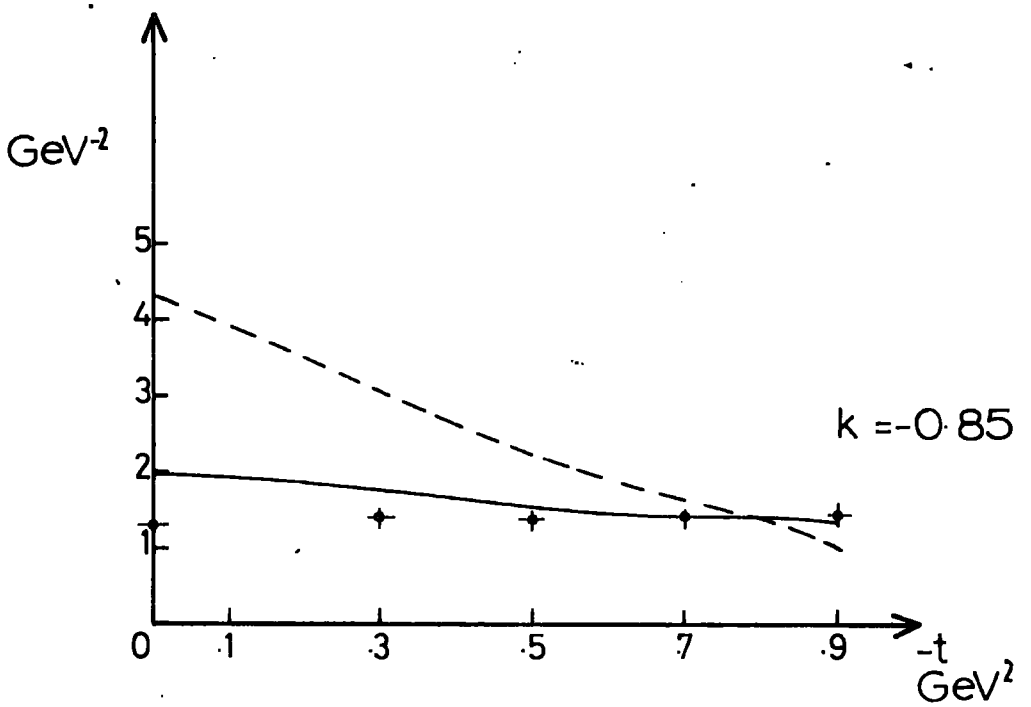

Fig. 4.1(b)

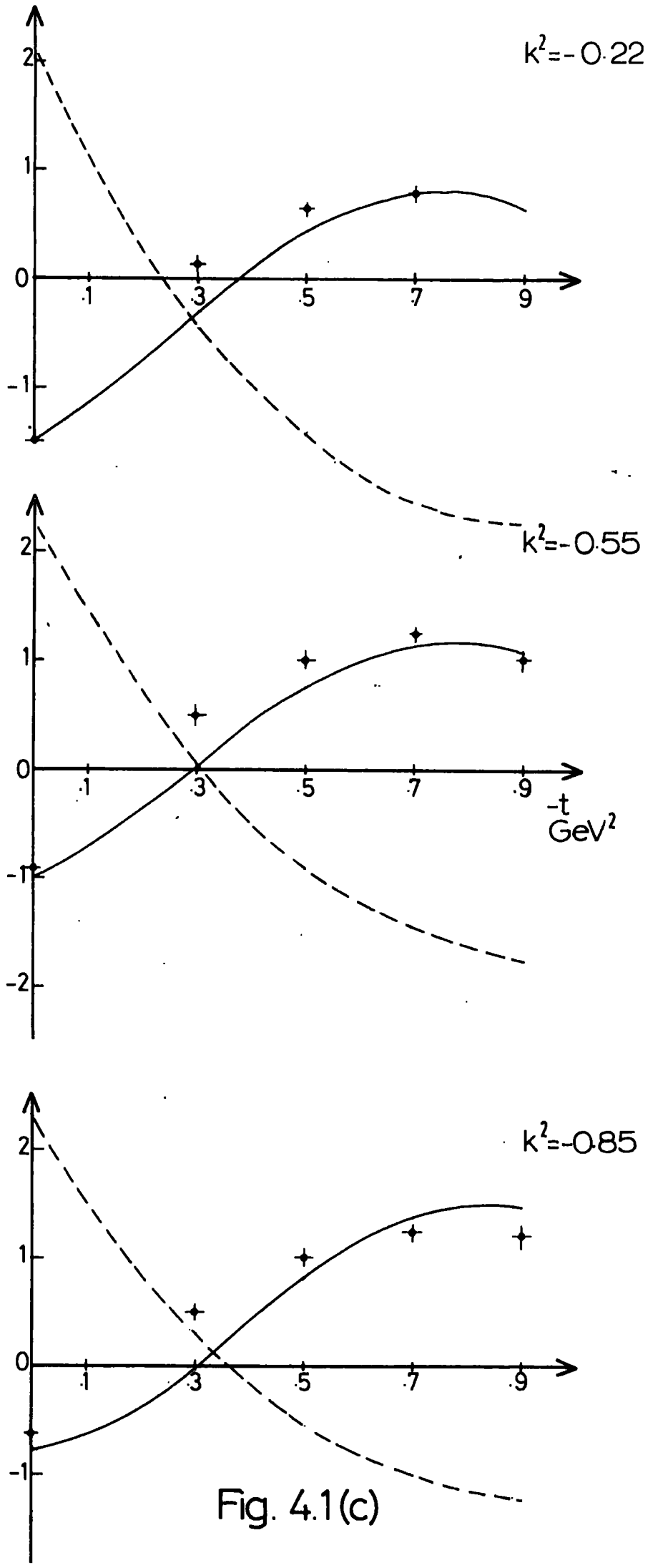

Fig. 4.1(c)

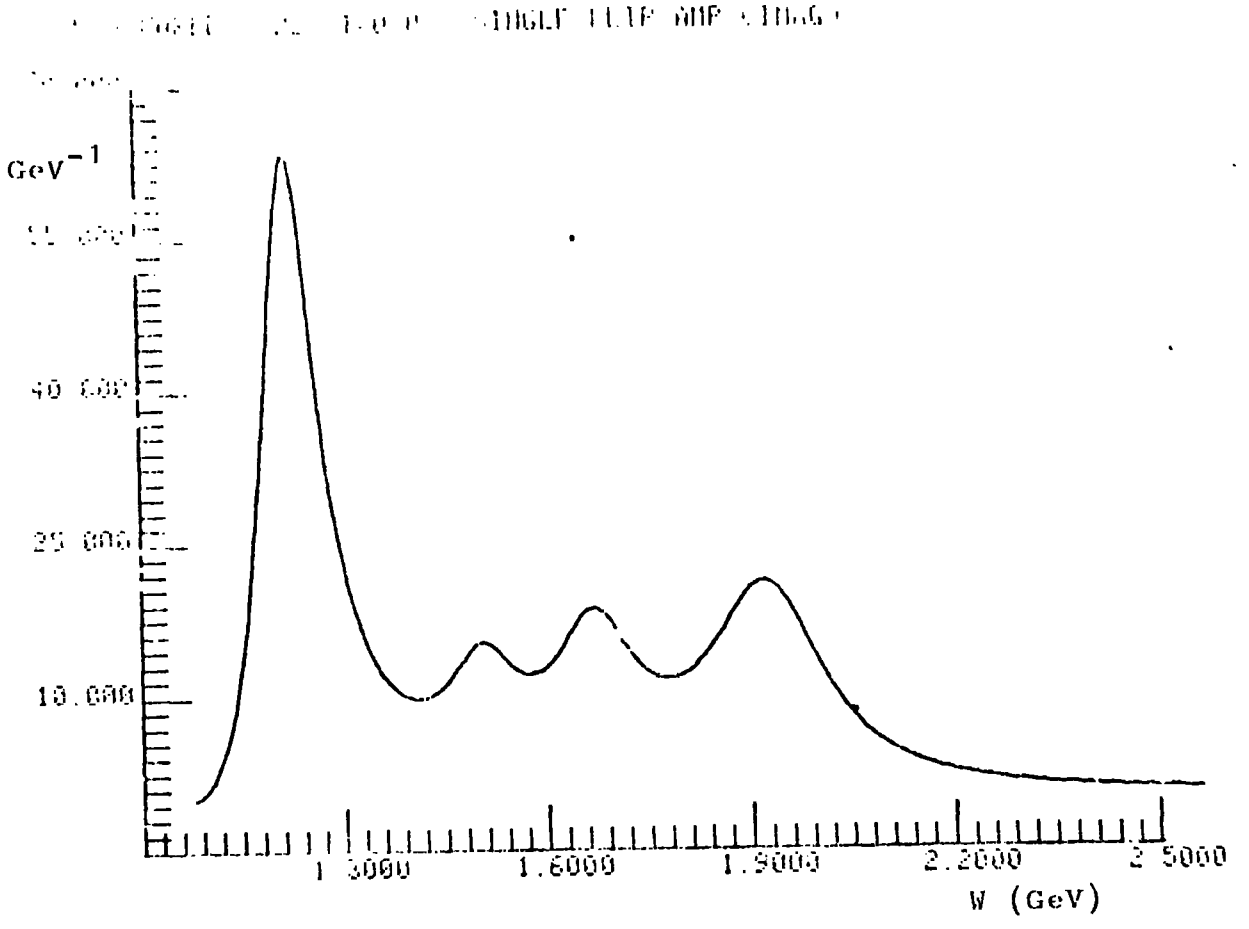
GeV^{-1}
40.000
25.000
10.000
1.3000
1.6000
1.9000
2.2000
2.5000
W (GeV)

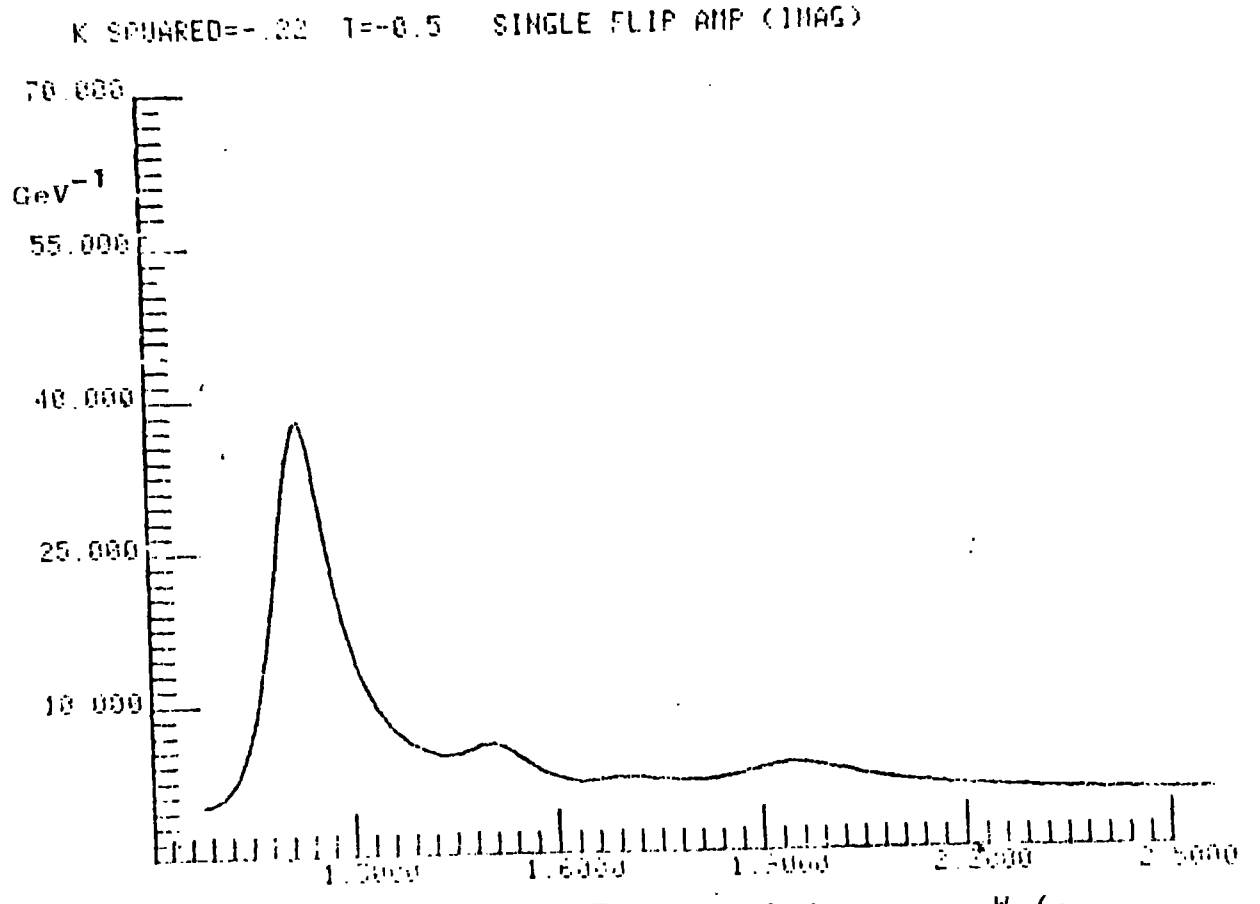
K SQUARED=-.22 T=-0.5 SINGLE FLIP AMP (IMAG)
70.000
GeV^{-1}
55.000
40.000
25.000
10.000
1.3000
1.6000
1.9000
2.2000
2.5000
W (GeV)

Fig 4.2(a)

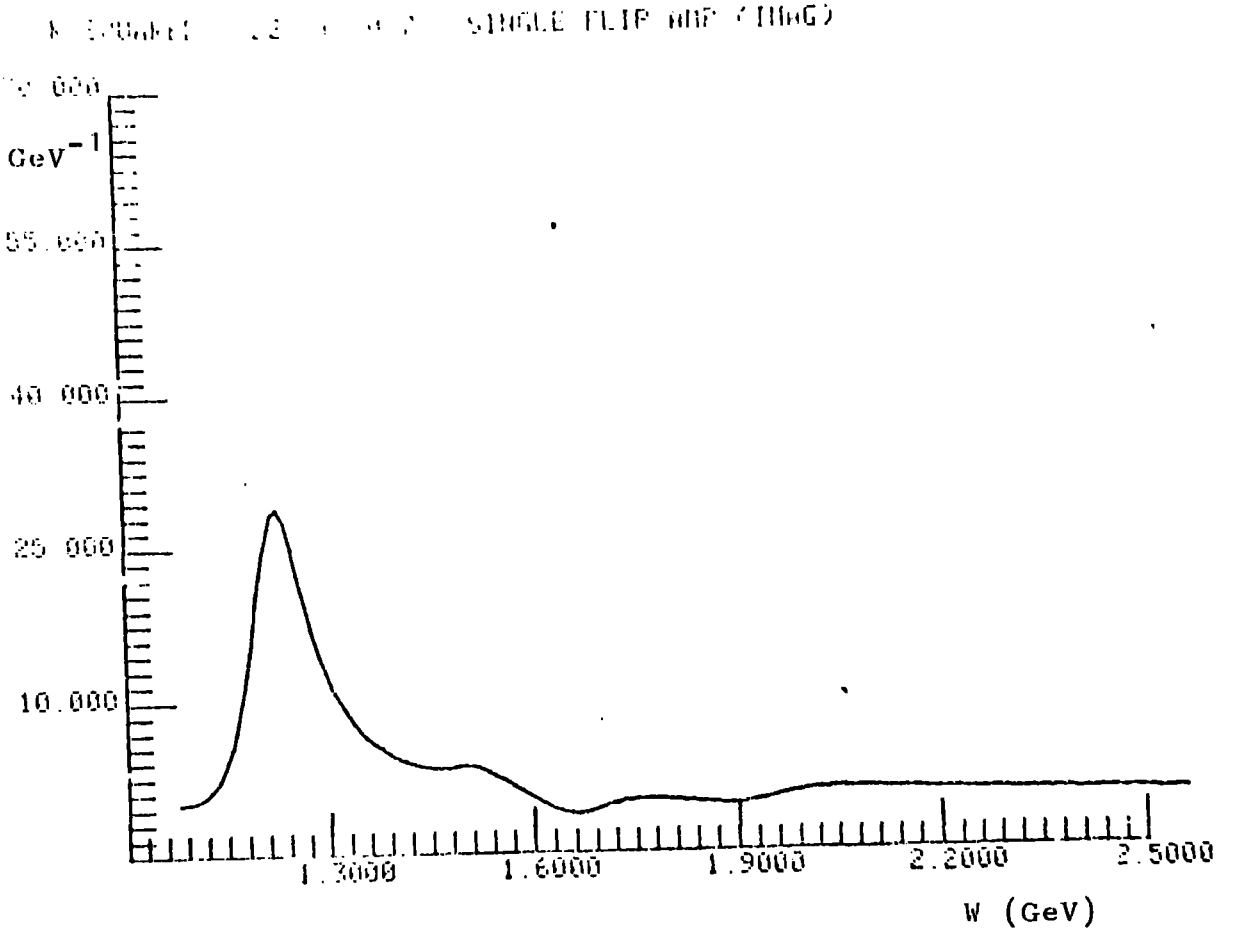
SINGLE FLIP AMP (IMAG)
GeV^{-1}
40 000
25 000
10.000
1.3000
1.6000
1.9000
2.2000
2.5000
W (GeV)

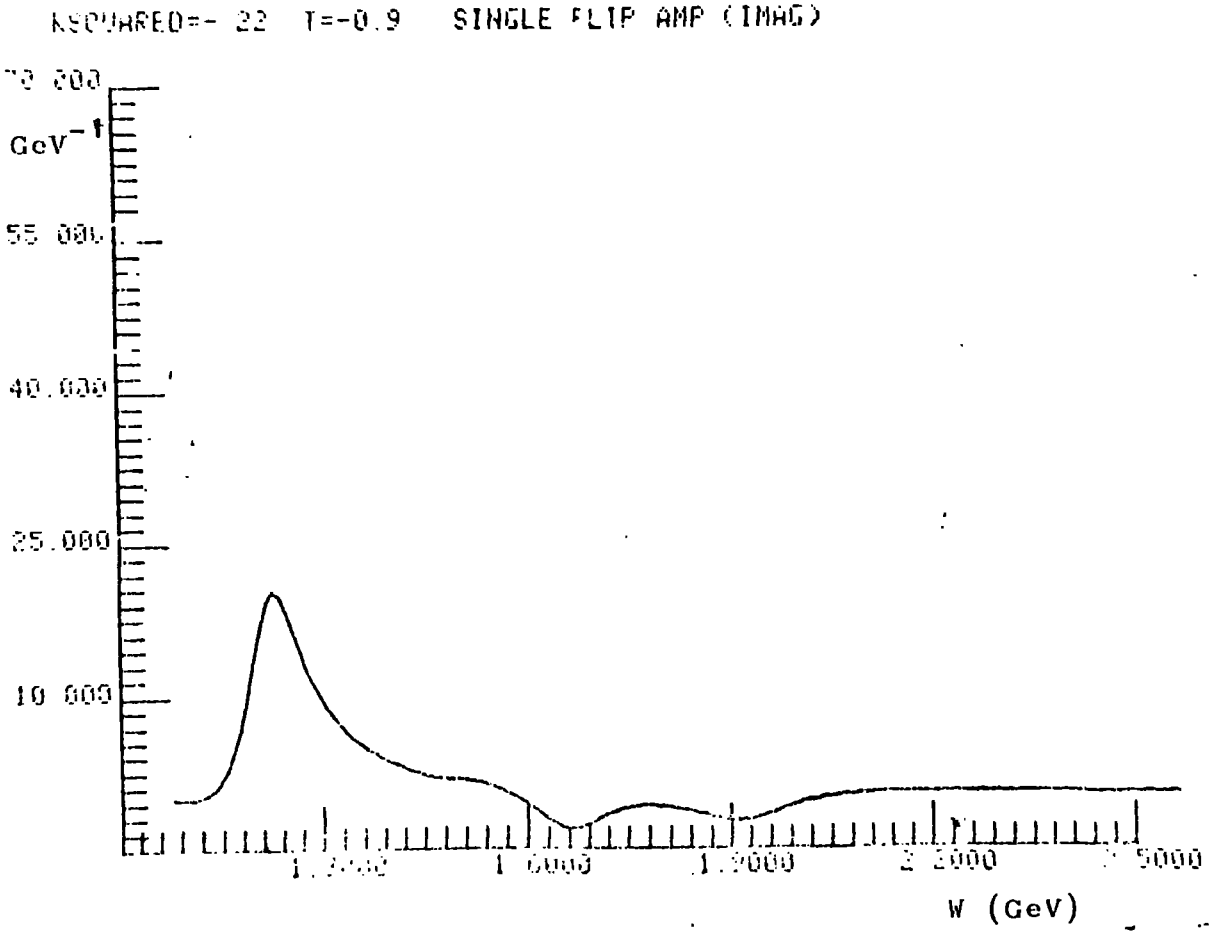
SINGLE FLIP AMP (IMAG)
GeV^{-1}
55 000
40.000
25.000
10 000
W (GeV)

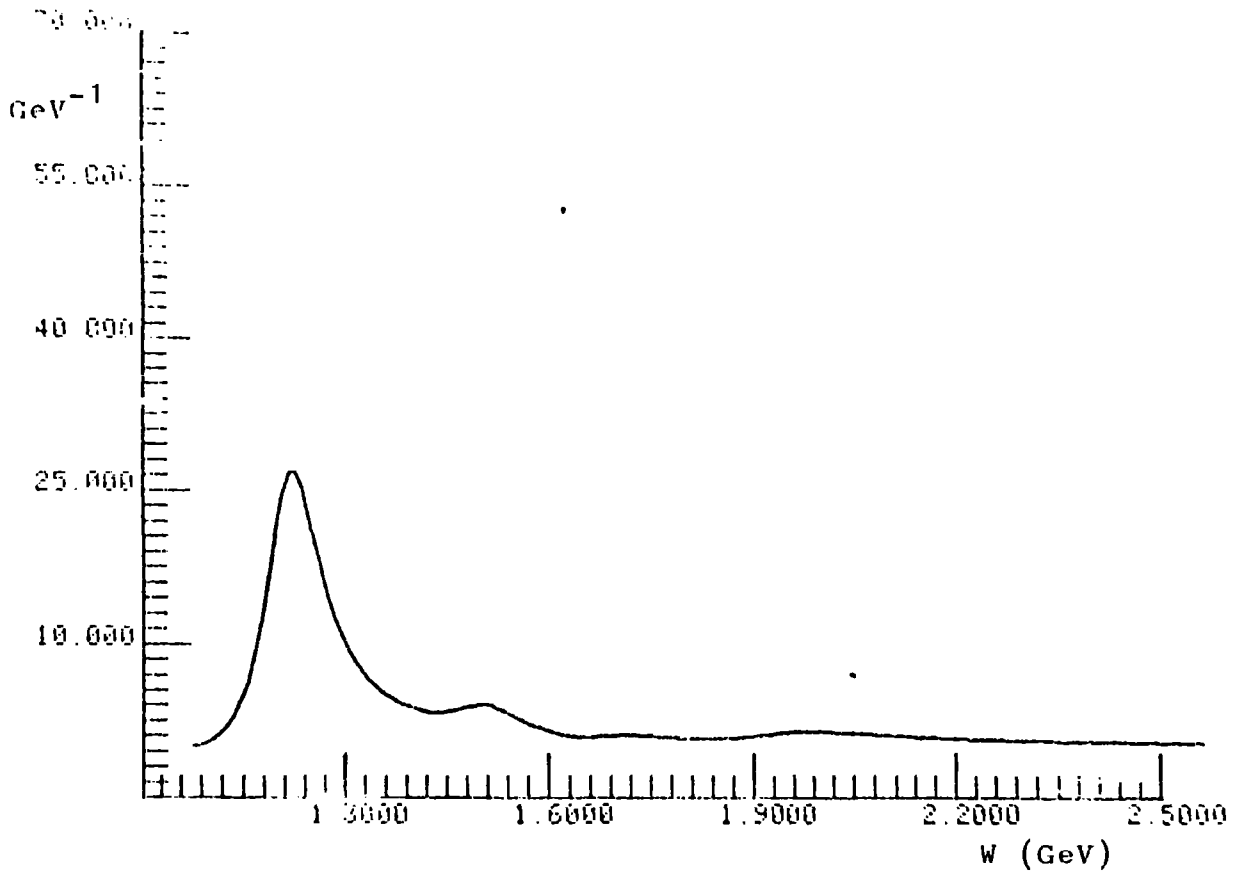

K SQUARED=- 55 T=-0.9 SINGLE FLIP AMP (IMAG)

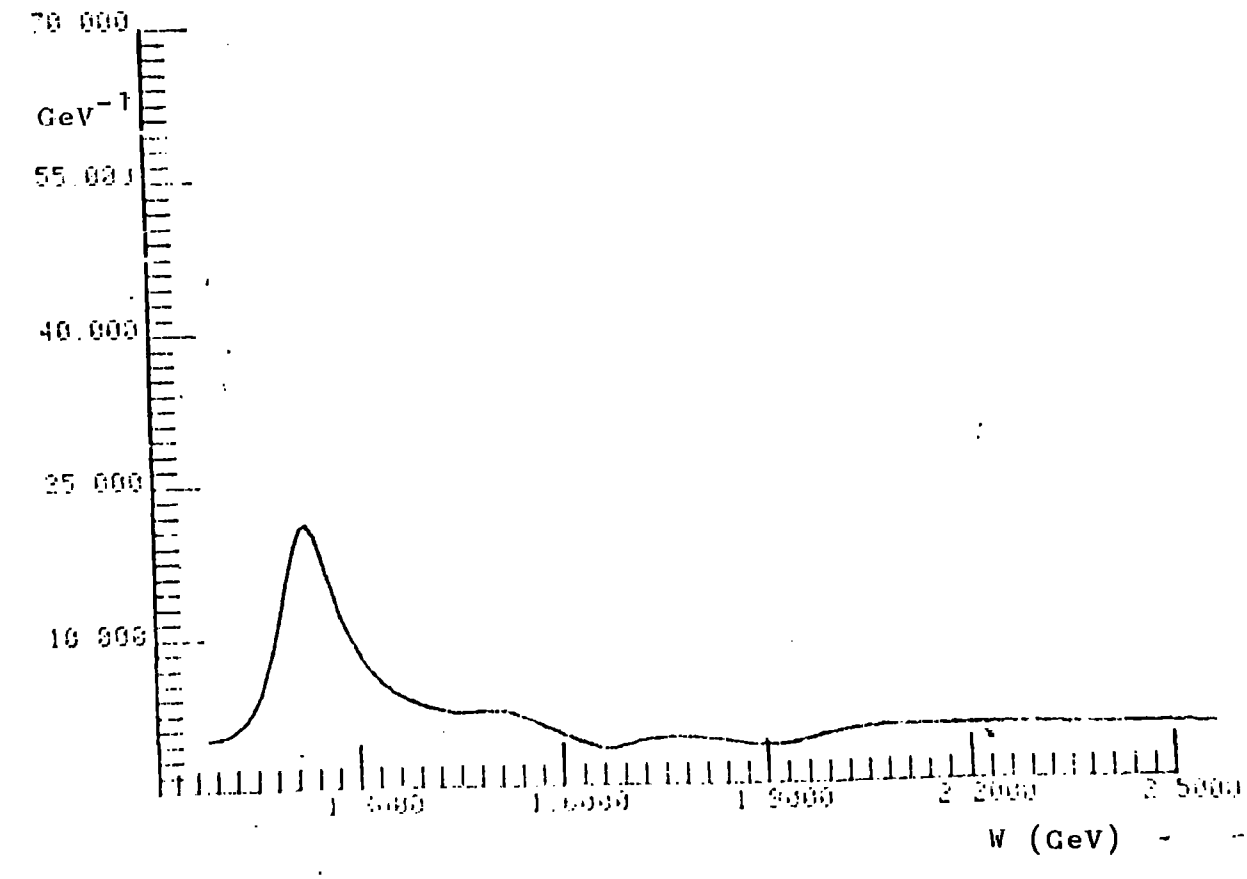

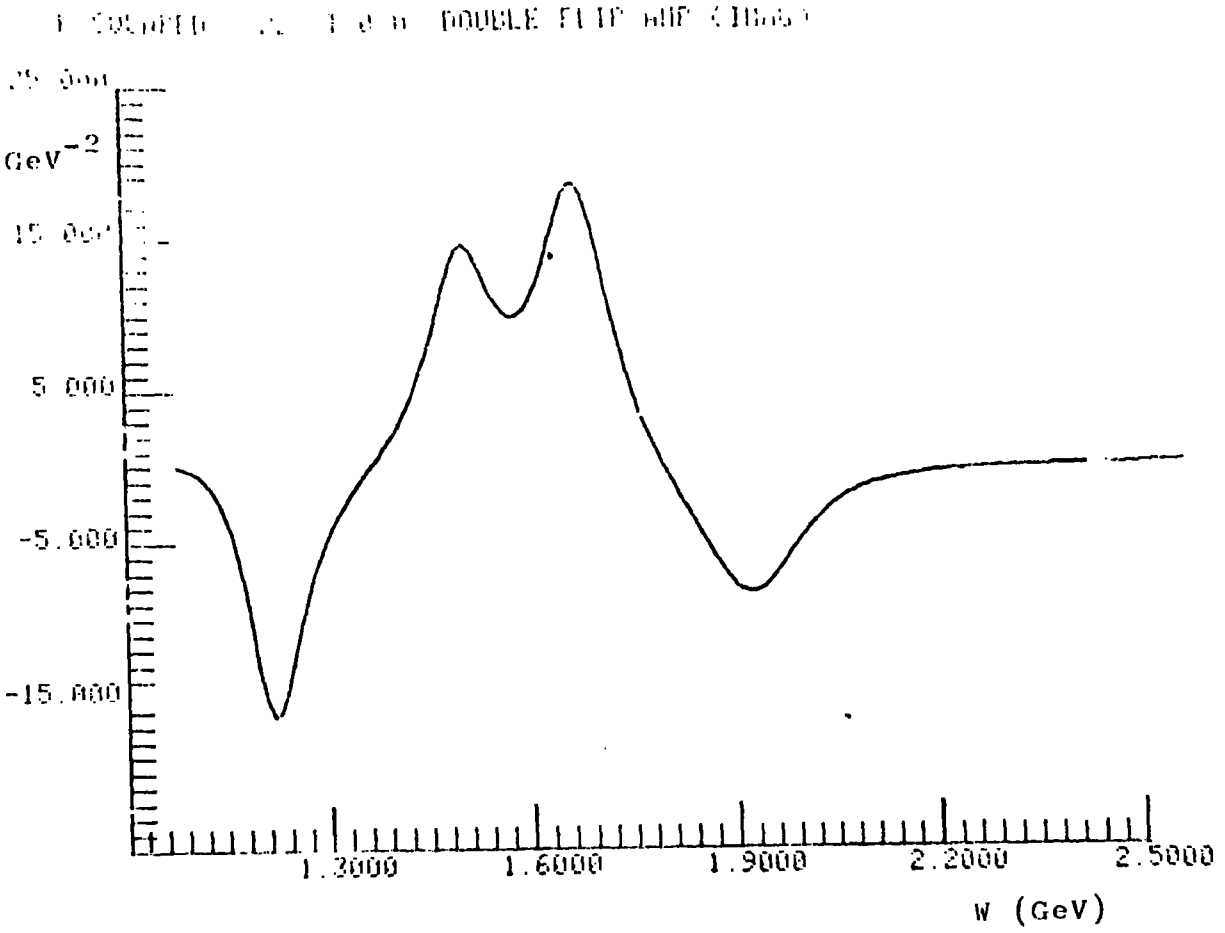
GeV^{-2}
5.000
-5.000
-15.000
1.3000
1.6000
1.9000
2.2000
2.5000
W (GeV)

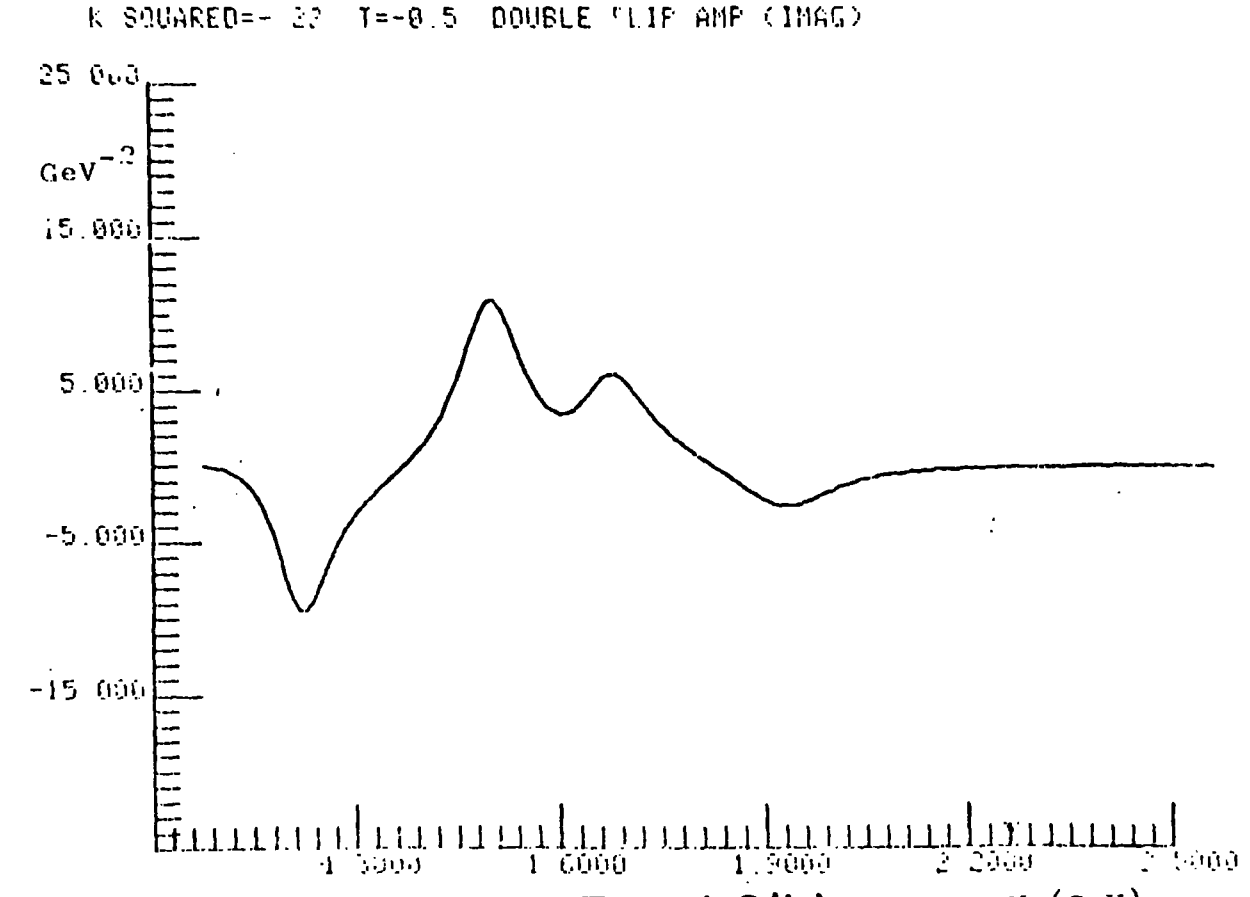
K SQUARED=- 3? T=-0.5 DOUBLE FLIP AMP (IMAG)
GeV^{-2}
15.000
5.000
-5.000
-15.000
W (GeV)

Fig. 4.2(b)

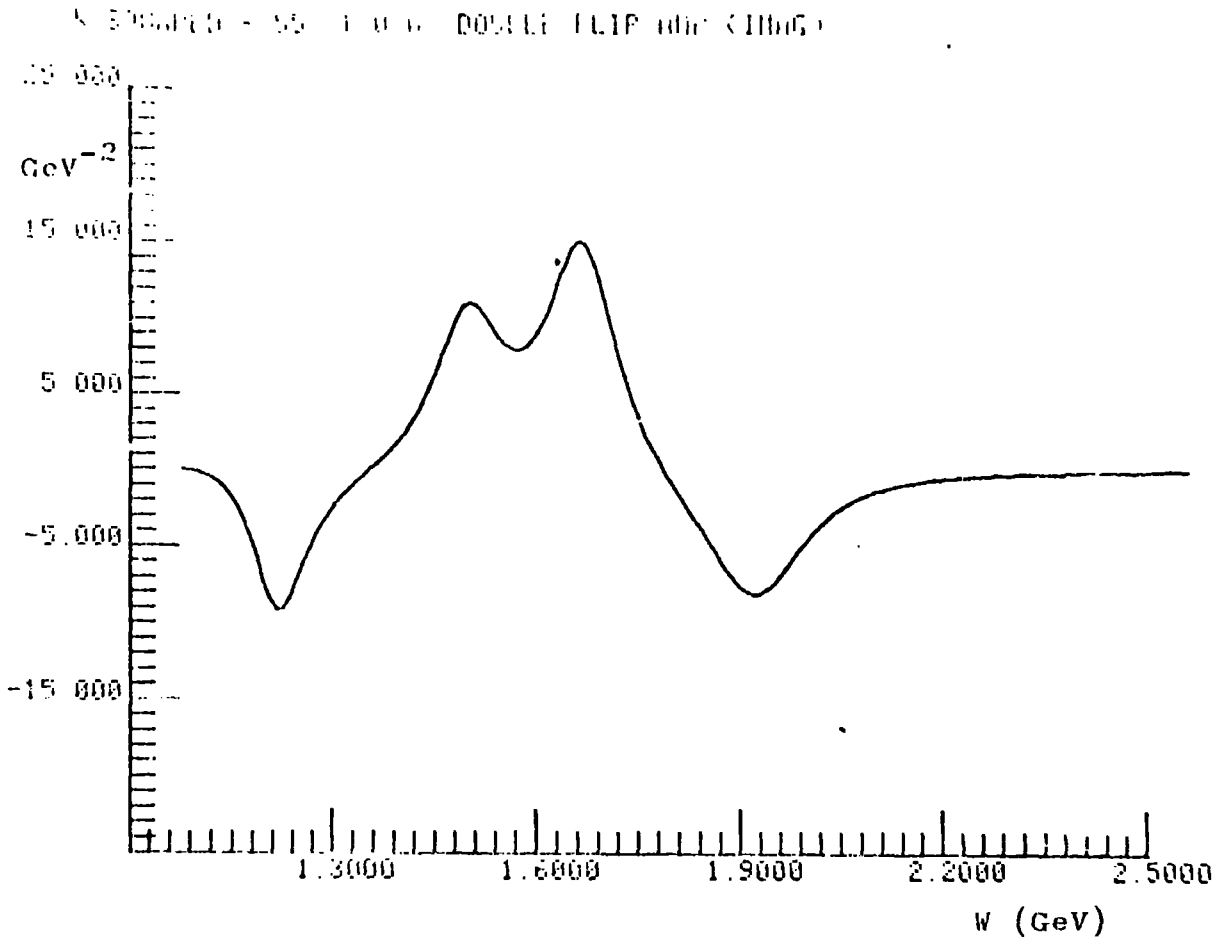

K SQUARED=- 55 T=-0 5 DOUBLE FLIP AMP (IMAG)

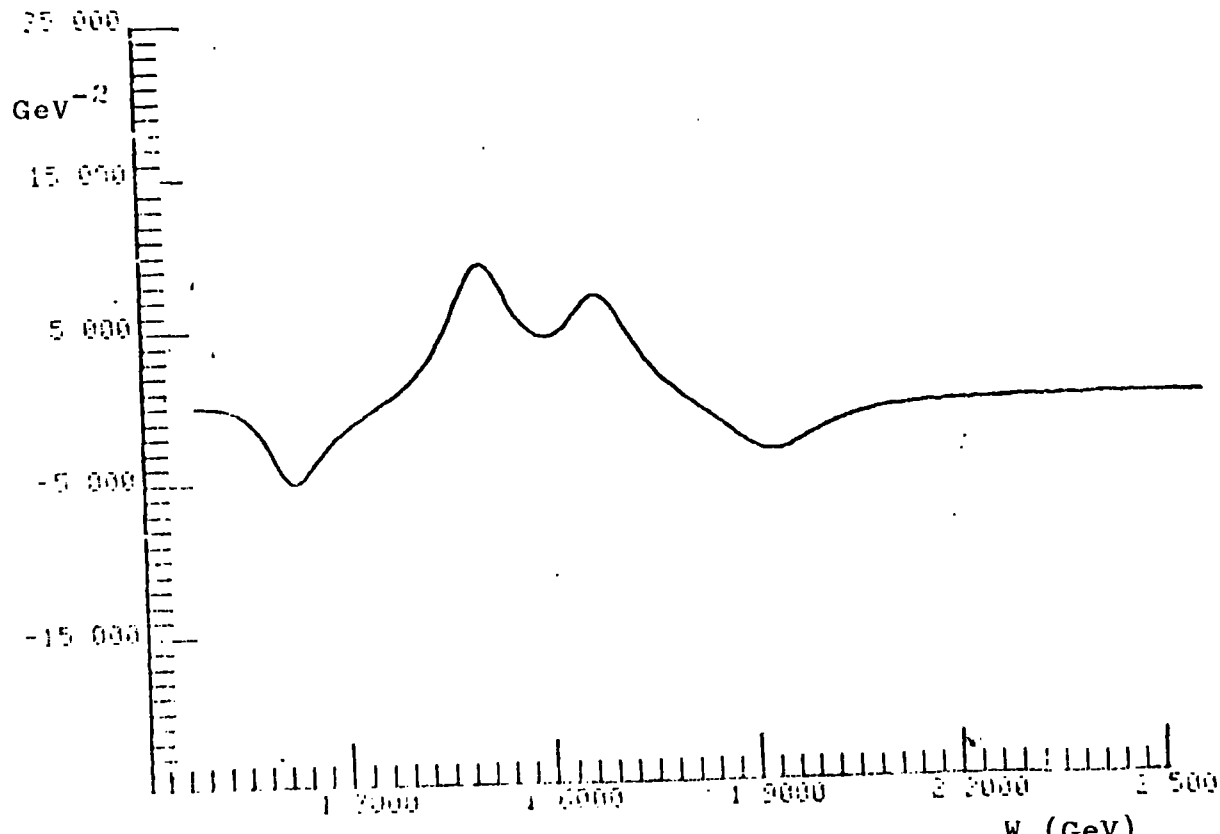

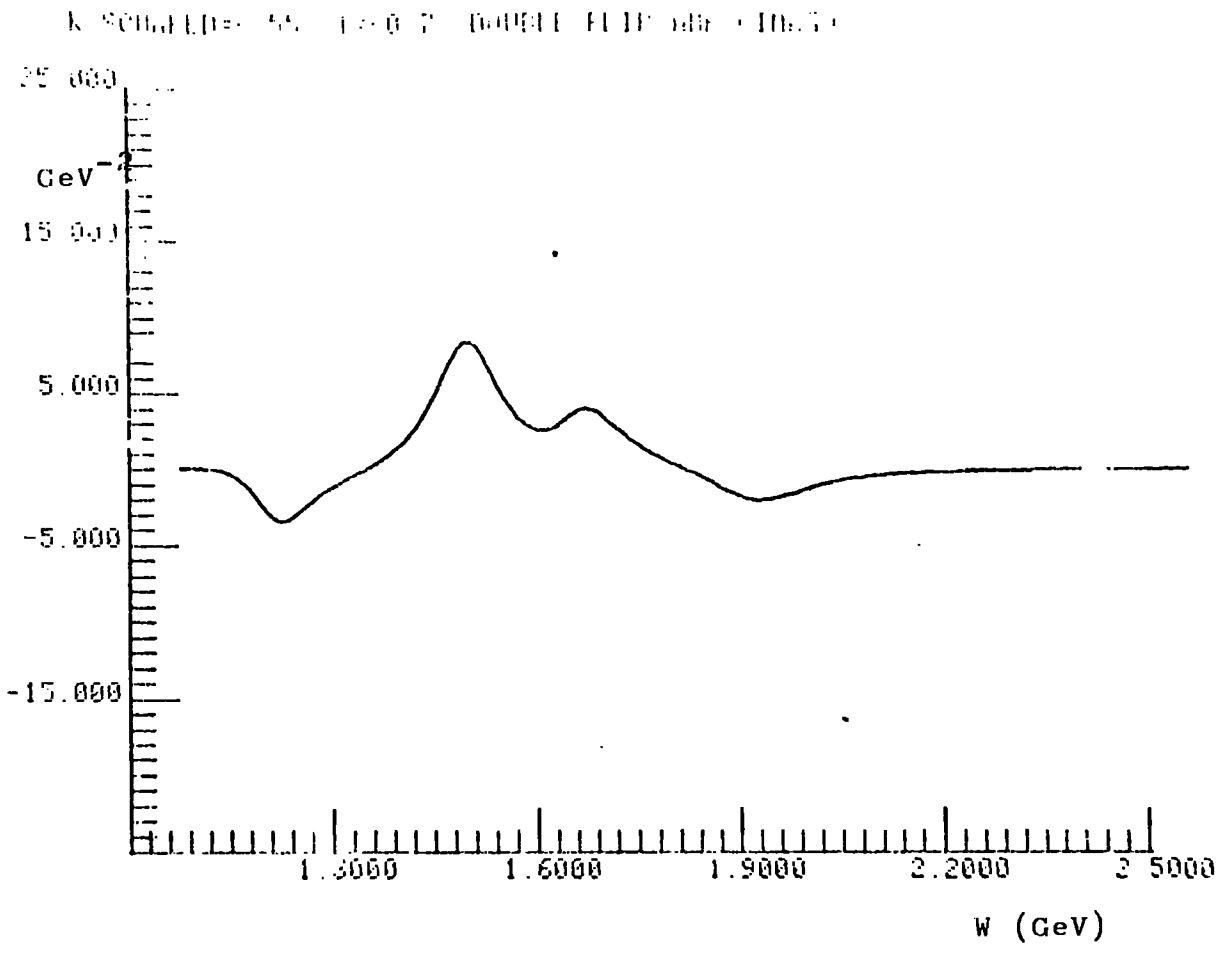

K SQUARED=- 55 T=-0.9 DOUBLE FLIP AMP (IMAG)

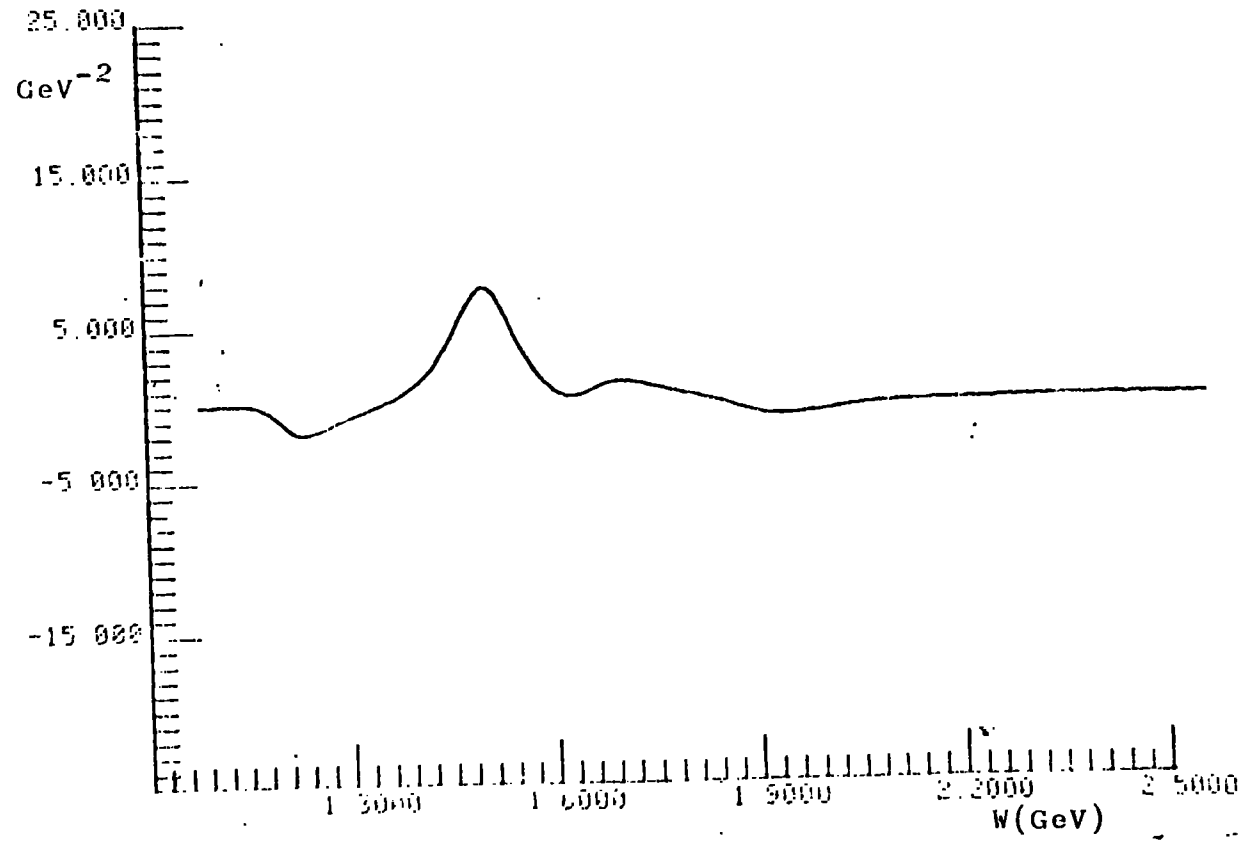

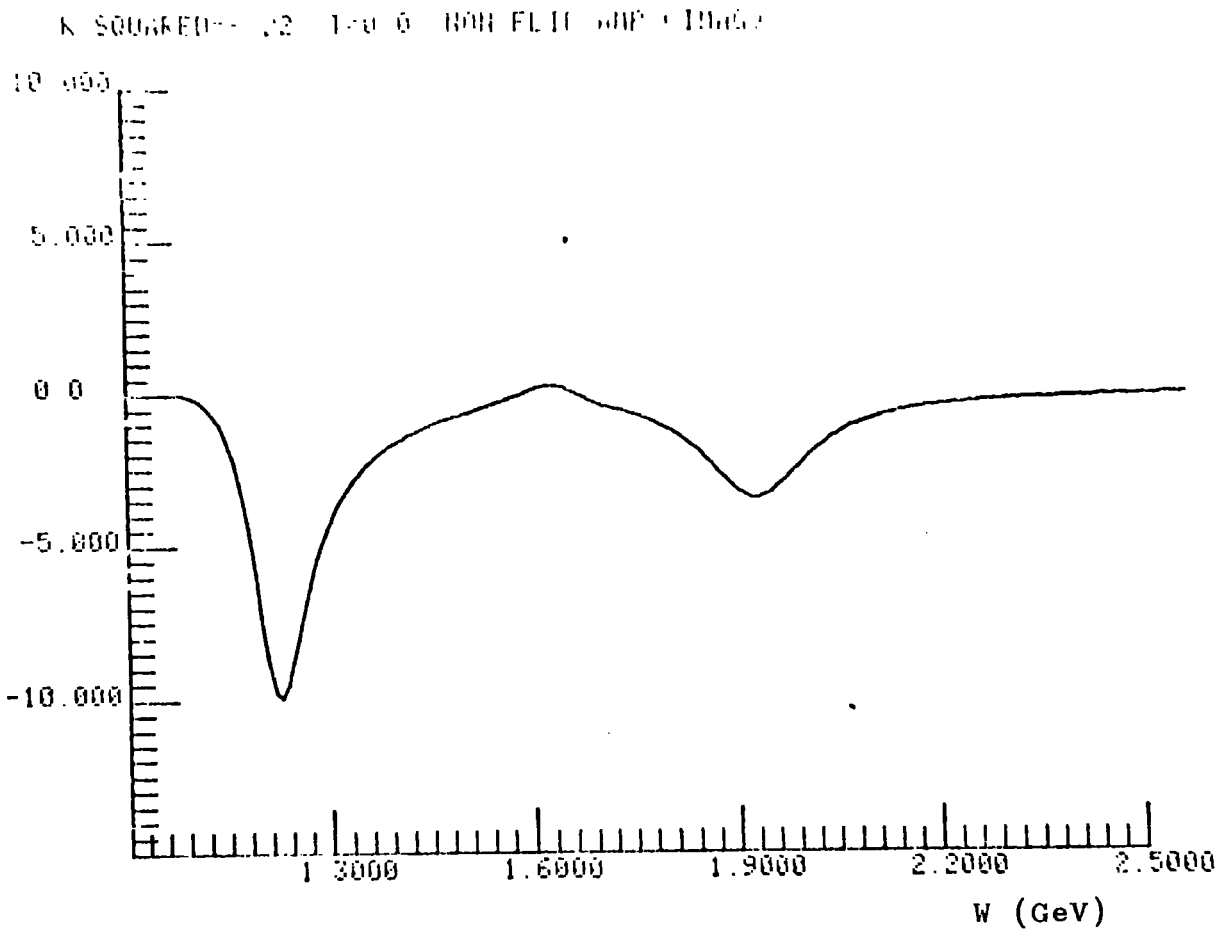
10.000
5.000
0.0
-5.000
-10.000
1.3000
1.6000
1.9000
2.2000
2.5000
W (GeV)

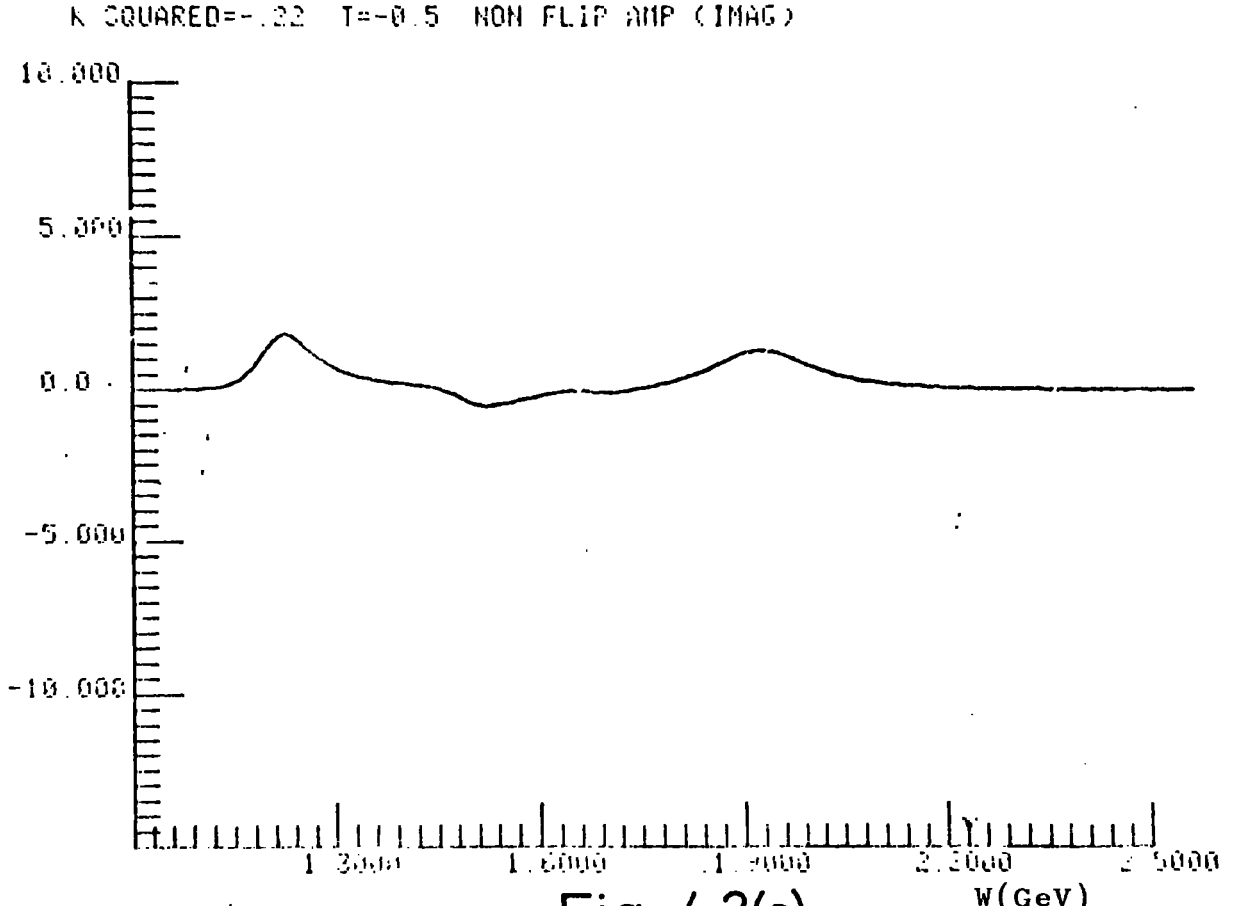
K SQUARED=-.22 T=-0.5 NON FLIP AMP (IMAG)
10.000
5.000
0.0
-5.000
-10.000
W(GeV)

Fig. 4.2(c)

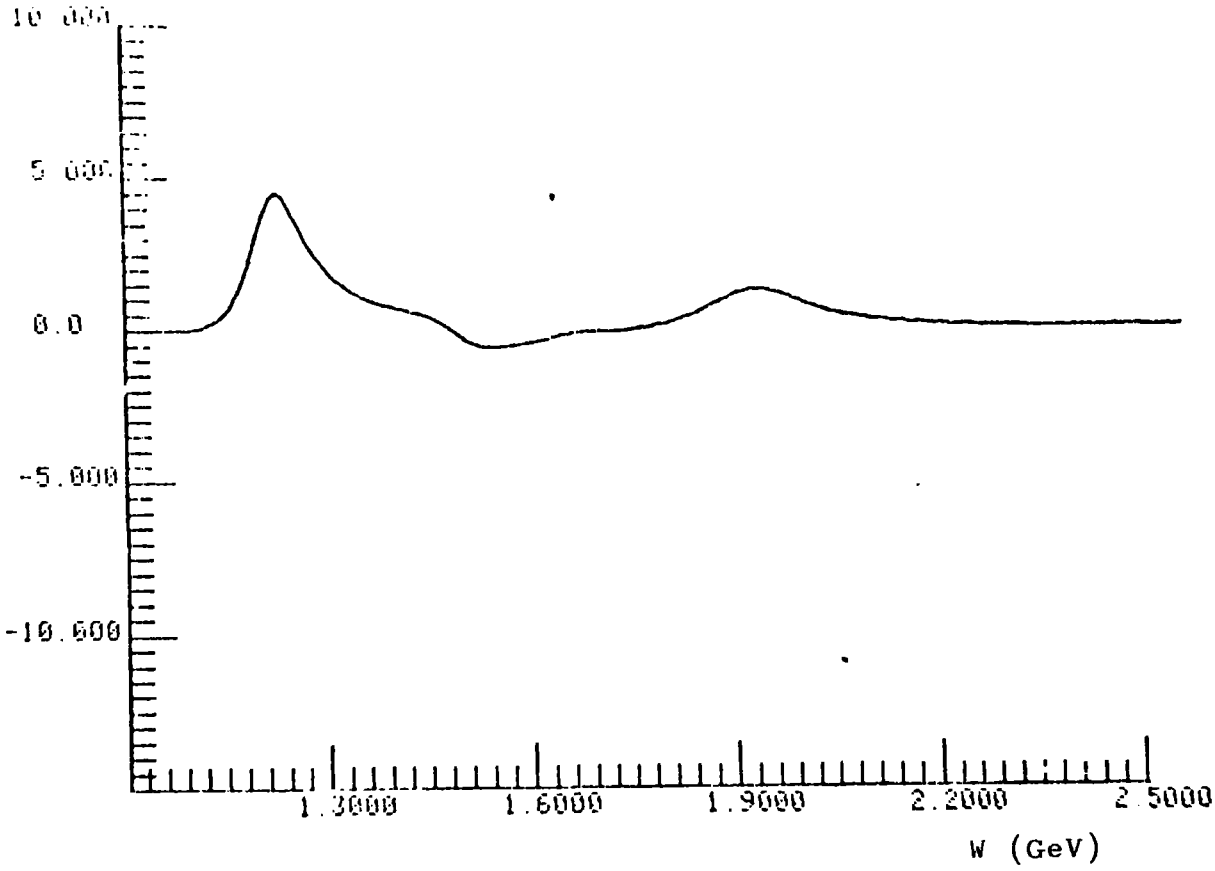

K SQUARED=-.22 T=-0.9 NON FLIP AMP (IMAG)

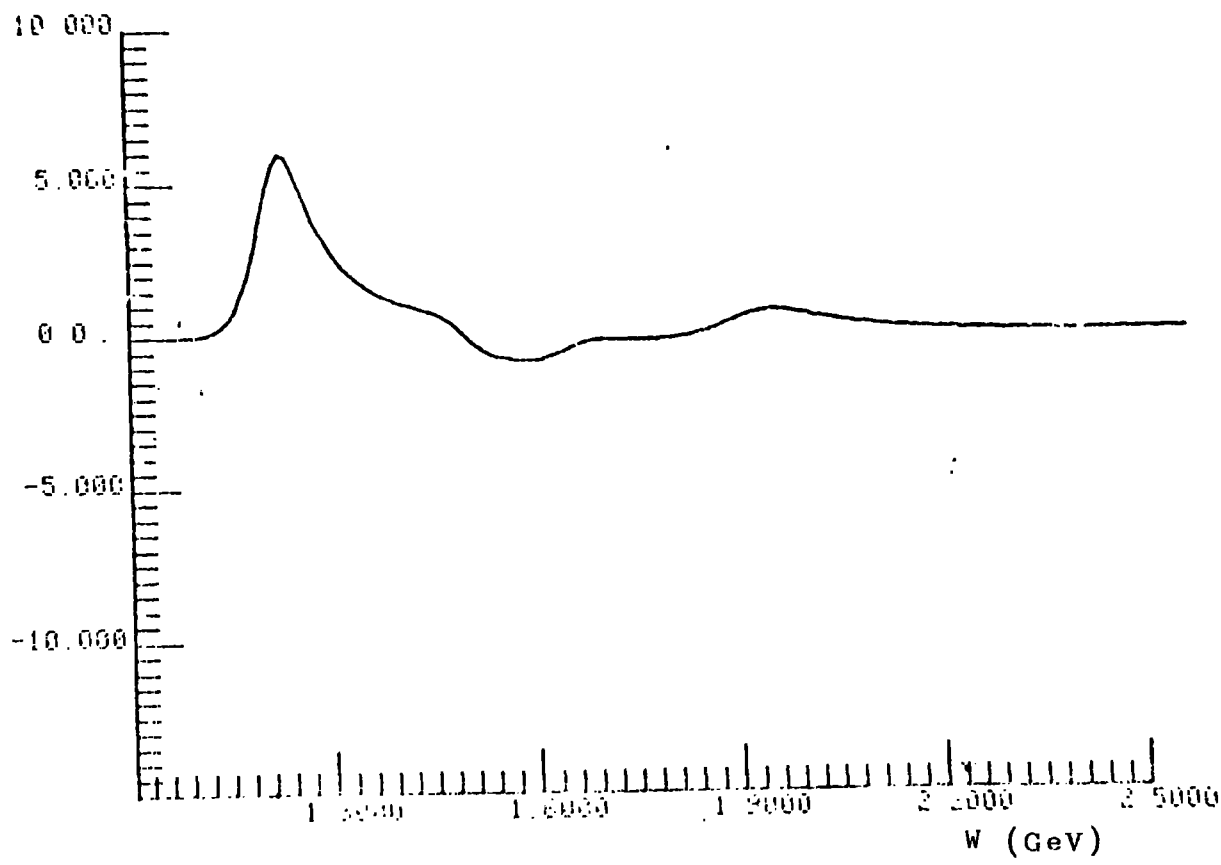

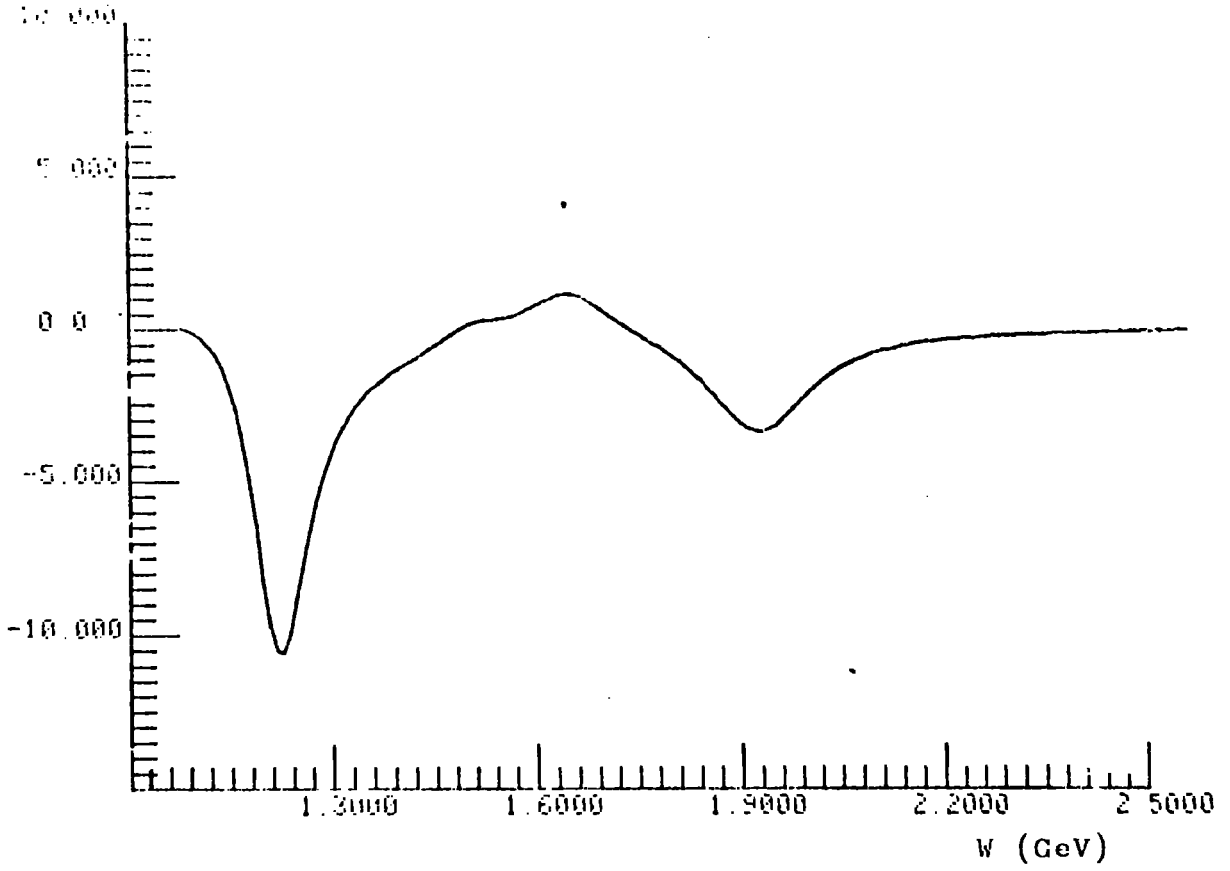

K SQUARED=-.55 T=-0.5 NON FLIP AMP (IMAG)

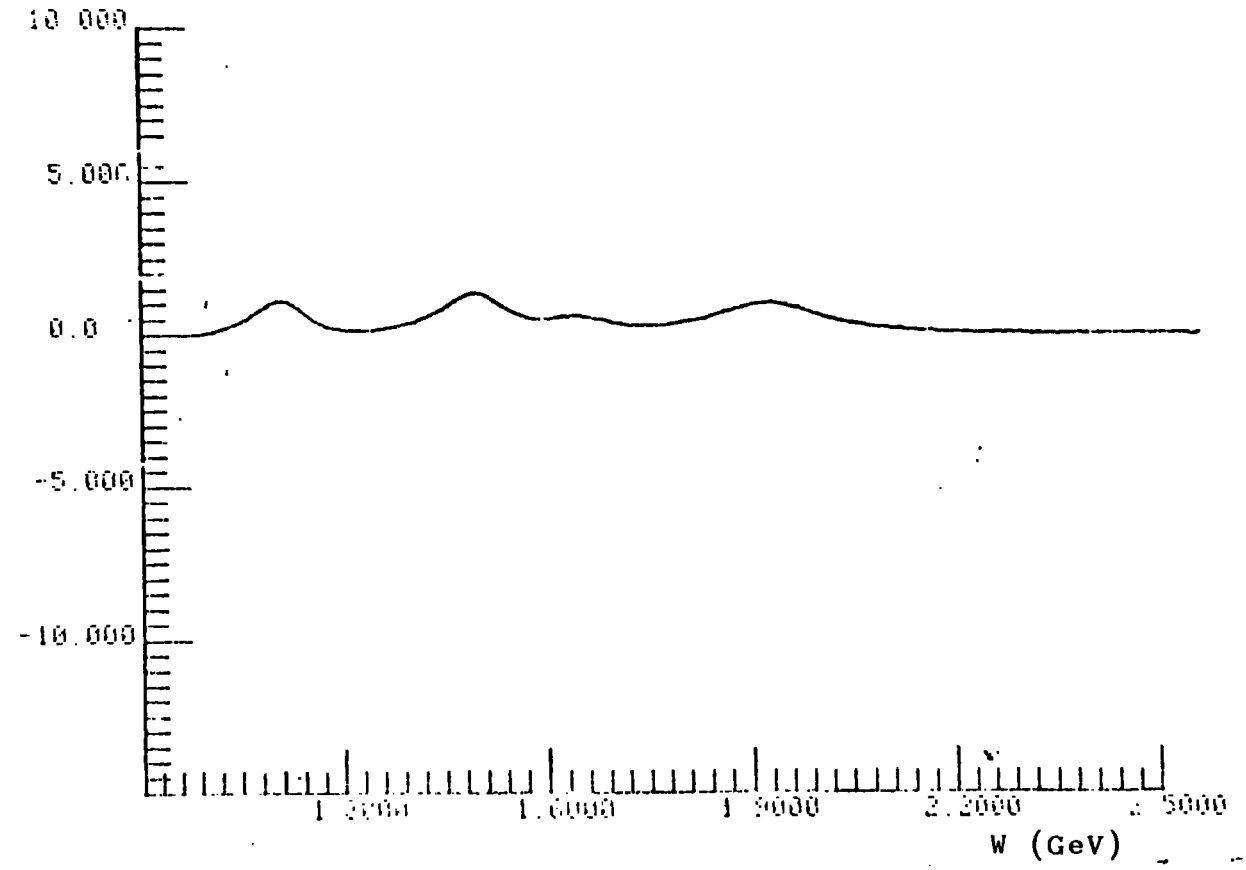

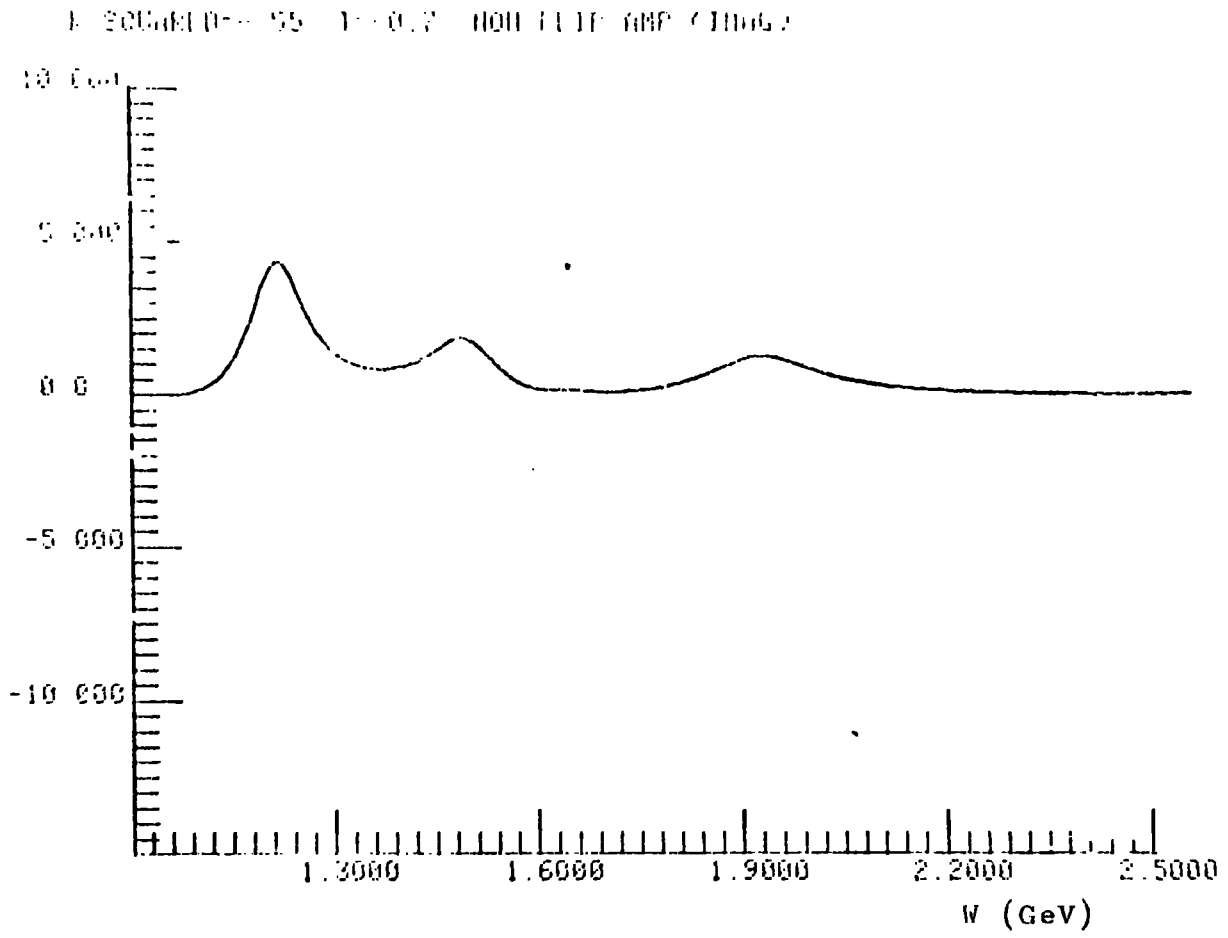
0 0
-5 000
-10 000
1.3000
1.6000
1.9000
2.2000
2.5000
W (GeV)

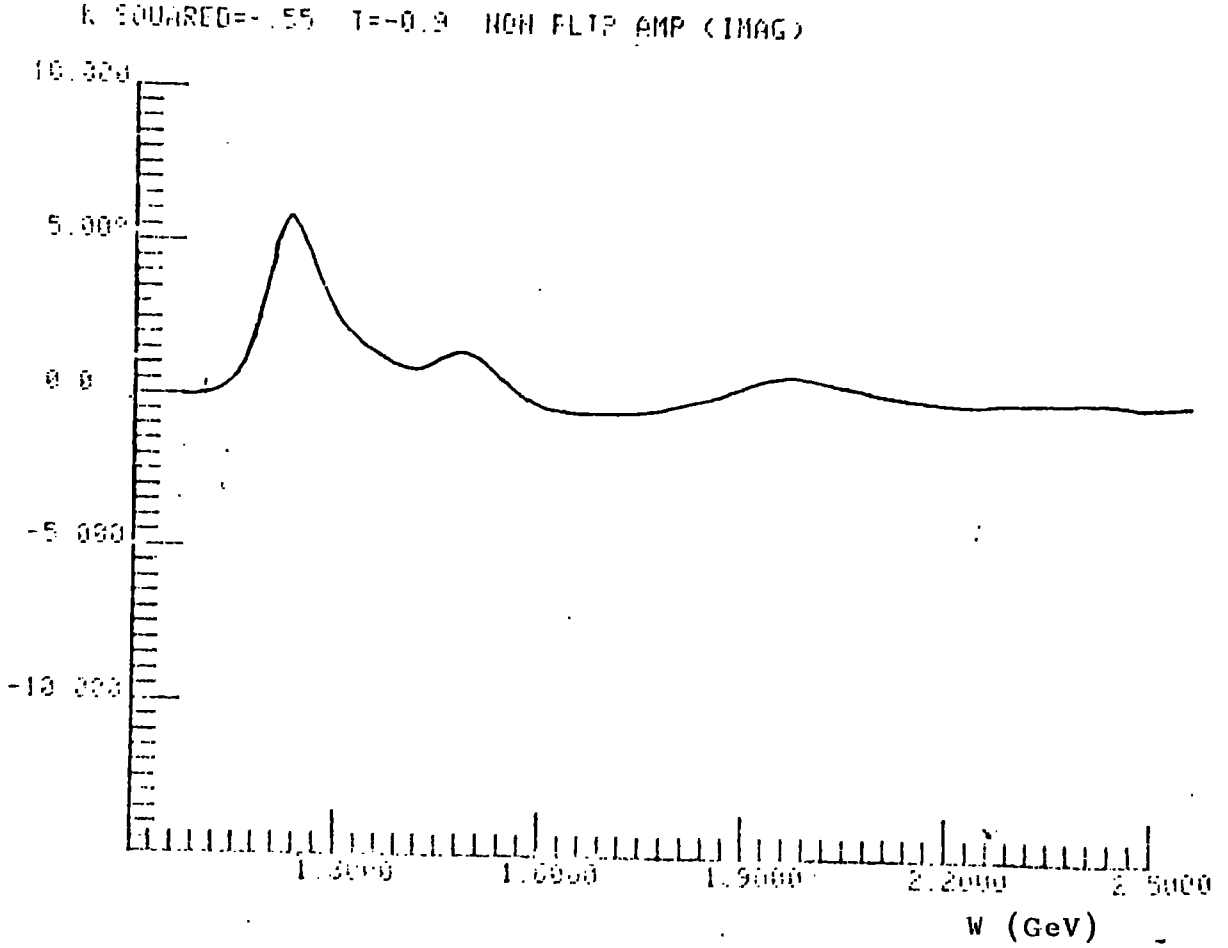
5.000
0 0
-5 000
-10 000
W (GeV)

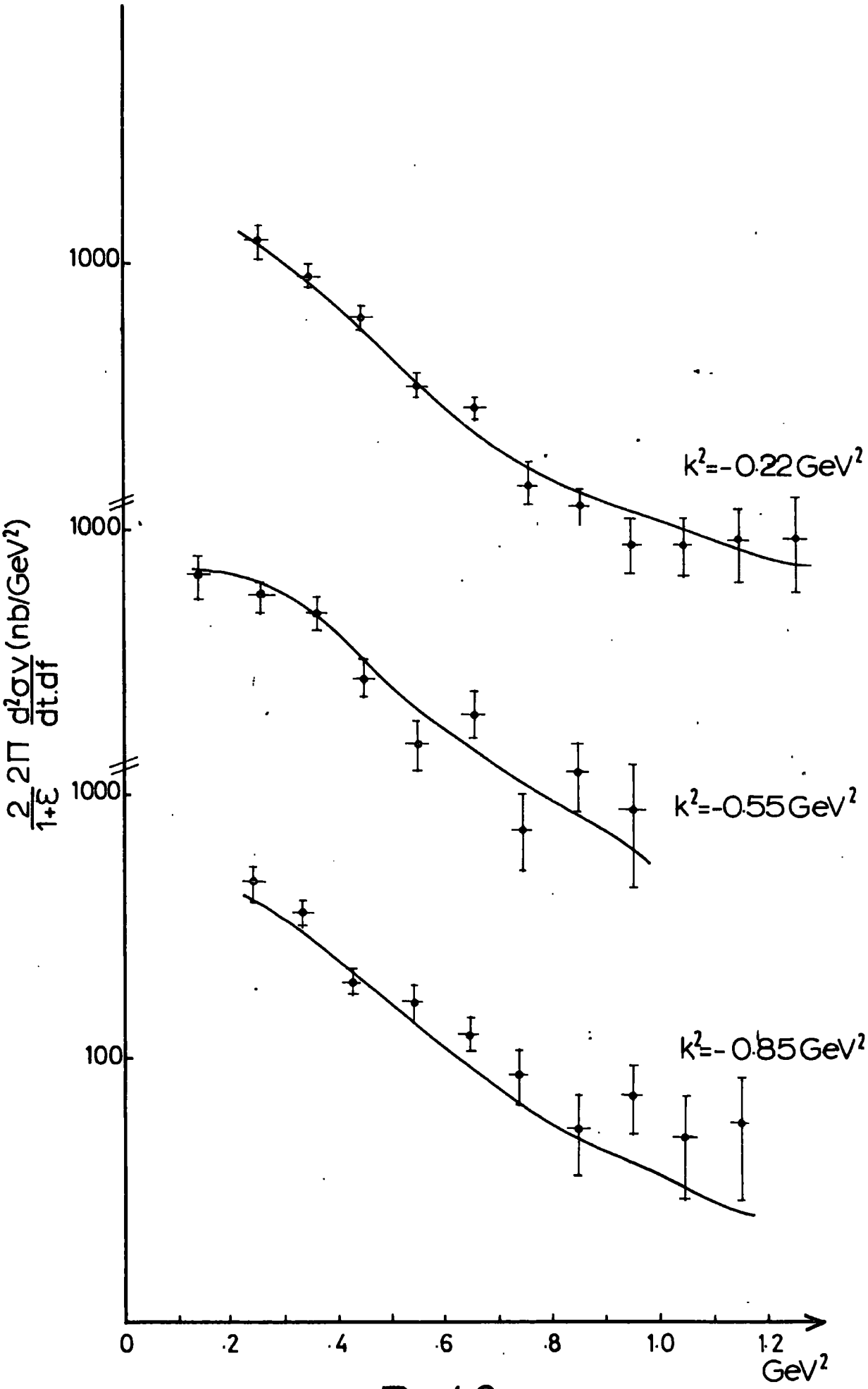
1000
1000
1000
100
$\frac{2}{1+\varepsilon}\frac{2\Pi}{}\frac{d^2\sigma_V}{dt.df}$ (nb/GeV²)
k²=-0.22 GeV²
k²=-0.55 GeV²
k²=-0.85 GeV²
0
.2
.4
.6
.8
1.0
1.2
GeV²

Fig. 4.3

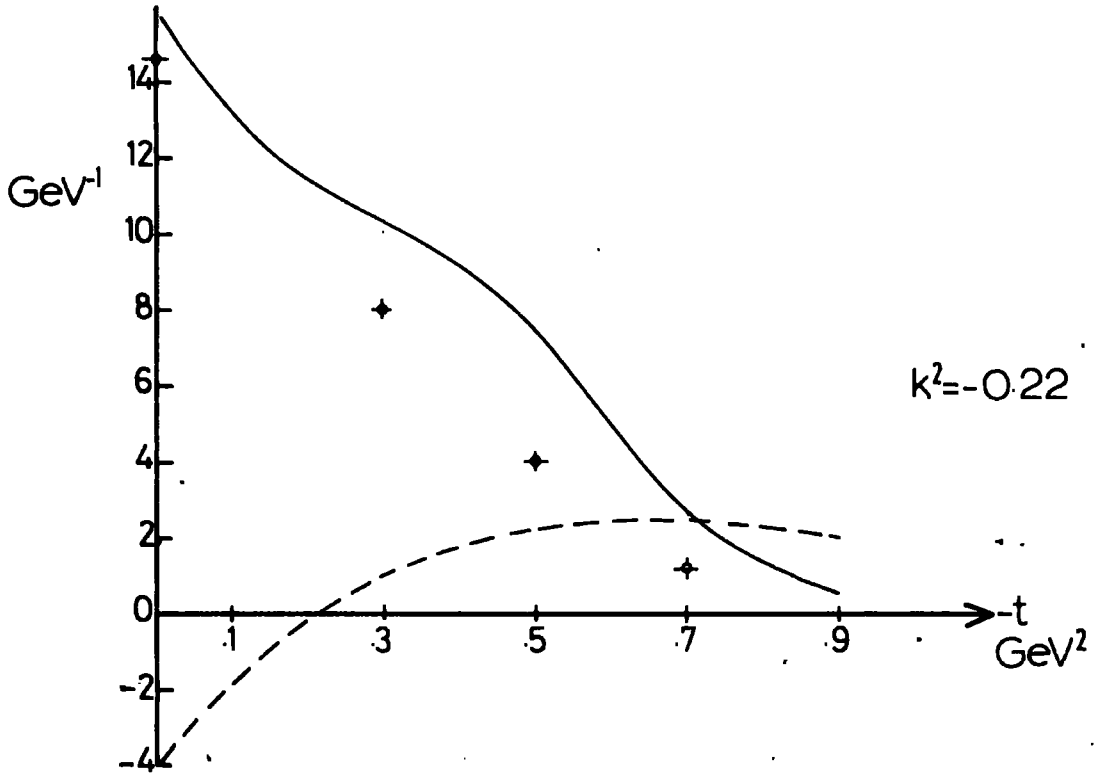
GeV⁻¹
14
12
10
8
6
4
2
0
-2
-4
.1
.3
.5
.7
.9
-t
GeV²
k²=-0·22

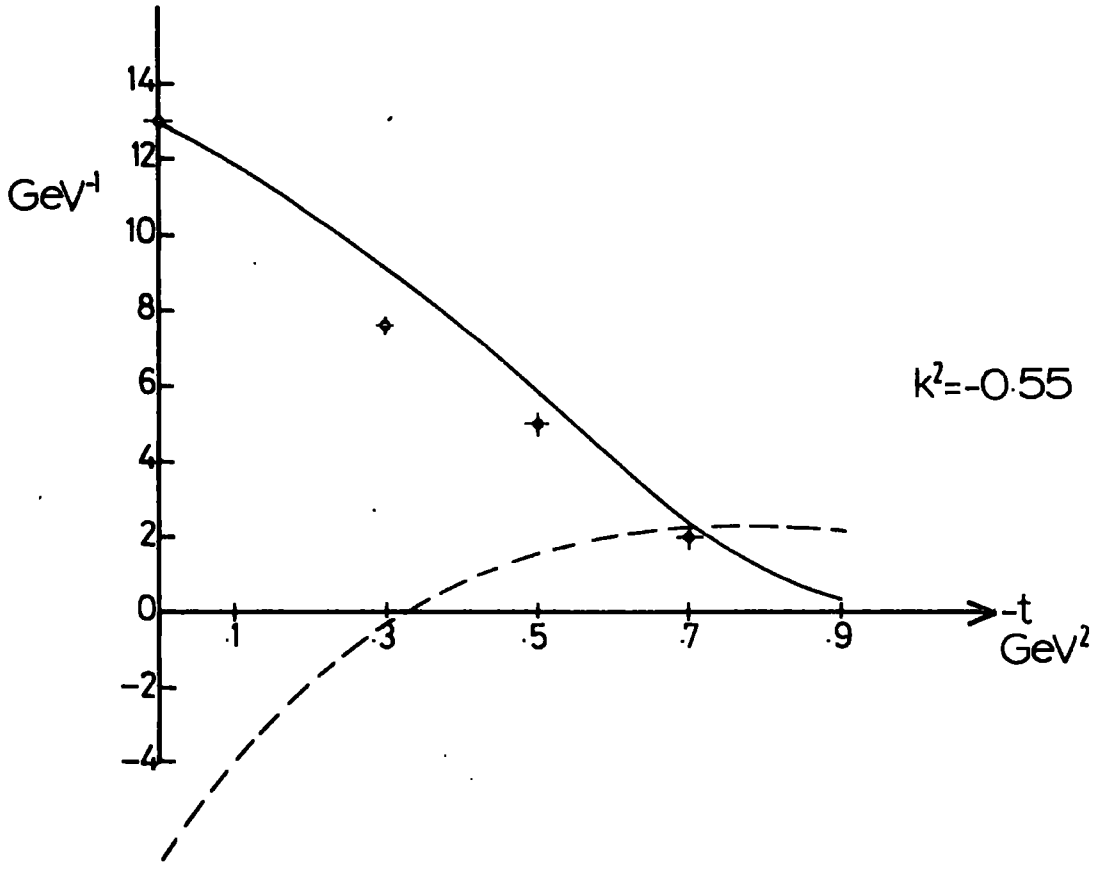
GeV⁻¹
14
12
10
8
6
4
2
0
-2
-4
.1
.3
.5
.7
.9
-t
GeV²
k²=-0·55

Fig. 4.4(a)

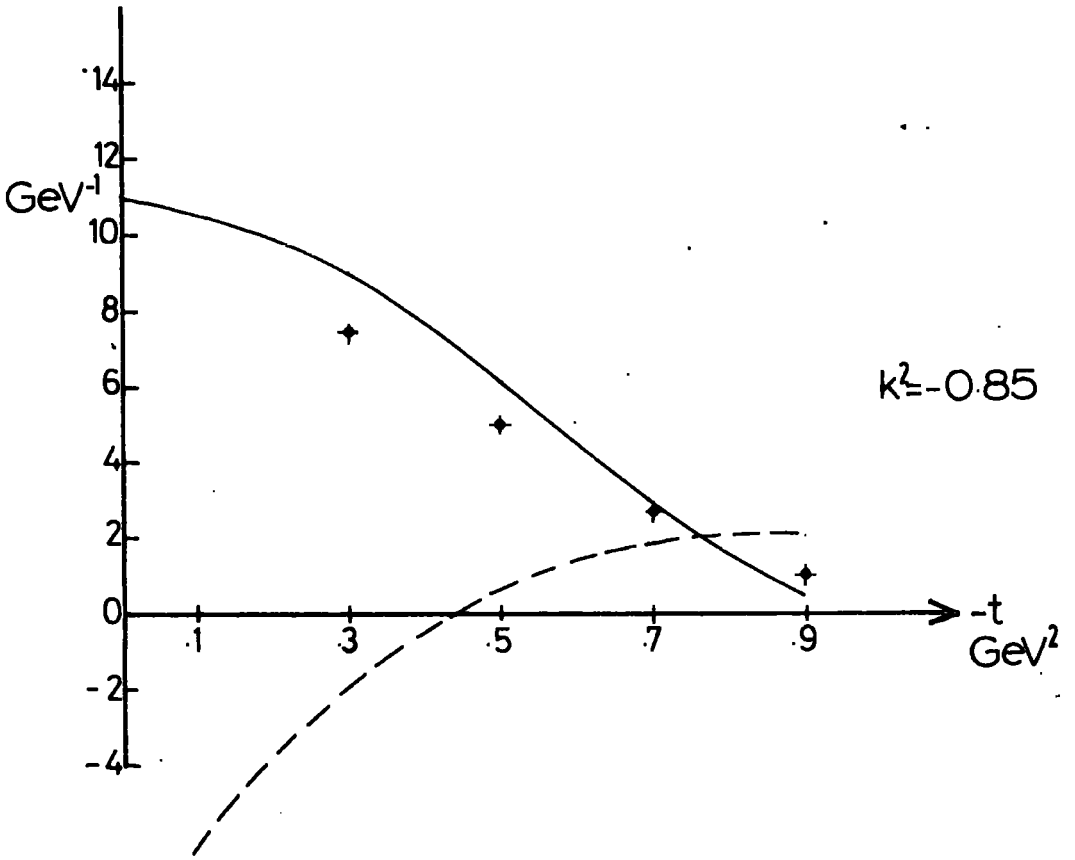

Fig.4.4(a)

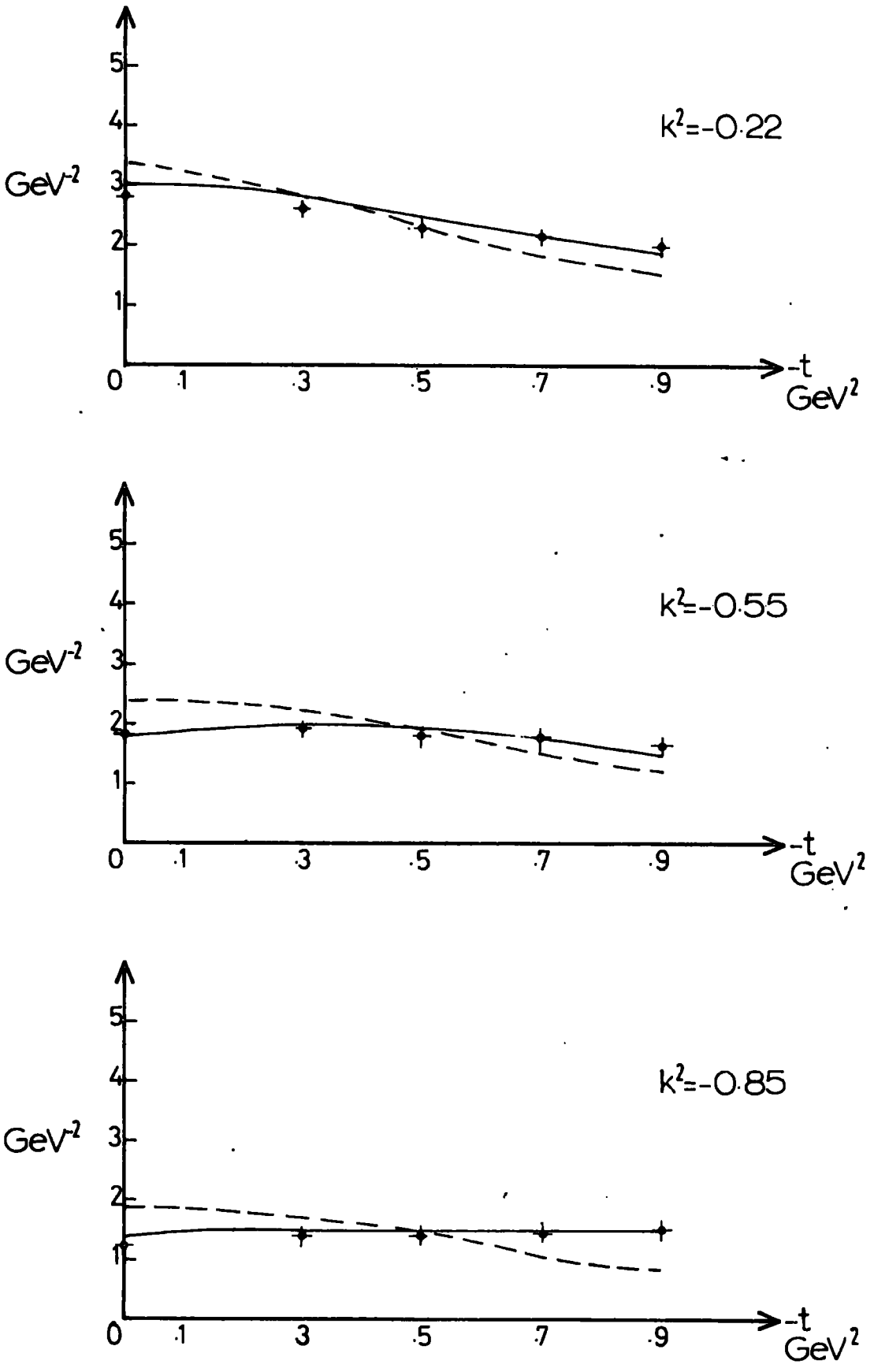

Fig.4.4 (b)

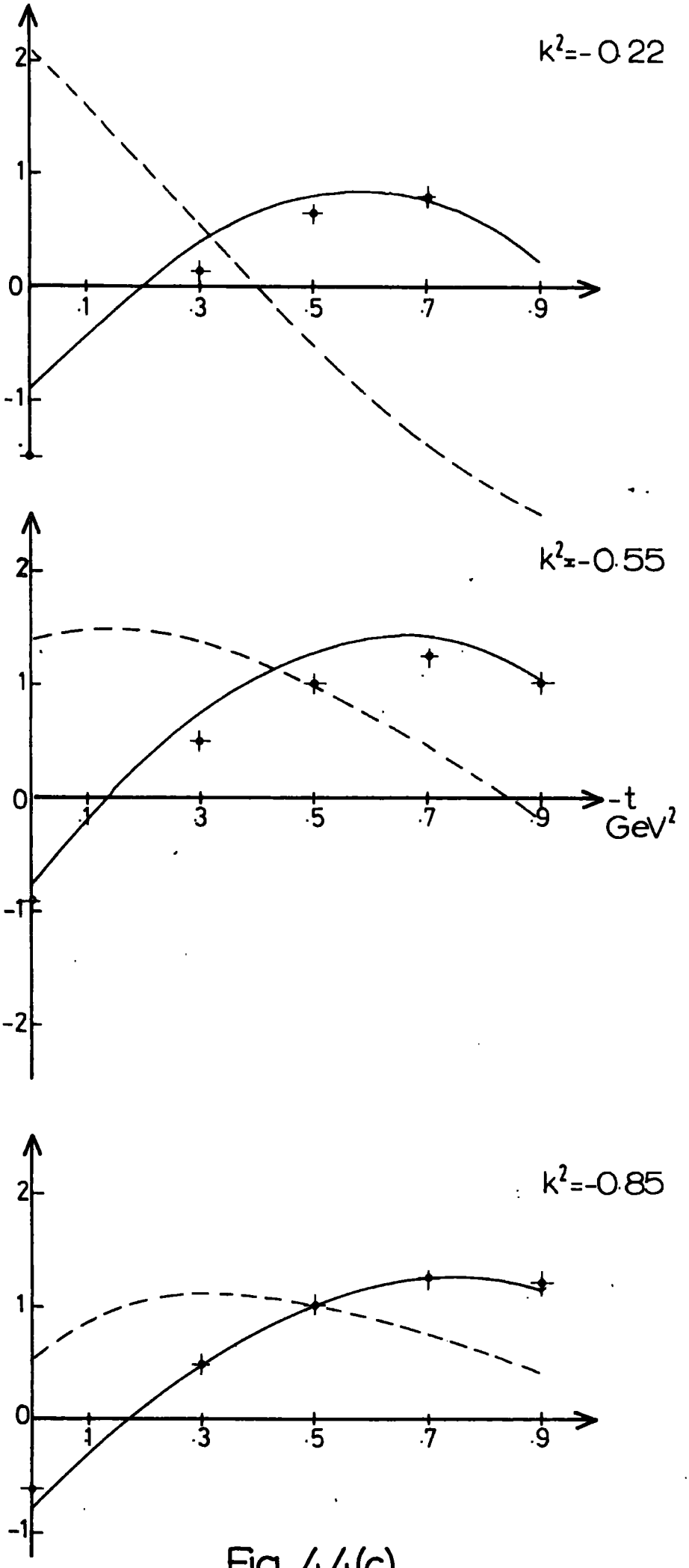

Fig. 4.4(c)

Chapter 5 : Conclusions and Predictions

Section 1 Discussion of electroproduction results

The parametrization presented in equation 4.9 of the preceeding chapter is remarkable in a number of respects. The first one is that it is the only modification of the Collins and Fitton photoproduction model which will fit the electroproduction data. Many alternative parametrizations were tried and had to be rejected as they yielded inferior fits (or, more properly, could not be made to fit the data). In particular, the behaviour of the poles and cuts was separately investigated: it was found that no modification to the pole amplitudes along the lines of equation 4.9 could be made to fit the data; neither could strengthening the cut residue alone (in the manner of equation 4.8) yield a fit; and the uselessness of strengthening the pole residue was quickly apparent. It is thus necessary to attempt to understand the implications of equation 4.9.

To take the slightest point first, it is reassuring that the value of m_v^2 is to close to the 0.6 GeV/c^2 which would have followed a pure ρ -component in the VMD model. This is remarkable, given the uncertainties associated with normalisation and systematic errors in the experiments. (Brasse et al assess their systematic

errors to be about 10%). The only element which can absorb such errors is the VMD factor $(1 - \frac{k^2}{m_v^2})^{-1}$, since it is common to all terms in the Regge model. Thus $m_v^2 = 0.6$ GeV/c^2 should not necessarily have been expected.

Superficially, the parametrization of the cut term as a function of k^2 is similar to that found by Irving (1975) for charged pion electroproduction. In his analysis, Irving noted a ~~hardening~~ strengthening of the cut contribution as a function of k^2 which he parametrized as

$$C(k^2, t) = (1 - 0.48\,k^2)\, G_c \exp\left((1 + 0.13k^2)\,at\right) \qquad 5.1$$

Since $k^2 < 0$ for electroproduction, this means that the value of the cut residue increases with $-k^2$, and that the "diffraction" peak broadens as $-k^2$ increases. This latter corresponds to a shrinkage in impact parameter space (b-space). Irving conjectures that this is related to a transition from a hadron-like photon (for $k^2 = m_\rho^2$, 0) to an increasingly point-like photon, as would be expected in deep-inelastic scattering. It should be noted in passing that the behaviour found by Irving is not that expected by Harari, as described in Chapter 1. Harari indeed expected the photon to shrink in b-space as $-k^2$ increased, but he expected that the diffractive

slope $c \sim \frac{1}{-k^2}$. Irving has $c \sim k^2$.

The results of Chapter 4 also indicate an increase in the cut residue. The effect, for neutral pion electroproduction, is some three times greater than in the charged pion case. However the size, and more especially the sign, of r is the main surprise of equation 4.9. We have several times remarked on the suddenness with which the anomalous behaviour of the electroproduction cross-section sets in. That the dip and secondary maximum vanish for so small a k^2 as -0.22, may make the magnitude of r acceptable: the k^2 modification to the CF model has to be dramatic, if the dramatic data are to be reproduced. The puzzle is the sign of r .

The results of Chapter 4 run counter to Irving's conclusion, noted above. As $-k^2$ increases, the diffractive peak of our absorbing amplitude shrinks. It will be more illuminating briefly to discuss this point in terms of the impact parameter representation of the scattering amplitudes.

The Collins and Fitton model, with which we have been concerned in this work, uses the eikonal prescription to calculate absorptive cuts for photoproduction. The details and motivation for the eikonal

model are exhaustively discussed in Collins (1977), and only the salient points will be rehearsed here. Using the distorted wave Born approximation, the scattering amplitude can be obtained as a function of s and b (impact parameter).

$$A(s,b) = \chi^R(s,b)\ \exp\left(i\,\chi^P(s,b)\right)$$

where we have made the simplifying assumption that the absorptive amplitude is purely pomeron exchange. (Note that it is precisely this assumption which Collins and Fitton showed untenable in pion photoproduction). For the photoproduction exchanges the eikonal amplitude has the form

$$\chi^R(s,b) = \frac{i\,G\,e^{\frac{i\pi\alpha(0)}{2}}}{8\pi s}\left(\frac{s}{s_0}\right)^{\alpha_0}\left(\frac{b}{2c}\right)^{n}\frac{e^{-b^2/4c}}{c} \qquad 5.2$$

The pomeron amplitude is identical except that, due to signature, the i term does not appear. The pomeron term is therefore almost purely imaginary. Equation thus becomes, on expanding the exponential and putting in cut enhancement terms (λ) explicitly,

$$A(s,b) \sim \chi^R + i\lambda\chi^R\chi^P \qquad 5.3$$

$$= \chi^R(1 - \lambda|\chi^P|)$$

For the non-flip eikonal amplitude (n=o) the Regge pole has a Gaussian b-dependence, but the effect of the cut's destructive interference is to kill the peak at b=o and enhance the amplitude for higher b. Depending on the value of the cut enhancement factor, λ , the small b region can be completely absorbed so that the scattering amplitude is dominated by $b \sim 1\,fm$ - peripheral scattering. For $n \neq 0$, the presence of a b^n factor in equation 5.2 means that the pole amplitudes are already peripheral, and so absorption has less effect.

Because the absorbing amplitude in the CF cut model has contributions from both P and P' , the absorption is no longer purely imaginary and the second line of equation 5.3 no longer holds. The complicated form of the absorbing amplitude also makes it rather difficult to calculate the exact eikonal. However, it is clear from equation 4.9 that, for the absorbing amplitude, $\frac{1}{4}c$ decreases as a function of $-k^2$. The Gaussian peak in b^2 of the absorbing amplitude corresponding to equation 5.2 therefore broadens as a function of $-k^2$, driving the peak of $(1 - \lambda |\chi^P|)$ out to higher b thus making the scattering more peripheral.

Unfortunately, it can easily be shown that the peripheral peak is driven out to such large values of impact parameter that a simple physical explanation

becomes difficult. For our purposes it will suffice to take only the single flip amplitude with the parameters of fit (b) from the previous chapter and to consider only pomeron exchange as the absorbing amplitude. As we have noted, this is only an approximation to the true amplitude, but the effect is so gross that a more complicated calculation is not required. Using this scheme, equation 5.3 was evaluated for p_L = 6 GeV/c and k^2 = 0, -0.22, -0.55, -0.85. The results are displayed on figure 5.1. It can clearly be seen that the effect of the k^2 modifications to the CF absorbing amplitude is to drive the peripheral peak from $b \sim 1.2$fm right out to $b \sim 4$-5fm. This is rather disappointing since it seems unlikely that such high values of impact parameter have any physical meaning. Conventionally, hadrons are regarded as having a spatial extension whose radius is $\sim$1fm. It is difficult to accommodate a value four times this.

Section 1a : Prediction

Since it was impossible to adjust the daughter contributions to account for the electroproduction data, it must be concluded that the form of the cross-section is not a low energy effect. The absence of dip and secondary maximum will persist (if an absence can be said to persist), at higher energies also.

This conclusion is at variance to Vanryckeghem, who chose to regard the cross-section's behaviour as a low energy effect. However, the size of the parameters in equation 4.9 do alter the ν dependence (as well as t-dependence). The conventional expression for the α of a R&P cut

$$\alpha_c = \alpha_R + \left(\frac{\alpha'_R \alpha'_P}{\alpha'_R + \alpha'_P}\right) t$$

assumes $\log\left(\frac{\nu}{\nu_0}\right) \gg a/\alpha'$, which clearly does not hold for our choice of parameters. To illustrate the energy dependence, we plot in figure 5.2 the predicted shape of the differential cross-section for p_L = 6 and 12 GeV/c and for k^2 = -0.22, -0.55, -0.85. For the purposes of comparison, we plot also the photoproduction differential cross-section, weighted by the factor

$$\left(1 - \frac{k^2}{0.68}\right)^{-2}$$

It may be seen that the dip and secondary maximum do not recur in higher energy electroproduction. (We have used the parameters from fit (a) of the preceeding chapter).

Section 2 : Conclusions

We have seen that the properties of photon-induced interactions are far more interesting than might have been expected from their apparent similarity to hadronic processes. Indeed we have seen that, at several crucial points, the photon has confounded reasonable expectations and predictions and that there are intriguing glimpses of a non-hadronic behaviour for the photon.

These points of difference arise as we extend the energy range and the mass-range under consideration. In neutral pion photoproduction, one of the first unusual features is that the process shows no signs of "Regge" shrinkage at large $|t|$ as the centre of mass energy is increased. Collins and Fitton interpreted this as evidence for "hard" rather than pole-dominated cuts in this reaction.

On the other hand, when neutral pion electroproduction is extended down in energy to the resonance region, the dip present in the high energy cross-section at $t \sim 0.5$ is not reflected in the experimental behaviour of the resonance amplitudes. A number of sophisticated Regge models of the high energy region have been proposed to accommodate this. However, it should be clear from the discussion of Chapter 2 that FESRs were originally proposed

(in other reactions) because the high energy dips were continued into the resonance region. This continuation was quite independent of any specific high energy model. We have seen that in a real sense the behaviour of the P_{33} in π^0 photoproduction is non-dual and have chosen to accommodate it by introducing a daughter term which does not contribute significantly at high energies. We have seen that Odorico attributes the resonance region behaviour to the kinematic complications of a spin-1 projectile. We have seen also that this conjecture might be confirmed by examining $\pi N \to \rho N$. The alternative approach seeks a dynamical explanation in terms of the electromagnetic nature of the photon or in the move away from the ρ mass shell. Since a predicted change in helicity structure of the resonances is actually seen in electroproduction, one might perhaps incline to the second explanation. However the agreement between the quark model and experiment is qualitative, and the model does not satisfactorily explain the photoproduction behaviour. Perhaps examining $\pi N \to \rho N$ is the only model independent way of checking this point.

Certainly, the off mass shell behaviour of the photon confounded all explanations. We have seen Harari's hopes for a definitive test of dip mechanisms shattered because the photon did not shrink (in b-space) as $-k^2$

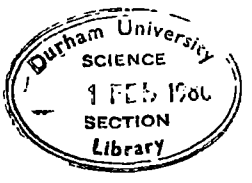

increased in diffractive electroproduction. We have seen that a strong cut Reggeized absorption model can fit neutral pion electroproduction data. To do so the slope in t of the absorptive part of the amplitude must be modified. Unfortunately, it foes not appear that the consequences of this modification have a simple physical explanation. As in Irving's investigation of charged pion electroproduction, we do not find the behaviour suggested by Harari. The form of the electroproduction differential cross-section, so different from that of photoproduction, is expected to persist to high energies.

Figure Captions

Fig. 5.1 The impact parameter profile of the single flip amplitude from fit (b) of Chapter 4 for p_L = 6 GeV/c and k^2 = 0.0, -0.22, -0.55, -0.85.

Fig. 5.2 a) The predicted shape of the electroproduction differential cross-sections at p_L = 6GeV/c and k^2 = -0.22, -0.55, -0.85. For comparison the photoproduction profile, weighted by $\left(1 - \frac{k^2}{0.68}\right)^{-2}$ is also shown.

b) The electroproduction cross-sections at p_L = 12 GeV/c. The photoproduction case is also shown. Note the change of scale with respect of a).

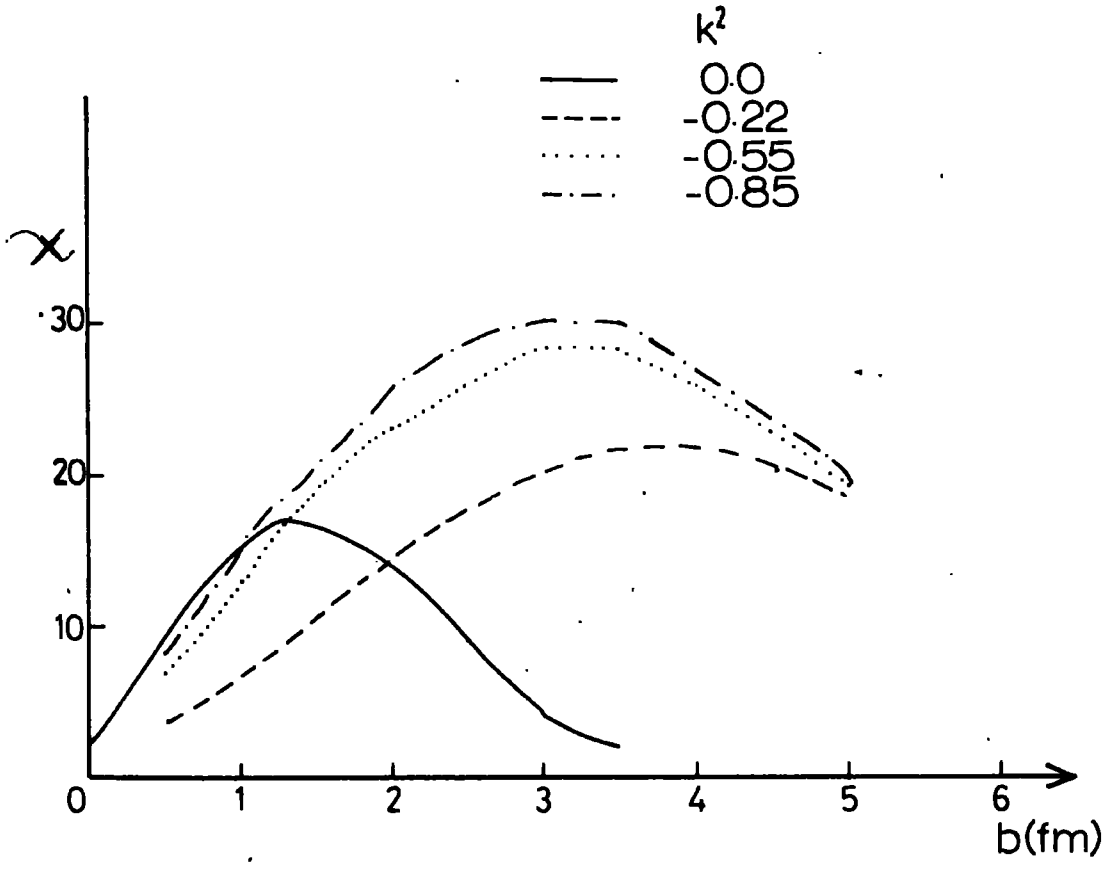

Fig. 5.1

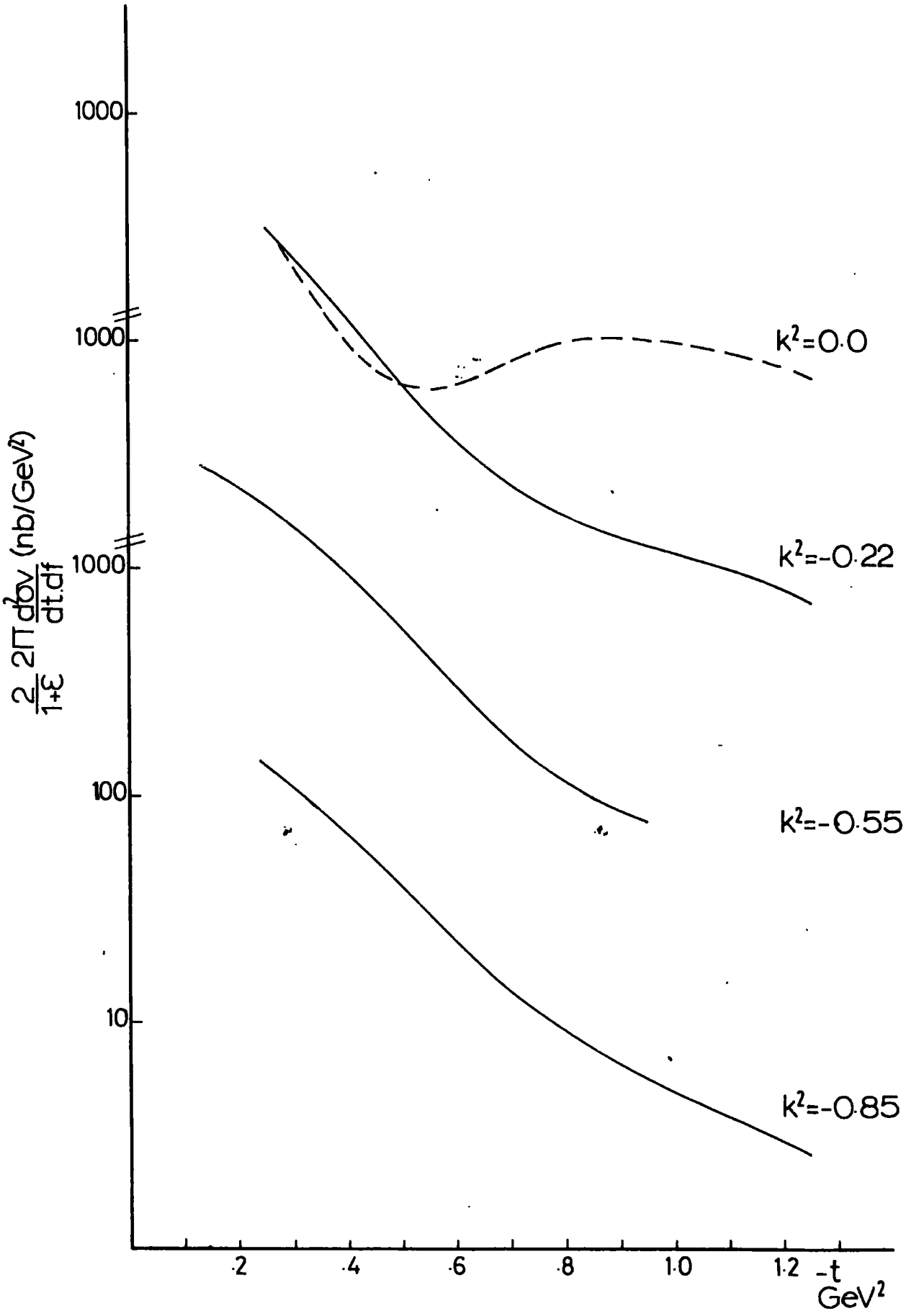
1000
1000
1000
100
10
$\frac{2}{1+\varepsilon}\frac{2\Pi d^2\sigma_V}{dt.df}$ (nb/GeV²)
k^2=0·0
k^2=-0·22
k^2=-0·55
k^2=-0·85
·2
·4
·6
·8
1·0
1·2
-t
GeV²

Fig. 5.2(a)

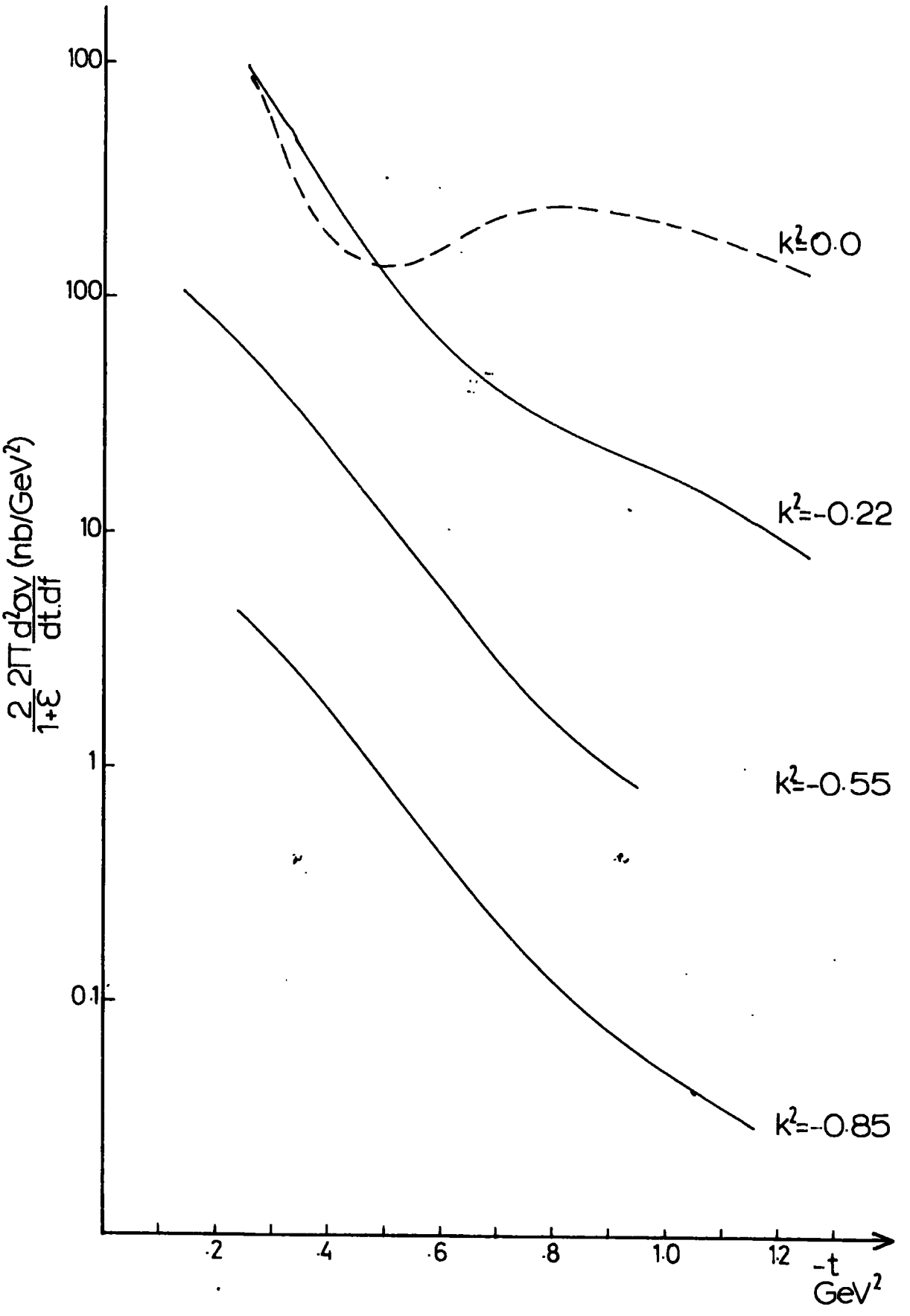
100
100
10
1
0.1
$\frac{2}{1+\varepsilon}\frac{2\pi d^2\sigma_V}{dt.df}$ (nb/GeV^2)
k^2=0.0
k^2=-0.22
k^2=-0.55
k^2=-0.85
.2
.4
.6
.8
1.0
1.2
-t
GeV^2

Fig.5.2(b)

Appendix A : Conventions

As stated in text, the formalism of electroproduction is complicated and subject to some confusion. In these appendices therefore, we give a complete and extensive account of the conventions, normalisations and formulae used throughout this thesis.

Dirac Matrices and Spinors

We choose the representation of the Dirac γ matrices to accord with that of Bjorken and Drell (1964). Thus,

$$\gamma_0 = \begin{bmatrix} 1 & 0 \\ 0 & -1 \end{bmatrix} \qquad \{\gamma^i\} = \underset{\sim}{\gamma} = \begin{bmatrix} 0 & \underset{\sim}{\sigma} \\ -\underset{\sim}{\sigma} & 0 \end{bmatrix}$$

$$\sigma^1 = \begin{bmatrix} 0 & 1 \\ 1 & 0 \end{bmatrix} \qquad \sigma^2 = \begin{bmatrix} 0 & -i \\ i & 0 \end{bmatrix} \qquad \sigma^3 = \begin{bmatrix} 1 & 0 \\ 0 & -1 \end{bmatrix}$$

$$\sigma^{\mu\nu} = \frac{i}{2}\left[\gamma^\mu, \gamma^\nu\right] \qquad \{\gamma^\mu, \gamma^\nu\} = 2 g^{\mu\nu}$$

$$\gamma^5 = i\gamma^0\gamma^1\gamma^2\gamma^3 = \gamma_5 = \begin{bmatrix} 0 & 1 \\ 1 & 0 \end{bmatrix}$$

$[\ ,]$ denotes commutation

$\{\ ,\}$ denotes anti-commutation

The metric tensor is chosen to be $g = \begin{bmatrix} 1 & 0 & 0 & 0 \\ 0 & -1 & 0 & 0 \\ 0 & 0 & -1 & 0 \\ 0 & 0 & 0 & -1 \end{bmatrix}$

The inner product of a four-vector and a γ matrix is denoted by $\gamma_\mu \varepsilon^\mu = \not{\varepsilon} = \gamma^0 \varepsilon^0 - \underset{\sim}{\gamma} \cdot \underset{\sim}{\varepsilon}$

Throughout, we are concerned to describe the kinomatics of pions, photons and nucleons (specifically protons). We therefore only require the Dirac spinor for a spin - $\frac{1}{2}$ particle travelling with three-momentum $\underset{\sim}{p}$. This will be denoted $u(\underset{\sim}{p})$

$$u = \frac{1}{\sqrt{E+m}} \begin{bmatrix} (E+m)\chi \\ \underset{\sim}{\sigma} \cdot \underset{\sim}{p}\, \chi \end{bmatrix} \qquad \text{(A1)}$$

ehrtr $p^0 = E$, and χ is a Pauli 2-spinor depending on the spin direction.

$\chi_+ = \begin{bmatrix} 1 \\ 0 \end{bmatrix}$ for a particle spinning parallel to its motion

$\chi_- = \begin{bmatrix} 0 \\ 1 \end{bmatrix}$ for a particle spinning anti parallel to its motion

To construct a matrix element one requires the hermitian conjugate of the Dirac spinor $u^\dagger$, easily obtained by noticing that $\sigma_i^\dagger = \sigma_i$, but a more useful expression is the adjoint spinor $\bar{u} = u^\dagger \gamma^0$

$$\bar{u}\gamma^5 = \frac{1}{\sqrt{E+m}} \left[\chi^\dagger(-\underset{\sim}{\sigma}\cdot\underset{\sim}{p}) \;,\; \chi^\dagger(E+m)\right] \qquad (2)$$

Note that in this convention $\bar{u}u = 2m$

At all times a contravariant four-vector will be denoted

$$p = p^{\mu} = (p^{0}, \underset{\sim}{p})$$

The magnitude of the three momentum will be denoted $|\underset{\sim}{p}|$ to distinguish it from the corresponding four-vector p.

$c = \hbar = 1$ throughout

Appendix B : Cross-sections and Normalisation

Kinematic Notation

Referring to fig B1 the following identifications may be made:

l_1 = incident electron	4 momentum	$l_1^2 = m_e^2$
l_2 = outgoing electron	4 momentum	
p_1 = incident nucleon	4 momentum	$p_1^2 = m^2$
p_2 = final nucleon	4 momentum	
q = final pion	4 momentum	$q^2 = \mu^2$
k = final photon	4 momentum	
$P = \frac{1}{2}(P_1 + P_2)$		

In almist all cases we work in the centre of mass (com) of the photon-nucleon system, that is, the one defined by

$$\underset{\sim}{p_1} = -\underset{\sim}{k} \qquad \underset{\sim}{p_2} = -\underset{\sim}{q}$$

We define two sets of the usual Mandelstam invariants: one referring to the complete lepton-hadron system; and the other to just the hadronic subsystem, regarding the photon as the incident projectile.

For the complete system

$S_T = (l_1 + P_1)^2$: the square of the total com energy

$k^2 = (l_1 - l_2)^2$: the square of the momentum transferred from the leptons to the hadronic system, and the square of the mass of the photon.

$= 4l_1^0 l_2^0 \sin^2 (\frac{\psi}{2})$

ψ is the angle between the two leptons.

For the hadronic system

$$s = (k + p_1)^2 = (k^0 + E_1)^2 = (E_\pi + E_2)^2 = P_H^2$$

$$p_1^0 = E_1 \,, \quad q^0 = E_\pi \,, \quad p_2^0 = E_2$$

$$t = (k - q)^2$$

$$= \mu^2 + k^2 + 2k^0 E_\pi - 2|\underset{\sim}{k}||\underset{\sim}{q}| \cos\Theta$$

where Θ is the angle between the incident photon and the scattered pion.

$$u = (k - P_2)^2$$

We shall find it convenient to use another variable

$$\nu = \frac{s-u}{2} = 2k.P = 2k^0 W - k^2 + \frac{t-\mu^2-k^2}{2}$$

$$= s - m^2 + \frac{t-\mu^2-k^2}{2}$$

In the centre of mass system

$$|\underset{\sim}{q}| = (E_2 + m)^{1/2} \; (E_2 - m)^{1/2}$$

$$|\underset{\sim}{k}| = (E_1 + m)^{1/2} \; (E_1 - m)^{1/2}$$

For the definition of cross-sections, we shall require the concept of Lorentz Invariant Phase Space (Lips) as explained in Pilkuhn (1967).

The volume element of one-particle Lorentz Invariant Phase Space

$$d\,\mathrm{Lips}\,(p) = \frac{d^3\underset{\sim}{p}}{2E(2\pi)^3} = \frac{d^4p}{(2\pi)^3}\;\delta(p^2 - m^2)$$

For n-particles with 4-momenta Pi ... Pn

$$d\,\mathrm{Lips}\,(s;\, p_1, \ldots p_n) = (2\pi)^4\;\delta^4\Big(p - \sum_i p_i\Big)(2\pi)^{-3n} \prod_{i=1}^{n} \frac{d^3\underset{\sim}{p}_i}{2E_i}$$

Cross-section Formulae

The use of Lorentz Invariant Phase Space requires covariant normalisation of momentum eigenstates $|\underset{\sim}{p}\rangle$

$$\langle \underset{\sim}{p}' | \underset{\sim}{p} \rangle = (2\pi)^3\; 2E\; \delta(\underset{\sim}{p}' - \underset{\sim}{p})$$

To obtain the scattering-matrix elements, we first decompose it into connected and disconnected parts (Eden et al; 1966) shown schematically in Fig B2. We can correspondingly define a transition matrix element from

$$\langle f | S | i \rangle = \delta_{fi} - i (2\pi)^4 \delta^3(\underset{\sim}{p}_f - \underset{\sim}{p}_i) T$$

where $|i\rangle$ denotes the pre-scattering eigenstate of the system, and $|f\rangle$ the post-scattering state. Clearly it is the elements of the T-matrix which describe any interaction which may have taken place, and their square is the probability of a given transition.

We seek an expression for the differential cross-section for both photo- and electroproduction of neutral pions off protons. The cross-section is the probability of producing a pion in an element of Lorentz Invariant Phase Space divided by unit incident flux; i.e.

$$d\sigma = \frac{1}{F} |T|^2 \, dLips(s_T; q, p_2, l_2)$$

The flux is the number of particles incident on unit area in unit time, which may easily be re-expressed as the ratio of the relative velocity of the two incident particles to the invariant normalisation volume;

$$F = |\underset{\sim}{v}_1 - \underset{\sim}{v}_2| \Big/ (2 l_1^\circ \, 2 E_1)^{-1}$$

$$= 4 l_1^\circ p_1^\circ |\underset{\sim}{v}_1 - \underset{\sim}{v}_2|$$

$$= 4\sqrt{s_T}\,|\underset{\sim}{l}_1|$$

where $|\underset{\sim}{l}_1|$ is the magnitude of the com 3-momentum for the incident lepton. (The use of this expression for the flux forces the covariant, $u\bar{u}$ = 2m normalisation of Dirac spinors on us).

$$d\sigma = \frac{1}{4\sqrt{s_T}\,|\underset{\sim}{l}_1|}\,|T|^2\, d\,Lips\,(s_T;\, q, p_2, l_2)$$

$$= \frac{1}{4\sqrt{s_T}\,|\underset{\sim}{l}_1|\,2\pi}\,|T|^2\, d\,Lips\,(s_T; P_H, l_2)\, d\,Lips\,(s; q, p_2)\, ds \qquad (B1)$$

where we have separated the leptonic and hadronic parts of the system, using a well-known recurrence relation. We may simplify further

$$d\,Lips\,(s_T;\, P_H, l_2) = \left(\frac{1}{2\pi}\right)^2 \frac{d^3\underset{\sim}{P}_H}{2W}\;\frac{d^3\underset{\sim}{l}_2}{2\,l_2^0}\;\delta(l_1 + p_1 - l_2 - P_H)$$

$$= \left(\frac{1}{2\pi}\right)^2 \frac{d^3\underset{\sim}{P}_H}{2W}\;\frac{d^3\underset{\sim}{l}_2}{2\,l_2^0}\;\delta(\sqrt{s_T} - l_2^0 - W)\,\delta(\underset{\sim}{l}_2 + \underset{\sim}{P}_H)$$

$$= \left(\frac{1}{2\pi}\right)^2 \frac{1}{2W}\;\frac{d^3\underset{\sim}{l}_2}{2\,l_2^0}\;\delta(\sqrt{s_T} - l_2^0 - W)$$

Defining $W_T = L_2^0 + W$, using $d^3k_2 = |\underset{\sim}{L}_2|^2 d|\underset{\sim}{L}_2| d\Omega_T$

$$dW_T = \frac{W_T}{W L_2^0} |\underset{\sim}{L}_2| d|\underset{\sim}{L}_2|$$

$$d\text{Lips}(s_T; P_H, L_2) = \left(\frac{1}{2\pi}\right)^2 \frac{|\underset{\sim}{L}_2|}{4W_T} d\Omega_T dW_T \delta(s_T^{1/2} - W_T)$$

$$= \frac{|\underset{\sim}{L}_2|}{(2\pi)^2} \frac{d\Omega_T}{4\sqrt{s_T}}$$

$$= \frac{dk^2 d\phi}{(2\pi)^2 8|\underset{\sim}{L}_1|\sqrt{s_T}}$$

using $k^2 = (L_1 - L_2)^2 = 2m_e^2 - 2L_1^0 L_2^0 + 2|\underset{\sim}{L}_1||\underset{\sim}{L}_2| \cos\psi$

Thus

$$d\text{Lips}(s_T; P_H, L_2) = \frac{dk^2 d\phi}{2^5 \pi^2 \sqrt{s_T} |\underset{\sim}{L}_1|}$$

Putting this expression into (B1) we obtain

$$\frac{d\sigma}{dk^2 d\phi ds} = \frac{1}{2^8 \pi^3 |\underset{\sim}{L}_1|^2 s_T} |T|^2 d\text{Lips}(s; q, P_2)$$

For the purposes of comparison with experiment it may be easier to express $|\underset{\sim}{q}_T| s_T$ in terms of laboratory frame measurements

$|\underset{\sim}{L}_1|^2 s_T = m^2 E_L$ where E_L is the lab energy of the incident electron.

similarly $|\underset{\sim}{p}_1| s^{1/2} = m k_L$ where k_L is the lab. energy of the virtual photon and $|\underset{\sim}{q}_H|$ is the com 3-momentum for the hadronic part of the system.

By a calculation exactly similar to the preceeding we can simplify

$$dLips(s; q, p_2) = \frac{1}{2^4 \pi \sqrt{s}\, |\underset{\sim}{p}_1|} dt \qquad (B2)$$

where, this time, we have integrated over the azimnthal angle.

We finally obtain an expression for the differential cross-section for pion electroproduction in terms only of quantities measurable in the laboratory:

$$\frac{d\sigma}{dk^2 d\phi\, ds\, dt} = \frac{|T|^2}{2^{12} \pi^4 m^3 E_L^2 k_L} \qquad (B3)$$

However, we wish to obtain a form for the electroproduction differential cross-section which is comparable with that for pion photoproduction. By use of the recurrence relation for Lorentz Invariant Phase Space we have kinematically separated the hadronic and leptonic parts. There remains a dynamical leptonic dependence in the matrix element which must be made explicit. This is a long and tedious process which will only be sketched here; a complete exposition may be found in Dombey (1969).

Making use of the one-photon approximation, we may write down an expression for the T matrix in terms of the electromagnetic current operator J_μ . For comparison with high energy photoproduction data, it will be useful to set down an equivalent expression in terms of helicity amplitudes. (We use s-channel helicity amplitudes throughout).

$$T = \frac{e}{k^2} \varepsilon_\mu T^\mu$$

$$= \frac{e}{k^2} \sum_\lambda a_\lambda e^{-i\lambda\phi} T_\lambda \qquad (B4)$$

where $e\varepsilon_\mu = \langle l_2 | J_\mu | l_1 \rangle$ - referring to leptonic vertex

$T_\mu = \langle N' | J_\mu | N \rangle$ - referring to hadronic vertex

λ = photon helicity

From QED, we know the dynamics of the lepton vertex and may write it down at once

$$\varepsilon_\mu = \bar{u}_2 \gamma_\mu u_1$$

To connect with the helicity amplitudes we may take

$$a_\lambda = e^*_\mu(\lambda)\, \varepsilon^\mu$$

where the polarisation vectors $e_\mu(\lambda)$ are

$$e_\mu(\pm 1) = \frac{1}{\sqrt{2}}\,(0, \mp 1, -i, 0)$$

$$e_\mu(0) = \frac{1}{\sqrt{|\underset{\sim}{k}^2|}}\,(|\underset{\sim}{k}|, 0, 0, k^0)$$

Assuming the leptons are unpolarized, one may now construct a photon polarization density matrix by summing over the spins of the electrons

$$\rho_{\lambda\lambda'} = \frac{1}{4} \sum a^*_\lambda a_{\lambda'}$$

$$\rho_{++} = \rho_{--} = \frac{1}{1-\varepsilon}\left(-\frac{k^2}{2}\right)$$

$$\rho_{+-} = \rho_{-+} = \frac{1}{1-\varepsilon}\left(\frac{\varepsilon k^2}{2}\right)$$

$$\rho_{+0} = \rho_{0+} = -\rho_{-0} = -\rho_{0-} = \frac{\sqrt{\varepsilon(1+\varepsilon)}}{1-\varepsilon}\,\frac{k^2}{2}$$

$$\rho_{00} = \frac{1}{1-\varepsilon}\left(-\varepsilon k^2\right)$$

Thus, for the unpolarised cross-section we require

$$\frac{1}{4}\sum_{\substack{\text{all}\\ \text{spins}}}|T|^2 = \frac{e^2}{k^4}\sum_{\lambda\lambda'}\rho_{\lambda\lambda'}\left[\sum_{\substack{\text{hadron}\\ \text{spins}}} T_\lambda\, T_{\lambda'}^{*}\, e^{-i\phi(\lambda-\lambda')}\right]$$

$$= \frac{e^2}{2k^2}\,\frac{1}{1-\varepsilon}\Big\{-|T_{+1}|^2-|T_{-1}|^2-2\varepsilon|T_0|^2+2\varepsilon\,\mathrm{Re}\,(T_{+1}T_{-1}^{*}\,e^{-2i\phi})+\sqrt{\varepsilon(1+\varepsilon)}\,2\,\mathrm{Re}\,(T_{+1}T_0\,e^{-i\phi}-T_{-1}T_0\,e^{i\phi})\Big\}$$

If we choose $\phi = 0$ along $\underset{\sim}{k}\times\underset{\sim}{q}$ fixes the helicity amplitude phases to be that of Jacob and Wick. Use of parity invariance allows the removal of the T_{-1} amplitudes. Putting $f_{\mu_2\mu_1\lambda}$ for T_λ where $\mu_2\,(\mu_1)$ denote final (initial) uncleon helicity we obtain:

$$\frac{1}{4}\Sigma|T|^2 = \frac{e^2}{k^2}\,\frac{1}{\varepsilon-1}\Big\{|f_{++1}|^2+|f_{+-1}|^2+|f_{-+1}|^2+|f_{--1}|^2+2\varepsilon\big(|f_{++0}|^2+|f_{-+0}|^2\big)-2\varepsilon\,\mathrm{Re}\,\big(f_{++1}f_{--1}^{*}-f_{+-1}f_{-+1}^{*}\big)\cos 2\phi$$

$$-\sqrt{2\varepsilon(\varepsilon+1)}\cos\phi\,\sqrt{2}\,\big(f_{++1}f_{++0}^{*}-f_{++0}f_{--1}^{*}+f_{+-1}f_{-+0}^{*}+f_{-+0}f_{-+1}^{*}\big)\Big\} \qquad (B5)$$

We wish to connect with photoproduction (for which the photon has only two helicities). The photoproduction cross-section is

$$d\sigma_\gamma = \frac{1}{4W|\underset{\sim}{k}|}\,|T_\gamma|^2\,dLips\,(s;q,p_2)$$

and using equation (B2)

$$\frac{d\sigma_\gamma}{dt} = \frac{1}{2^6 \pi s |\underset{\sim}{k}|^2} |T_\gamma|^2$$

$$= \frac{1}{2^6 \pi (s-m^2) m k_L} \left(|f_{++1}|^2 + |f_{+-1}|^2 + |f_{-+1}|^2 + |f_{--1}|^2\right)$$

$$= \frac{1}{2^5 \pi (s-m^2)^2} \left(|f_{++1}|^2 + |f_{+-1}|^2 + |f_{-+1}|^2 + |f_{--1}|^2\right) \quad (B6)$$

Using this as our starting point, we may now <u>define</u> the virtual photon differential cross-section to be

$$\frac{d\sigma_v}{dt} = \frac{1}{2^5 \pi (s-m^2)^2} \left\{|f_{++1}|^2 + |f_{+-1}|^2 + |f_{-+1}|^2 + |f_{--1}|^2 \right.$$

$$+ 2\varepsilon \left(|f_{++0}|^2 + |f_{-+0}|^2\right) - 2 Re \left(f_{++1} f^*_{--1} - f_{+-1} f^*_{-+1}\right) \varepsilon \cos 2\phi$$

$$- 2\sqrt{\varepsilon(1+\varepsilon)} \cos\phi \, Re \left(f_{++1} f^*_{+-0} - f_{++0} f^*_{--1} + f_{+-1} f^*_{-+0}\right.$$

$$\left.\left. + f_{-+0} f^*_{-+1}\right)\right\} \quad (B7)$$

$$= \frac{d\sigma}{dt}_u + \varepsilon \frac{d\sigma}{dt}_s + \frac{d\sigma}{dt}_T \varepsilon \cos 2\phi + \frac{d\sigma}{dt}_I \sqrt{2\varepsilon(1+\varepsilon)} \cos\phi$$

in a familiar notation.

Comparing this expression with equations (B5) and (B3) we have

$$\frac{d\sigma}{dk^2\, d\varphi\, ds\, dt} = \frac{1}{2^{12}\,\pi^4\, m^3\, E_L^{\,2}\, k_L}\ \frac{1}{4}\sum_{\text{spins}} |T|^2$$

$$= \frac{1}{2^{12}\,\pi^4\, m^3\, E_L^{\,2}\, k_L}\left(\frac{e^2}{-k^2}\right)\frac{1}{1-\varepsilon}\ \sum |T_v|^2$$

$$= \frac{1}{2^{12}\,\pi^4\, m^2\, E_L^{\,2}}\left(\frac{e^2}{-k^2}\right)\frac{1}{1-\varepsilon}\ 2^6\pi\,(s-m^2)\ \frac{d\sigma_v}{dt}$$

$$= \frac{s-m^2}{2^6\,\pi^3\, m^2\, E_L^{\,2}\,(1-\varepsilon)}\left(\frac{e^2}{-k^2}\right)\ \frac{d\sigma_v}{dt}$$

$$= \Gamma\ \frac{d\sigma_v}{dt} \qquad \text{(B8)}$$

where $\Gamma = \frac{s-m^2}{2^6\,\pi^3\, m^2\, E_L^{\,2}\,(1-\varepsilon)}\left(\frac{e^2}{-k^2}\right)$ is the conventional factor, extracted to show the correspondence of electroproduction and photoproduction cross-sections.

Note that in the first line of the above we have explicitly inserted the spin-average for electroproduction, this was not present in equation (B3).

Finally, lengthy calculation and use of the identity

$$\frac{1}{4}\sum_{\substack{\text{electron}\\ \text{spin}}} \varepsilon_\mu\, \varepsilon_\nu^{*} = \frac{1}{2}\, g_{\mu\nu}\, k^2 + l_{1\mu}\, l_{2\nu} + l_{1\nu}\, l_{2\mu}$$

will yield an expression for the polarisation parameter ε

$$\varepsilon^{-1} = 1 - 2\,\frac{|\underset{\sim}{k}_L|}{k^2}\,\tan^2\frac{\psi_L}{2}$$

where ψ_L is the laboratory scattering angle.

Figure Captions

Fig B1 The one photon approximation for neutral pion electroproduction.

Fig B2 The decomposition of the S-matrix into connected and disconnected parts.

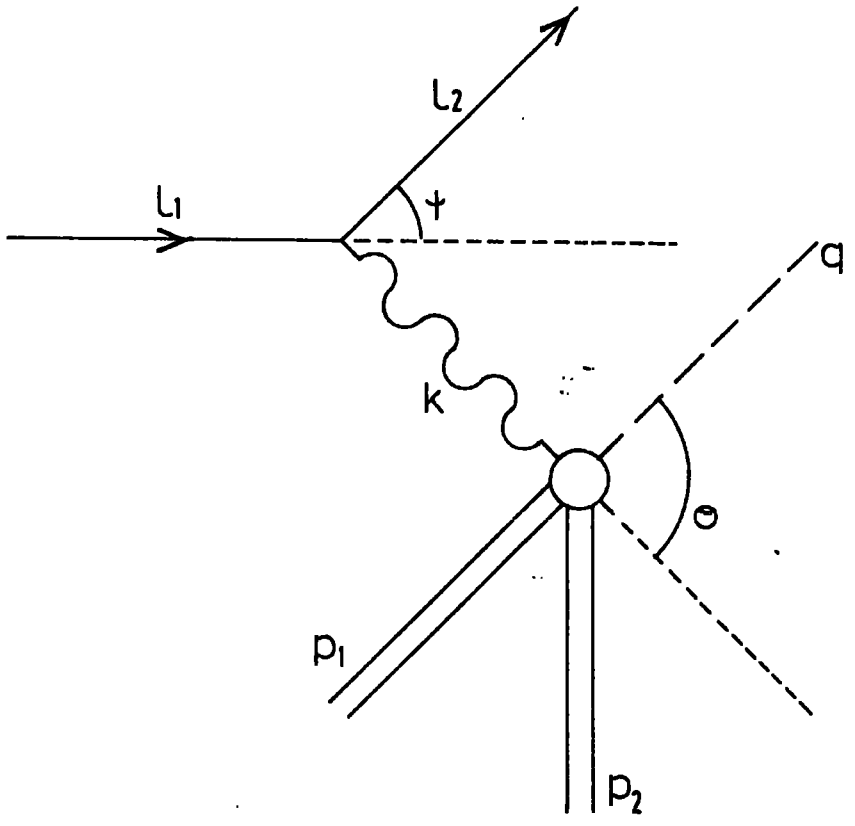

Fig.B1

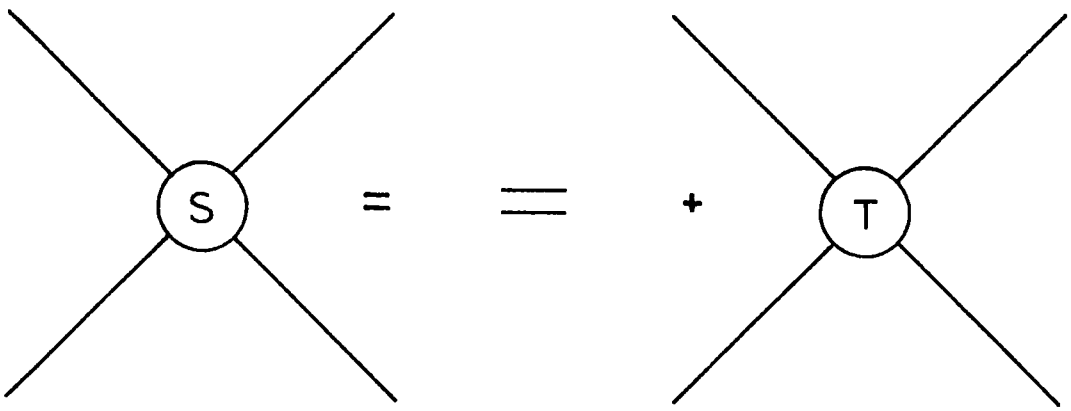

Fig.B2

Appendix C

a) The Invariant Amplitudes

There does not yet exist a complete analysis of neutral pion electroproduction in the resonance region. As mentioned in the text, there are a number of partial wave analyses of photoproduction available: Devenish et al (1973); Metcalf and Walker (1974); Moorhouse et al. (1974); some of which rely on dispersion relation techniques. The desire to perform dispersion relation calculations indicates the use of kinematical singularity free (KSF) amplitudes. Some discussion of this point is contained in Berends et al (1967), but that reference is heavily oriented to photoproduction. In particular an "explicitly gauge invariant" set of amplitudes (Dennery (1961)) is manifestly unsuitable for continuation to electroproduction processes. We therefore choose the set of amplitudes due to Ball (1961) which have been shown to be free of kinematic singularity in s, t, and k^2 (Hearn (1961)).

We introduce a maximal set of kinematic covariants M^i_μ $(i = 1,\ldots 8)$ which depend on hadron spins and momenta and have the Ball amplitudes B^i as dynamical coefficients. As this is an electromagnetic process, parity is conserved; for a weak process, there would be 16 amplitudes.

Referring to equation (B4)

$$T = \frac{e}{k^2} \varepsilon_\mu T^\mu$$

Let $$T_\mu = \sum_i M_\mu^i B_i$$

$$M_\mu^1 = \bar{u} \gamma_5 \tfrac{1}{2} (\gamma_\mu \not{k} - \not{k} \gamma_\mu) u$$

$$M_\mu^2 = \bar{u} \gamma_5 2 P_\mu u \qquad \text{(C1)}$$

$$M_\mu^3 = \bar{u} \gamma_5 2 q_\mu u$$

$$M_\mu^4 = \bar{u} \gamma_5 2 k_\mu u$$

$$M_\mu^5 = \bar{u} \gamma_5 (-\gamma_\mu) u$$

$$M_\mu^6 = \bar{u} \gamma_5 \not{k} P_\mu u$$

$$M_\mu^7 = \bar{u} \gamma_5 \not{k} k_\mu u$$

$$M_\mu^8 = \bar{u} \gamma_5 \not{k} q_\mu u$$

$$T = \frac{e}{k^2} \bar{u}_2 \gamma_5 \left\{ \frac{\not{\varepsilon}\not{k} - \not{k}\not{\varepsilon}}{2} B^1 + 2P.\varepsilon B^2 \right. \qquad \text{(C2)}$$

$$+ 2q.\varepsilon B^3 + 2k.\varepsilon B^4 - \not{\varepsilon} B^5 + \not{k} P.\varepsilon B^6$$

$$\left. + \not{k} k.\varepsilon B^7 + \not{k} q.\varepsilon B^8 \right\} u,$$

b) Current Conservation

The above expression is modified somewhat because the electromagnetic current is a conserved quantity. In particular we show how two of the kinematical covariants may be removed to yield a maximum of six amplitudes for electroproduction (cf the six helicity amplitudes of equation (B7)). The basic result comes from QED:

$$e\,\varepsilon_\mu = \langle l_2 |\, J_\mu(0) \,| l_1 \rangle$$

$$T_\mu = \langle N' |\, J_\mu(0) \,| N \rangle$$

From QED $\varepsilon_\mu = \bar{u}_2 \gamma_\mu u_1$

The photon current is conserved at both vertices i.e.

$$\partial_\mu J^\mu(x) = 0$$

which, in momentum space, gives us the two relations

$$k_\mu \varepsilon^\mu = 0$$

$$k_\mu T^\mu = 0 \qquad \text{(C3)}$$

It is apparent from the first of these why the photon polarisation density matrix in Appendix B had no time-like

parts. Using the invariant amplitude decomposition of T_μ (C2) the second relation becomes

$$2k^2 B_4 = (t-k^2-\mu^2) B_3 - \frac{s-u}{2} B_2$$

$$k^2 B_7 = B_5 - \frac{s-u}{4} B_6 + \frac{t-k^2-\mu^2}{2} B_8 \qquad (C4)$$

However, the first of the current conservation conditions tells us that neither B_4 nor B_7 appear in the electroproduction matrix element.

The only constraint placed on the Bi's by current conservation occurs for zero photon mass squared and is

$$(t-\mu^2) B_3 = \frac{s-u}{2} B_2$$

$$2B_5 = \frac{s-u}{2} B_6 - (t-\mu^2) B_8 \qquad (C5)$$

By itself, current conservation allows the elimination of two redundant amplitudes out of the original eight. It does not place any restriction on the form of the electroproduction transition matrix T. This may be seen "geometrically": the first of the two conditions states that ε_μ and k_μ are perpendicular (in 4-space); thus $T = T^\mu \varepsilon_\mu$ does not involve any component of T^μ parallel to k_μ ; the second condition, however, tells us that any such parallel component is zero (Lyth 1971).

The photoproduction matrix element contains only 4 amplitudes. This is because, in addition to current conservation, a massless photon is gauge invariant: i.e. the photoproduction matrix element is invariant with respect to substitutions of the form $\varepsilon_\mu \rightarrow \varepsilon_\mu - \lambda k_\mu$ Clearly, this satisfies $k_\mu \varepsilon^\mu = 0$ only for $k^2 = 0$, and is a special case of $k_\mu T^\mu = 0$. A massive photon is not gauge invariant.

Current conservation also imposes conditions on the amplitudes ϕ_i which will be introduced in the next section:

$$\phi_1 + \hat{\underset{\sim}{k}} \cdot \hat{\underset{\sim}{q}}\, \phi_3 + \phi_5 - \frac{k^\circ}{|\underset{\sim}{k}|}\, \phi_8 = 0$$

$$\phi_6 + \hat{\underset{\sim}{k}} \cdot \hat{\underset{\sim}{q}}\, \phi_4 - \frac{k^\circ}{|\underset{\sim}{k}|}\, \phi_7 = 0 \qquad (C6)$$

c) The Multiple Amplitudes

In order to connect the matrix element with the eigen-amplitudes of parity and angular momentum i.e. in order to perform partial wave analysis, we first split the expression (C2) involving Dirac 4-spinors into an equivalent one involving Pauli spinors. This is essentially the procedure of Chew et al (1957) (hereafter referred to as CGLN).

Equations (A2) now become:

$$\bar{u}_2 \gamma_5 = (E_2+m)^{-1/2} \left[\chi^\dagger \, \underset{\sim}{\sigma}\cdot\underset{\sim}{q} \, , \; \chi^\dagger (E_2+m) \right]$$

$$u_1 = (E_1+m)^{-1/2} \begin{bmatrix} (E_1+m)\,\chi \\ -\underset{\sim}{\sigma}\cdot\underset{\sim}{k}\,\chi \end{bmatrix}$$

because we are working in the hadronic com where

$$\underset{\sim}{p}_1 = -\underset{\sim}{k} \qquad \underset{\sim}{q} = -\underset{\sim}{p}_2$$

Use of the identities

$$\not{\varepsilon} = \begin{bmatrix} \varepsilon^\circ & -\underset{\sim}{\sigma}\cdot\underset{\sim}{\varepsilon} \\ \underset{\sim}{\sigma}\cdot\underset{\sim}{\varepsilon} & -\varepsilon^\circ \end{bmatrix} \qquad \not{k} = \begin{bmatrix} k^\circ & -\underset{\sim}{\sigma}\cdot\underset{\sim}{k} \\ \sigma\cdot k & -k^\circ \end{bmatrix}$$

and

$$\tfrac{1}{2}(\not{\varepsilon}\not{k} - \not{k}\not{\varepsilon}) = \begin{bmatrix} i\,\underset{\sim}{\sigma}\cdot\underset{\sim}{k}\times\underset{\sim}{\varepsilon} & k^\circ\underset{\sim}{\sigma}\cdot\underset{\sim}{\varepsilon} - \varepsilon^\circ\underset{\sim}{\sigma}\cdot\underset{\sim}{k} \\ k^\circ\underset{\sim}{\sigma}\cdot\underset{\sim}{\varepsilon} - \varepsilon^\circ\underset{\sim}{\sigma}\cdot\underset{\sim}{k} & i\,\underset{\sim}{\sigma}\cdot\underset{\sim}{k}\times\underset{\sim}{\varepsilon} \end{bmatrix}$$

quickly shows that there are eight independent kinematical factors which may be written $\left(\hat{\underset{\sim}{q}}\ |\underset{\sim}{q}| = \underset{\sim}{q}\right)$

$$\mathcal{F} = \underset{\sim}{\sigma}\cdot\underset{\sim}{\varepsilon}\ \phi_1 + i\,\underset{\sim}{\sigma}\cdot\hat{\underset{\sim}{q}}\ \underset{\sim}{\sigma}\cdot\hat{\underset{\sim}{k}}\times\underset{\sim}{\varepsilon}\ \phi_2 + \underset{\sim}{\sigma}\cdot\hat{\underset{\sim}{k}}\ \hat{\underset{\sim}{q}}\cdot\underset{\sim}{\varepsilon}\ \phi_3 + \underset{\sim}{\sigma}\cdot\hat{\underset{\sim}{q}}\ \hat{\underset{\sim}{q}}\cdot\underset{\sim}{\varepsilon}\ \phi_4$$

$$+ \underset{\sim}{\sigma}\cdot\hat{\underset{\sim}{k}}\ \hat{\underset{\sim}{k}}\cdot\underset{\sim}{\varepsilon}\ \phi_5 + \underset{\sim}{\sigma}\cdot\hat{\underset{\sim}{q}}\ \hat{\underset{\sim}{k}}\cdot\underset{\sim}{\varepsilon}\ \phi_6 - \underset{\sim}{\sigma}\cdot\hat{\underset{\sim}{q}}\ \varepsilon^0\ \phi_7 - \underset{\sim}{\sigma}\cdot\hat{\underset{\sim}{k}}\ \varepsilon^0\ \phi_8 \qquad (C7)$$

By convention, the ϕ_i are chosen to be such that

$$\sum_{i=1}^{8} B_i\, M_\mu^i\, \varepsilon^\mu = \chi_2^+\, \mathcal{F}\, \chi_1 \qquad (C8)$$

This immediately leads to the following identifications

$$\phi_1 = (E_1+m)^{1/2}(E_2+m)^{1/2}\left((W-m)B^1 - B^5\right)$$

$$\phi_2 = -(E_1-m)^{1/2}(E_2-m)^{1/2}\left((W+m)B^1 + B^5\right)$$

$$\phi_3 = (E_1-m)^{1/2}(E_2-m)^{1/2}(E_2+m)\left(2B^3 - B^2 + (W+m)\left(\frac{B^6}{2} - B^8\right)\right)$$

$$\phi_4 = (E_1+m)^{1/2}(E_2+m)^{1/2}(E_2-m)\left(B^2 - 2B^3 + (W-m)\left(\frac{B^6}{2} - B^8\right)\right)$$

$$\phi_5' = (E_1+m)^{1/2}(E_2+m)^{1/2}(E_1-m)\left(2B^4 - B^1 - B^2 + (W+m)\left(\frac{B^6}{2} - B^7\right)\right)$$

$$\phi_6' = (E_1-m)^{1/2}(E_2-m)^{1/2}(E_1+m)\left(B^2 - (E_1+m)^{-1}\left(k^0 B^1 + B^5\right) - 2B^4 + (W-m)\left(\frac{B^6}{2} - B^7\right)\right)$$

$$\phi_7' = -(E_2-m)^{1/2}(E_1+m)^{1/2}\left(B^1(E_1-m) + (E_1+E_2)B^2 + 2E_\pi B^3 - B^5\right.$$
$$\left. + (W-m)\left(\frac{B^6}{2}(E_1+E_2) + E_\pi B^8\right) + k^0\left(2B^4 + (W-m)B^7\right)\right)$$

$$\phi_8' = (E_1-m)^{1/2}(E_2+m)^{1/2}\ B^1(E_1-m) + (E_1+E_2)B^2 + 2E_\pi B^3 + B^5$$
$$- (W+m)\left(\frac{B^6}{2}(E_1+E_2) + E_\pi B^8\right) + k^0\left(2B^4 - (W+m)B^7\right)$$

Current conservation allows us to express B^4 and B^7 in terms of the other B^i; and ϕ_8' and ϕ_7' in terms of the other ϕ_i . We thus obtain:-

$$\phi_1 = (E_1+m)^{1/2}(E_2+m)^{1/2}\left((W-m)B' - B^5\right)$$

$$\phi_2 = -(E_1-m)^{1/2}(E_2-m)^{1/2}\left((W+m)B' + B^5\right)$$

$$\phi_3 = (E_1-m)^{1/2}(E_2-m)^{1/2}(E_2+m)\left(2B^3 - B^2 + (W+m)\left(\frac{B^6}{2} - B^8\right)\right)$$

$$\phi_4 = (E_1+m)^{1/2}(E_2+m)^{1/2}(E_2-m)\left(B^2 - 2B^3 + (W-m)\left(\frac{B^6}{2} - B^8\right)\right)$$

$$\phi_5 = \frac{1}{k^2}(E_1-m)^{1/2}(E_2+m)^{1/2}\left\{(E_1+m)\left(k^2B' - (W-m)B^5 - (E_1-m)2W\right.\right. \tag{C9}$$

$$\left.\left(B^2 - (W+m)\frac{B^6}{2}\right)\right) + \left(k^0\,\frac{t-\mu^2-k^2}{2} + k^2E_\pi\right)\left(2B^3 - B^2 + (W+m)\left(\frac{B^6}{2} - B^8\right)\right)\Big\}$$

$$\phi_6 = \frac{1}{k^2}(E_1+m)^{1/2}(E_2-m)^{1/2}\left\{-(E_1-m)k^2B' + (W+m)B^5 - (E_1+m)2W\right.($$

$$\left.B^2 + (W-m)\frac{B^6}{2}\right)) + \left(k^0\,\frac{t-\mu^2-k^2}{2} + k^2E_\pi\right)\left(B^2 - 2B^3 + (W-m)\left(\frac{B^6}{2} - B^8\right)\right)\Big\}$$

The ϕ_i have a simple relation to the eigenamplitudes of parity and angular momentum, originally defined by CGLN. However, because of the relation (C8) there is a multiplicative factor of $8\pi W$ connecting our ϕ_i and the conventional $\mathcal{F}_i$.

$$
\begin{aligned}
\phi_1 &= 8\pi W \sum_l \left(l M_{l+} + E_{l+}\right) P'_{l+1}(z) + \left(M_{l-} (l+1) + E_{l-}\right) P'_{l-1}(z) \\
\phi_2 &= 8\pi W \sum_l \left(M_{l+} (l+1) + l M_{l-}\right) P'_l(z) \\
\phi_3 &= 8\pi W \sum_l \left(E_{l+} - M_{l+}\right) P''_{l+1}(z) + \left(E_{l-} + M_{l-}\right) P''_{l-1}(z) \\
\phi_4 &= 8\pi W \sum_l \left(M_{l+} - E_{l+} - M_{l-} - E_{l-}\right) P''_l(z) \\
\phi_5 &= 8\pi W \sum_l (l+1) S_{l+} P'_{l+1}(z) - l S_{l-} P'_{l-1}(z) \\
\phi_6 &= 8\pi W \sum_l \left(l S_{l-} - (l+1) S_{l+}\right) P'_l(z)
\end{aligned}
\qquad \text{(C10)}
$$

The E, M, S are the electric, magnetic and scalar transition amplitudes respectively. We display their relationships in table C1.

d) Helicity Amplitudes

In Appendix B, we obtained an expression for the differential cross-section for pion-electroproduction using helicity amplitudes. We are now in a position to connect the invariant amplitudes and the helicity amplitudes.

Our starting point is equation (C8):

$$T = \frac{e}{k^2} \chi_2^+ \mathcal{F} \chi_1$$

Following Jones (1965), we take the photon 3-momentum to define the positive z-axis, and the x-axis lying in the hadronic scattering plane (diagram C1). The

polarisation vectors for a photon with helicity ± 1 or 0 become $e^{\pm 1}_{\mu} = \frac{1}{\sqrt{2}}(0, \mp 1, -i, 0)$ $e^{0}_{\mu} = \frac{1}{k}(|\underset{\sim}{k}|, 0, 0, k^0)$ where the photon momentum $k_\mu = (k^0, 0, 0, |\underset{\sim}{k}|)$

With the above convention, an initial-state proton with 2-spinor $\begin{pmatrix}1\\0\end{pmatrix}$ i.e. spin along the z-axis has negative helicity: χ_- Similarly, in the final state, a proton with 2-spinor $\begin{pmatrix}\cos\Theta/2\\ \sin\Theta/2\end{pmatrix}$ i.e. spin up along Θ -direction, has negative helicity. By making a conventional assumption of $\varphi = 0$ and evaluating the 2-spinor decomposition explicitly one may obtain the identification of the helicity amplitudes and the multipole amplitudes:

$$f_{++1} = \sqrt{2}\sin\Theta/2\left\{\phi_1 + \phi_2 + \cos^2\Theta/2\,(\phi_3 + \phi_4)\right\}$$

$$f_{--1} = -\sqrt{2}\sin\Theta/2\cos^2\Theta/2\,(\phi_3 + \phi_4)$$

$$f_{+-1} = \sqrt{2}\sin^2\Theta/2\cos\Theta/2\,(\phi_3 - \phi_4)$$

$$f_{-+1} = -\sqrt{2}\cos\Theta/2\left\{\phi_1 - \phi_2 - \sin^2\Theta/2\,(\phi_3 - \phi_4)\right\} \qquad \text{(C11)}$$

$$f_{++0} = \frac{k}{|\underset{\sim}{k}|}\cos\Theta/2\,(\phi_5 + \phi_6)$$

$$f_{-+0} = \frac{k}{|\underset{\sim}{k}|}\sin\Theta/2\,(\phi_5 - \phi_6)$$

The first two amplitudes are the single flip amplitudes present in photoproduction; $f_{+-|}$ is the double flip amplitude; $f_{-+|}$ is the non-flip amplitude. The last two are present only in electroproduction.

With the three sets of equations (C9, C10, C11) we have the fundamental, properly normalised relations between the amplitudes. It will, however, be useful to write down the inversion of equations (C9), i.e. to find the expression for the invariant amplitudes in terms of the sums of multipoles.

For brevity, we identify

$$Z_1 = (E_1+m)^{1/2} \qquad Z_2 = (E_2+m)^{1/2}$$

$$Y_1 = (E_1-m)^{1/2} \qquad Y_2 = (E_2-m)^{1/2}$$

$$B_1 = \frac{1}{2W}\left\{ \frac{\phi_1}{Z_1 Z_2} - \frac{\phi_2}{Y_1 Y_2} \right\}$$

$$B_2 = \frac{1}{4W^2|\underset{\sim}{k}|^2}\left\{(s-m^2-k^2)k^2 B_1 - 2mk^2 B_5 + \left(k^0\frac{\mu^2-k^2-t}{2} - k^2 E_\pi\right)\right.$$

$$\left.\left(\frac{(W+m)\phi_4}{Z_1 Z_2 Y_2^2} - \frac{(W-m)\phi_3}{Y_1 Y_2 Z_2^2}\right) + k^2\left(\frac{(W+m)\phi_6}{Z_1 Y_2} - \frac{(W-m)\phi_5}{Y_1 Z_2}\right)\right\}$$

$$B_3 = \frac{B_2}{2} + \frac{1}{2W}\left\{\frac{(W-m)\phi_3}{Y_1 Y_2 Z_2^2} - \frac{(W+m)\phi_4}{Z_1 Z_2 Y_2^2}\right\}$$

$$B_5 = -\frac{1}{2W}\left\{\frac{(W+m)\phi_1}{Z_1 Z_2} + \frac{(W-m)\phi_2}{Y_1 Y_2}\right\} \qquad \text{(C12)}$$

$$B_6 = \frac{1}{2W^2|\underset{\sim}{k}|^2}\left\{-2mk^2 B_1 + (s-m^2-k^2)B_5 + \left(k^0\frac{\mu^2-k^2-t}{2} - k^2 E_\pi\right)\right.$$

$$\left.\left(\frac{\phi_3}{Y_1 Y_2 Z_2^2} + \frac{\phi_4}{Z_1 Z_2 Y_2^2}\right) + k^2\left(\frac{\phi_5}{Y_1 Z_2} + \frac{\phi_6}{Z_1 Y_2}\right)\right\}$$

$$B_8 = \frac{1}{2}B_6 - \frac{1}{2W}\left\{\frac{\phi_3}{Y_1 Y_2 Z_2^2} + \frac{\phi_4}{Z_1 Z_2 Y_2^2}\right\}$$

e) Other Amplitudes

To ease comparison with other work, we give below the relationship of the Ball amplitudes to the invariant amplitudes used by Dennery (1961) and Donnachie (1971).

$$
\begin{aligned}
A_1 &= B_1 - m B_6 \\
A_2 &= \frac{2 B_2}{t-\mu^2} \\
A_3 &= -B_9 \\
A_4 &= -\tfrac{1}{2} B_6 \\
A_5 &= \frac{2}{t-\mu^2-k^2}\left(B_1 + 2B_4 + \frac{s-u}{t-\mu^2}\,\tfrac{1}{2} B_2\right) \\
A_6 &= B_7
\end{aligned}
\qquad \text{(C13)}
$$

It is clear that these "gauge invariant" amplitudes have kinematical singularities. Although these are outside the physical region, we prefer to use the Ball amplitudes in the dispersion relations (and the FESRs derived therefrom). Note that if the kinematical covariants used by Fubini et al (1958) are adopted, the singularities may occur within the physical region.

Table C1

The multipole amplitude for pion electroproduction.

J	L	Parity	Multipole	Notation	Lowest l
$l + \frac{1}{2}$	$L = j+\frac{1}{2} = l+1$	$(-1)^L$	2^L	E_{l+}	0
$l - \frac{1}{2}$	$L = j-\frac{1}{2} = l-1$	$(-1)^L$	2^L	E_{l-}	2
$l + \frac{1}{2}$	$L = j-\frac{1}{2} = l$	$(-1)^{L+1}$	2^L	M_{l+}	1
$l - \frac{1}{2}$	$L = j+\frac{1}{2} = l$	$(-1)^{L+1}$	2^L	M_{l-}	1
$l + \frac{1}{2}$	$L = j+\frac{1}{2} = l+1$	$(-1)^L$	2^L	S_{l+}	0
$l - \frac{1}{2}$	$L = j-\frac{1}{2} = l-1$	$(-1)^L$	2^L	S_{l-}	1

l = angular momentum of pion-nucleon final state

j = total angular momentum of pion-nucleon final state

L = total orbital angular momentum of photon

Only (E_{l+}, M_{l-}) contribute to photoproduction

Appendix D

1) Asymptotic Behaviour of Helicity Amplitudes

We evaluate finite energy sum rules (FESRs) of the helicity amplitudes discussed in the previous appendix. The helicity amplitudes contain various kinematical singularities (factors of $(E_1 - m)^{1/2}$, $\sin\theta/2$ ...) as functions of energy and k^2; we require to eliminate these in order that the FESRs may be integrals over functions containing only dynamical singularities.

Using equations C11 and C9 we can show that the helicity amplitudes approximate to singularity free combinations of the Ball amplitudes, for large values of s.

a) Single Flip Amplitude

$$f_{++1} + f_{--1} = \sqrt{2}\,\sin\theta/2\,(\phi_1 + \phi_2)$$

$$= \sqrt{\frac{-t}{2|\underset{\sim}{q}||\underset{\sim}{k}|}}\left\{z_1 z_2\left((W-m)B_1 - B_5\right) - Y_1 Y_2\left((W+m)B_1 + B_5\right)\right\}$$

$$\simeq \sqrt{\frac{-t}{2|\underset{\sim}{q}||\underset{\sim}{k}|}}\;\frac{1}{2W}\left\{2m\,(s-m^2)B_1 - 2(s+m^2)B_5 + (k^2+\mu^2)(mB_1 + B_5)\right\}$$

Put $B_5 = B_5' + \frac{s-u}{4}B_6$ (see over)

$$\Rightarrow f_{++1} + f_{--1} \simeq -\sqrt{\frac{-t}{2}}\;\nu B_6 \qquad \nu = \frac{s-u}{2}$$

The approximations used are already reasonable for

$\underset{\sim}{p}_L = 5$ GeV.

b) Double Flip Amplitude

$$f_{+-1} = \sqrt{2}\ \cos\Theta/2 \sin^2\Theta/2\ (\phi_3 - \phi_4)$$

$$= \frac{-t}{2\sqrt{2}}\left\{ \frac{z_2}{z_1}\left(2B_3 - B_2 + (W+m)\left(\tfrac{1}{2}B_6 - B_8\right)\right) + \frac{y_2}{y_1}\left(2B_3 - B_2 - (W-m)\left(\tfrac{1}{2}B_6 - B_8\right)\right)\right\}$$

$$\simeq \frac{-t}{2\sqrt{2}}\left\{ 4B_3 - B_2 + 2m\left(\tfrac{1}{2}B_6 - B_8\right) + \ldots \right\} \qquad (D2)$$

$$\Rightarrow \quad f_{+-1} \simeq -t\sqrt{2}\ B_3$$

c) Non-flip Amplitude

$$f_{-+1} = \sqrt{2}\ \cos\Theta/2 \left\{ -(\phi_1 - \phi_2)\right\} + f_{+-1}$$

$$\simeq -\sqrt{2}\ \nu\left(B_1 - m B_6\right) - t\sqrt{2}\ B_3 \qquad (D3)$$

2) Asymptotic Behaviour of Invariant Amplitudes

Using Ball & Jacob's expression (1968) for the Ball amplitudes in terms of t-channel helicity amplitudes, and assuming a Regge-type energy dependence of $s^{\alpha-1}$ for the helicity amplitudes, we obtain the following high energy behaviour for the Ball amplitudes:

$B_1, B_2, B_5', B_6, B_8 \quad \sim s^{\alpha-1}$

$B_3, B_5 \quad \sim s^{\alpha}$

and we define

$$B_5' = B_5 - \frac{\varepsilon - u}{4} B_6$$

Appendix E : Isospin and Crossing

1) Isospin Decomposition

It is conventionally assumed that the isotopic spin properties of the electromagnetic current are those of an isoscalar and the third component of an isovector, (but Sanda & Shaw (1971) suggest an isotensor component). Thus

$$J^{\mu} = J^{\mu}_{V_3} + J^{\mu}_{S}$$

This allows an isospin decomposition of the invariant amplitudes originally due to Watson (1954)

$$\begin{aligned} B &= B^{S} + B^{V} \\ &= B^{0}\tau_{\beta} + B^{+}\delta_{\beta 3} + B^{-}\tfrac{1}{2}[\tau_{\beta},\tau_{3}] \\ &= B^{0}\mathcal{I}^{0} + B^{+}\mathcal{I}^{+} + B^{-}\mathcal{I}^{-} \end{aligned}$$

where τ_{β}, τ_{3} are Pauli (iso)spin matrices and β is the isospin index of the outgoing pion. The matrix elements of the various charge states are shown on table E1.

Careful attention should be paid to the definition of the charge conjugation properties of the pion-nucleon state. We follow Martin and Spearman (1970) (p268)

$$C|\pi^{\pm}\rangle = -|\pi^{\mp}\rangle$$

The usual field-theoretic convention is $C|\pi^{\pm}\rangle = +|\pi^{\mp}\rangle$ in accord with $C|\pi^{0}\rangle = +|\pi^{0}\rangle$

One may connect the isovector transition amplitudes $B^{\pm}$ with those of definite isospin $\frac{1}{2}$, $\frac{3}{2}$ in the final s-channel state $B^{1/2}$, $B^{3/2}$

$$B^{+} = \tfrac{1}{3} B^{1/2} + \tfrac{2}{3} B^{3/2}$$

$$B^{-} = \tfrac{1}{3} \left(B^{1/2} - B^{3/2}\right)$$

Thus one obtains

$$\langle \pi^{0} p | T | \gamma p \rangle = B^{0} + \tfrac{2}{3} B^{3/2} + B^{1/2}$$

$$\langle \pi^{+} n | T | \gamma p \rangle = -\sqrt{2}\, B^{0} + \tfrac{\sqrt{2}}{3} \left(B^{3/2} - B^{1/2}\right)$$

$$\langle \pi^{-} p | T | \gamma n \rangle = \sqrt{2}\, B^{0} + \tfrac{\sqrt{2}}{3} \left(B^{3/2} - B^{1/2}\right)$$

$$\langle \pi^{0} n | T | \gamma n \rangle = -B^{0} + \tfrac{2}{3} B^{3/2} + B^{1/2}$$

Thus it is only by investigating γ-scattering off neutrons as well as protons that a separation of the ρ-like and ω-like contributions can be made.

2. Crossing

For the process $\gamma p \to \pi^0 p$ only, the amplitudes have the definite crossing properties ($s \leftrightarrow u$ symmetry)

$$B_1(\nu) = B_1(-\nu) \qquad B_3(\nu) = -B_3(-\nu)$$

$$B_2(\nu) = B_2(-\nu) \qquad B_5(\nu) = -B_5(-\nu)$$

$$B_6(\nu) = B_6(-\nu) \qquad B_8(\nu) = -B_8(-\nu)$$

The above follows from the simple expression for $\gamma p \to \pi^0 p$ in terms of definite isospin amplitudes:

$$B^{\pi^0 p} = B^0 + B^+$$

Table E1

Matrix elements of $J^{(t,o)}$ for all charge configurations

	$\gamma p \to \pi^0 p$	$\gamma n \to \pi^0 n$	$\gamma p \to \pi^+ n$	$\gamma n \to \pi^- p$
J^+	1	1	0	0
J^-	0	0	$-\sqrt{2}$	$-\sqrt{2}$
J^0	1	-1	$-\sqrt{2}$	$\sqrt{2}$

Appendix F

1. Form Factors

From the use of the Ball invariant amplitudes, the behaviour of the multipole form factors, and the constraints they must satisfy, can be easily derived. We follow the approach of Devenish and Lyth (1975). Devenish et al (1977) arrive at consistent conclusions in an intensely detailed paper.

We express each multipole in terms of combinations of the Bi.

$$E_{L+} = \frac{1}{8\pi W}\frac{1}{2(L+1)}\int_{-1}^{1} dz \left\{ \phi_1 P_L(z) - \phi_2 P_{L+1}(z) + L\phi_3 \frac{P_{L-1}(z) - P_{L+1}(z)}{2L+1} + \phi_4 (L+1) \frac{P_L(z) - P_{L+2}(z)}{2L+3} \right\}$$

$$E_{L-} = \frac{1}{8\pi W}\frac{1}{2L}\int_{-1}^{1} dz \left\{ \phi_1 P_L(z) - \phi_2 P_{L-1}(z) - \phi_3 (L+1) \frac{P_{L-1}(z) - P_{L+1}(z)}{2L+1} - L\phi_4 \frac{P_{L-2}(z) - P_L(z)}{2L-1} \right\}$$

$$M_{L+} = \frac{1}{8\pi W}\frac{1}{2(L+1)}\int_{-1}^{1} dz \left\{ \phi_1 P_L(z) - \phi_2 P_{L+1}(z) - \phi_3 \frac{P_{L-1}(z) - P_{L+1}(z)}{2L+1} \right\} \qquad \text{(F1)}$$

$$M_{L-} = \frac{1}{8\pi W}\frac{1}{2L}\int_{-1}^{1} dz \left\{ -\phi_1 P_L(z) + \phi_2 P_{L-1}(z) + \phi_3 \frac{P_{L-1}(z) - P_{L+1}(z)}{2L+1} \right\}$$

$$S_{L+} = \frac{1}{8\pi W}\frac{1}{2(L+1)}\int_{-1}^{1} dz \left\{ \phi_6 P_{L+1}(z) + \phi_5 P_L(z) \right\}$$

$$S_{L-} = \frac{1}{8\pi W}\frac{1}{2L}\int_{-1}^{1} dz \left\{ \phi_6 P_{L-1}(z) + \phi_5 P_L(z) \right\}$$

The notation is as in Appendix C. The inversions above may be accomplished by liberal use of the formulae:

$$\int_{-1}^{1} P_\ell(z)\, P'_{\ell+1}(z)\, dz = 2 \qquad \int_{-1}^{1} P_\ell(z)\, P'_{\ell-1}(z)\, dz = 0$$

$$\int_{-1}^{1} P_\ell(z)\, P'_{\ell+3}(z)\, dz = 2$$

$$\int_{-1}^{1} P_\ell(z)\, P'_{\ell+5}(z)\, dz = 2$$

and $$\int_{-1}^{1} P_n(z)\, P''_m(z)\, dz = m(m+1) - n(n+1) \quad \text{for } m = n+2,\ n+4,\ n+6$$

The ϕ_i are combinations of Ball amplitudes with kinematic coefficients.

$$\phi_1 = z_1 z_2 F_1 = X_1 F_1 \qquad \phi_4 = z_1 z_2 Y_2^2 F_4 = X_4 F_4$$

$$\phi_2 = Y_1 Y_2 F_2 = X_2 F_2 \qquad \phi_5 = \tfrac{1}{k^2} Y_1 z_2 F_5 = X_5 F_5$$

$$\phi_3 = Y_1 Y_2 z_2^2 = X_3 F_3 \qquad \phi_6 = \tfrac{1}{k^2} z_1 Y_2 F_6 = X_6 F_6$$

Now $$(E_1 \pm m)^{1/2} = \frac{(W \pm m)}{\sqrt{2W}} \left(1 - \frac{k^2}{(W \pm m)^2}\right)^{1/2} = \frac{m_\pm}{\sqrt{2 m_R}}\, \phi_\pm \qquad \text{(F2)}$$

from which it may be seen that as $k^2 \to (m_R \pm m)^2$ the Xi have the following behaviour:

$$X_1, X_4, X_6 \sim \phi_+ \qquad k^2 \to m_+^2$$

$$X_2, X_3, X_5 \sim \phi_- \qquad k^2 \to m_-^2$$

Since the F_i are combinations of the Ball amplitudes which do not involve kinematical singularities, the above gives the behaviour of the ϕ_i at the threshold and pseudo-threshold in k^2. It remains only to derive the threshold behaviour of the legendre polynomials $P_L(z)$.

Since there are no kinematic singularities within the F_i, a fixed - s dispersion relation may be assumed for the imaginary part (Jones (1965)). This may be inserted into the expression for the multipoles, and the order of integration interchanged.

Schematically, for any multipole M_L

$$M_L \sim \sum_i a_i X_i \int_{-1}^{1} dz \; Im\, F_i(s,t,k^2)\, P_{L_i}(z)$$

a_i = numerical coefficient

on substituting the fixed-s dispersion relation this becomes

$$\sim \sum_i a_i X_i \int_{-1}^{1} dz\, P_{L_i}(z) \int_{4\mu^2}^{\infty} \frac{Im\, F_i}{t'-t}\, dt'$$

However,

$$-\frac{1}{2}\int_{-1}^{1} \frac{dz'\, P_L(z')}{z'-z} = Q_L(z)$$

where the $Q_L(z)$ are legendre functions of the second kind.

$$\Rightarrow M_L \sim \sum_i \frac{a_i X_i}{|\underset{\sim}{q}|\,|\underset{\sim}{k}|} \int_{4\mu^2}^{\infty} dt'\, Q_{L_i}(z')\, \mathrm{Im}\, F_i(s,t',k^2)$$

where we have used: $t'-t = |\underset{\sim}{q}|\,|\underset{\sim}{k}|\,(z'-z)$

The full expression for z' is

$$z' = \frac{1}{|\underset{\sim}{q}|\,|\underset{\sim}{k}|}\left(\frac{t'-\mu^2-k^2}{2} + k^0 E_\pi\right)$$

where

$$|\underset{\sim}{k}| = \frac{m_+ m_-}{2 m_R}\, q_+ q_-$$

Thus for the thresholds $q_\pm \to 0$, $k \to 0$, and, for finite t'

$z' \to \infty$.

The constraints on the multipoles therefore appear at the lower end of the above integration. For large z' the behaviour of $Q_L(z')$ is

$$Q_L(z') \sim z'^{-L-1} \sim |\underset{\sim}{k}|^{L+1}$$

From this we made finally deduce the behaviour of the multipoles at the thresholds in k^2:

$$M_i \sim \sum_i a_i X_i\, |\underset{\sim}{k}|^{L_i}\, \mathrm{Im}\, F_i \qquad \text{(F3)}$$

We shall briefly illustrate the method by deriving the constraints which must exist between E_{l+} and S_{L+} at the thresholds. We shall then just quote the relationships for the other multipoles.

We shall require a recurrence formula for legendre Polynomials (Sueddon 1956) : $z P_L(z) = \frac{1}{2L+1}\left((L+1)P_{L+1}(z) + L P_{L-1}(z)\right)$

$$\phi_5 = \frac{1}{k^2} Y_1 z_2 \left\{ z_1^2 \left[k^2 B_1 - (W-m) B_5 - 2W(E_1 - m)\left(B_2 - (W+m)\tfrac{1}{2} B_8\right)\right] + \left(k^0 \underset{\sim}{q}\cdot\underset{\sim}{k} - |\underset{\sim}{k}|^2 E_\pi\right) F_3 \right\}$$

$$\phi_6 = \frac{1}{k^2} z_1 Y_2 \left\{ - Y_1^2 \left[k^2 B_1 + (W+m) B_5 - 2W(E_1 + m)\left(B_2 + (W-m)\tfrac{1}{2} B_8\right)\right] + \left(k^0 \underset{\sim}{q}\cdot\underset{\sim}{k} - |\underset{\sim}{k}|^2 E_\pi\right) F_4 \right\}$$

Which as $\phi_+ \to 0$ become

$$\phi_5 \sim k^0 |\underset{\sim}{q}| |\underset{\sim}{k}| z F_3$$

$$\phi_6 \sim - \phi_+ 2m(W+m) F_2 + \phi_+ k^0 |\underset{\sim}{k}| |\underset{\sim}{q}| z F_4$$

And as $\phi_- \to 0$ become

$$\phi_5 \sim \phi_- 2m(W-m) F_1 + \phi_- k^0 |\underset{\sim}{k}| |\underset{\sim}{q}| z F_3$$

$$\phi_6 \sim k^0 |\underset{\sim}{k}| |\underset{\sim}{q}| z F_4$$

Now

$$E_{L+} = \frac{1}{8\pi W}\,\frac{1}{2(L+1)}\,\frac{1}{|\underset{\sim}{q}||\underset{\sim}{k}|}\int_{4m^2}^{\infty} dt'\Big\{Q_L(z')\,Z_1 Z_2\,\mathrm{Im}F_1 - Q_{L+1}(z')\,Y_1 Y_2\,\mathrm{Im}F_2 +$$

$$Y_1 Y_2 Z_2^2\,\mathrm{Im}F_3\,\frac{L}{2L+1}\left(Q_{L-1}(z') - Q_{L+1}(z')\right) + \mathrm{Im}F_4\,Z_1 Z_2 Y_2^2\,\frac{L+1}{2L+3}\left(Q_L(z') - Q_{L+2}(z')\right)\Big\}$$

and

$$S_{L+} = \frac{1}{8\pi W}\,\frac{1}{2(L+1)}\,\frac{1}{k^2|\underset{\sim}{q}||\underset{\sim}{k}|}\int_{4m^2}^{\infty} dt'\Big\{-Z_1 Y_1^2 Y_2\left(k^2 B_1 + (W+m)\,B_5\right)Q_{L+1}(z')$$

$$+ Z_1 Y_2\,k^0|\underset{\sim}{q}||\underset{\sim}{k}|\,\mathrm{Im}F_4\,\frac{1}{2L+3}\left((L+2)Q_{L+2}(z') + (L+1)Q_L(z')\right) + Y_1 Z_2\,k^0|\underset{\sim}{q}||\underset{\sim}{k}|$$

$$\mathrm{Im}F_3\,\frac{1}{2L+1}\left((L+1)\,Q_{L+1}(z') + L\,Q_{L-1}(z')\right)\Big\}$$

The relevant relationships appear as we pick out the slowest dependence on $Z_1 \to 0$, $z' \to \infty$, $|\underset{\sim}{k}| \to 0$, $k^2 \to m_+^2$ giving

$$E_{L+} \sim \frac{1}{8\pi W}\,\frac{1}{2(L+1)}\,\frac{1}{|\underset{\sim}{q}||\underset{\sim}{k}|}\,Y_1 Y_2 Z_2^2\,\mathrm{Im}F_3\left(\frac{L}{2L+1}\right)Q_{L-1}(z)$$

$$S_{L+} \sim \frac{1}{8\pi W}\,\frac{1}{2(L+1)}\,\frac{1}{k^2|\underset{\sim}{q}||\underset{\sim}{k}|}\,Y_1 Z_2\,k^0|\underset{\sim}{q}||\underset{\sim}{k}|\,\mathrm{Im}F_3\left(\frac{L}{2L+1}\right)Q_{L-1}(z)$$

$$\Rightarrow E_{L+} \sim \frac{Y_2 Z_2}{k^0|\underset{\sim}{q}||\underset{\sim}{k}|}\,S_{L+}$$

$$\sim \frac{k^2}{k^0|\underset{\sim}{k}|}\,S_{L+}$$

$$\sim \frac{k^0}{|\underset{\sim}{k}|}\,S_{L+} \qquad \text{when } k^2 = m_+^2$$

We have therefore

$$S_{L+} \rightarrow \frac{|\underset{\sim}{k}|}{k^0} E_{L+} \quad : \phi_+ \rightarrow 0$$

$$S_{L-} \rightarrow -\frac{L-1}{L} \frac{|\underset{\sim}{k}|}{k^0} E_{L-} : \phi_- \rightarrow 0$$

$$S_{L-} \rightarrow \frac{|\underset{\sim}{k}|}{k^0} \frac{1}{L} \left(M_{L-} - (L-1) E_{L-}\right) : \phi_+ \rightarrow 0$$

(F4)

References

J.P. Ader, M. Capdeville and H. Navelet, Nuovo Cim. 56A, 315 (1968)

L. Ahrens et al, Phys. Rev. D9, 1894 (1974)

J.W. Alcock, W.N. Cottingham and A.C. Davis, Phys. Lett. 69B, 457 (1977)

R.L. Anderson et al, Phys. Rev. D4, 1937 (1971)

H.K. Armenian et al, Semi-Local Duality in π° Photoproduction, Tufts University Preprint (1974)

J.S. Ball, Phys. Rev. 124, 2014 (1961)

J.S. Ball, W.R. Frazer and M. Jacob, Phys. Rev. Lett. 20, 518, (1968)

J.S. Ball and M. Jacob, Nuovo Cim. 54A, 620 (1968)

V. Barger and D. Cline, Phys. Rev. 155, 1792 (1967)

V. Barger and R.J.N. Phillips, Phys. Rev. 187, 2210 (1969)

I. Barker, A. Donnachie and J. Storrow, Nucl. Phys. B79, 431 (1974)

I. Barker and J. Storrow, Nucl. Phys. B135, 285 (1978)

F.A. Behrends, A. Donnachie and D.L. Weaver, Nucl. Phys. B4, 1 (1967)

Ch. Berger et al, Nucl. Phys. B137, 1 (1978)

A. Bietti et al, Phys. Lett. 26B, 457 (1968)

J.D. Bjorken and S. Drell, Relativistic Quantum Mechanics (McGraw-Hill, 1964)

J.D. Bjorken, J.B. Kogut and D.E. Soper, Phys. Rev. D3, 1382 (1971)

F.W. Brasse et al, Nucl. Phys. B58, 467 (1975)

S.J. Brodsky et al, Phys. Rev. D6, 177 (1972)

J. Bronzan and C.E. Jones, Phys. Rev. 160, 1494 (1967)

A. Capella, J. Tran Thanh Van and A.P. Contogonris, Nucl. Phys. B12, 167 (1969)

J.L. Cardy, Nucl. Phys. B79, 319 (1974)

J.L. Cardy and A.R. White, Nucl. Phys. B80, 12 (1974)

H. Cheng and T.T. Wu, Phys. Rev. 183, 1324 (1969)

G. Chadwick, Y. Eisenberg and E. Kogan, Phys. Rev. D8, 1067 (1973)

G.F. Chew, M.L. Goldberger, F.E. Low and Y. Nambu, Phys. Rev. 106, 1345 (1957)

C.B. Chiu, R.L. Heimann and A. Schwimmer, Phys. Rev. D4, 3177 (1971)

F.E. Close and F.J. Gilman, Phys. Lett. 38B, 541 (1972)

P.D.B. Collins, An Introduction to Regge Theory and High Energy Physics (CUP, 1977)

P.D.B. Collins and A. Fitton, Nucl. Phys. B68, 125 (1974) Nucl. Phys. B91, 332 (1975)

P.D.B. Collins, R.C. Johnson and E.J. Squires, Phys. Lett. 26B, 223, (1968), Phys. Lett. 27B, 23 (1968)

P.D.B. Collins and R.A. Swetman, Nuovo Cim. Lett. 5, 793 (1972)

A.P. Contogouris, J. Tran Thanh Van and H.J. Lubatti, Phys. Rev. Lett. 19, 1352 (1967)

L.A. Copley, G. Karl and E. Obryk, Nucl. Phys. B13, 303, (1969)

D.J. Crennell et al, Phys. Rev. Lett. 27, 1674 (1971)

Ph. Dennery, Phys. Rev. 124, 2000 (1961)

R.C.E. Devenish, T. Eisenschitz and J.G. Korner, Electromagnetic N-N Transition Form Factors, DESY Preprint 75/48 (1975)

R.C.E. Devenish and D.H. Lyth, Nucl. Phys. B93, 109 (1975)

R.C.E. Devenish, D.H. Lyth and W.A. Rankin, Nucl. Phys. B59, 237 (1973)

P. DiVecchia et al, Phys. Lett. 27B, 296 (1968), Phys. Lett. 27B, 521 (1968)

R. Dixon et al, Phys. Rev. Lett. 39, 516 (1977)

R. Dolen, D. Horn and C. Schmid, Phys. Rev. Lett. 19, 4 (1967)

N. Dombey, Rev. Mod. Phys. 41, 236 (1969)

A. Donnachie, Invited paper at the Royal Society Symposium on Resonances, Regge Poles and Duality (1969)

A. Donnachie, in Hadronic Interactions of Electrons and Photons (Academic Press, 1971)

R.J. Eden et al, The Analytic s-matrix (CUP, 1966)

F. Elvekjaer and B.R. Martin, Nucl. Phys. B75, 388 (1974)

C. Ferro Fontan, N.M. Queen and G. Violini. Riv. del Nuovo Cirn. 2, 357 (1972)

R.P. Feynman, M. Kisslinger and F. Ravndal, Phys. Rev. D3, 2706 (1971)

H. Fraas, B.J. Read and D. Schilkklnecht, Nucl. Phys. B86, 346 (1975)

W.R. Francis et al, Phys. Rev. Lett 38, 633 (1977)

S. Fubini, Y. Nambu and V. Wataghin, Phys. Rev. 111, 329 (1958)

S. Fubini and G. Veneziano, Nuovo Cim. 64A, 811 (1969)

R. Gatto, Phys. Lett. 18, 803 (1967)

F.D. Gault, A.D. Martin and G. Kane, Nucl. Phys. B32, 429 (1971)

F. Gliozzi, Nuovo Cim. Lett. 4, 1160 (1970)

B. Haber et al, Phys. Rev. D10, 1387 (1974)

H. Harari, Phys. Rev. Lett. 27, 1028 (1971)

J. Harnard, Ph.D. Thesis, Oxford. Quoted in R.J.N. Phillips, Proc. Amsterdam Conference (1972)

A.C. Hearn, Nuovo Cim. 21, 333 (1961)

A.C. Irving, Nucl. Phys. B86, 125 (1975)

J.D. Jackson and C. Quigg, Phys. Lett. 29B, 236 (1969); Nucl. Phys. B22, 301 (1970)

H.F. Jones, Nuovo Cim. 10, 1018 (1965)

P. Joos et al, Nucl. Phys. B113, 53 (1976)

G.L. Kane et al, Phys. Rev. Lett. 25, 1519 (1970)

R.L. Kelly, Phys. Lett. 39B, 635 (1972)

M. LeBellac, Phys. Lett. 25B, 524 (1967)

E. Leader, Phys. Rev. 166, 1599 (1968)

D.H. Lyth, Proc. Daresbury Study Weekend No. 3 (DNPL/R15, 1971)

A.D. Martin and T.D. Spearman, Elementary Particle Theory (North-Holland, 1970)

W.J. Metcalf and R.L. Walker, Nucl. Phys. B76, 253 (1974)

W. Michael and G. Gidal, Phys. Rev. Lett. 28, 1475 (1972)

R.G. Moorhouse, H. Oberlack and A.H. Rosenfeld, Phys. Rev. D9, 1 (1974)

R.G. Moorhouse, Rapporteur's talk at Palermo Conference (1975)

R. Odorico, Phys. Rev. D15, 1384 (1977); Nucl. Phys. B101, 480 (1975); Phys. Lett. 61B, 263 (1976)

D. Olive et al, Phys. Rep 9C, 201 (1974)

H. Pilkuhn, The Interactions of Hadrons (Wiley, 1967)

M. Ross, F. Henyey and G.L. Kane, Nucl. Phys. B23, 269 (1970)

J.J. Sakurai, Ann Phys. 11, 1 (1960)

A.I. Sanda and G. Shaw, Phys. Rev. D3, 243 (1971)

I.N. Sneddon, Special functions of mathematical physcis and chemistry (Oliver and Boyd, 1956)

P. Stichel, Z. Physik 180, 170 (1964)

R. Talman, Proc. Bonn Lepton-Photon Symposium (1973)

L.G.F. Vanryckeghem, Neutral pion electroproduction at intermediate and high energies, Liverpool University Preprint (1976)

G. Veneziano, Nuovo Cim. 57A , 190 (1968)

K.M. Watson, Phys. Rev. 95, 228 (1954)

R.P. Worden, Nucl. Phys. B37, 253 (1972); Nucl. Phys. B58, 205 (1973)

I declare that, except where due reference is made in the text or acknowledgements, the work presented herein is original. It has not been presented, either in whole or in part, to any other university.

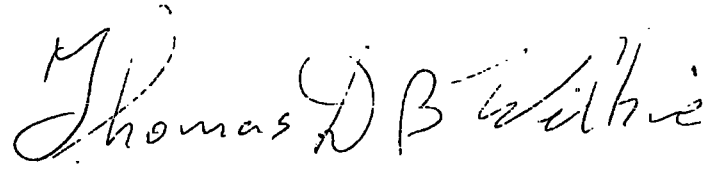

Thomas D.B. Wilkie

Better is the end of a thing than the beginning thereof.

Ecclesiastes